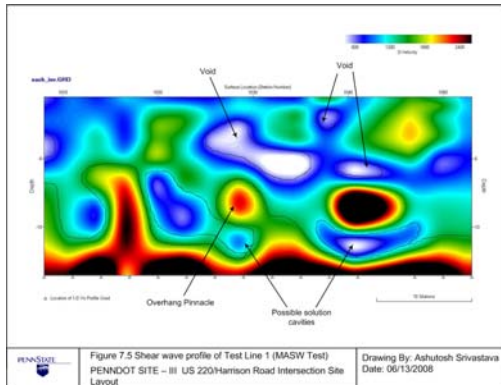


---

**COMMONWEALTH OF PENNSYLVANIA  
DEPARTMENT OF TRANSPORTATION**

**PENNDOT RESEARCH**



**SINKHOLE VOID GROUT TREATMENT**

**FINAL REPORT**

**Work Order No. PSU001  
Intergovernmental Agreement, No. 510602**

**October 10, 2008**

**By A. J. Schokker, J. A. Laman and A. Srivistava**

**PENNSSTATE**



---

**The Thomas D. Larson  
Pennsylvania Transportation Institute**

**The Pennsylvania State University  
Transportation Research Building  
University Park, PA 16802-4710  
(814) 865-1891 www.pti.psu.edu**



<b>1. Report No.</b> FHWA-PA-2008-004-PSU 001		<b>2. Government Accession No.</b>		<b>3. Recipient's Catalog No.</b>	
<b>4. Title and Subtitle</b> Sinkhole Void Grout Treatment			<b>5. Report Date</b> October 10, 2008		
			<b>6. Performing Organization Code</b>		
<b>7. Author(s)</b> Andrea J. Schokker, Jeffrey A. Laman and Ashutosh Srivistava			<b>8. Performing Organization Report No.</b> PTI 2009-02		
<b>9. Performing Organization Name and Address</b> The Thomas D. Larson Pennsylvania Transportation Institute The Pennsylvania State University 201 Transportation Research Building University Park, PA 16802-4710			<b>10. Work Unit No. (TRAIS)</b>		
			<b>11. Contract or Grant No.</b> 510602, PSU 001		
<b>12. Sponsoring Agency Name and Address</b> The Pennsylvania Department of Transportation Bureau of Planning and Research Commonwealth Keystone Building 400 North Street, 6 <sup>th</sup> Floor Harrisburg, PA 17120-0064			<b>13. Type of Report and Period Covered</b> Final Report: 4/16/2007 – 10/15/2008		
			<b>14. Sponsoring Agency Code</b>		
<b>15. Supplementary Notes</b> COTR: Alfred Picca					
<b>16. Abstract</b> Active karst areas in Pennsylvania are plagued by sinkhole activity, causing potential damage to the infrastructure and resulting in a public safety issue. A number of techniques such as full excavation and replacement, pin piles to bedrock, pressure grouting, polymer injection, and combinations of techniques are available for sinkhole remediation. These approaches may vary widely in cost, feasibility, speed, and effectiveness. Each of these approaches needs to be thoroughly investigated, with positives and negatives for various scenarios clearly defined so that PennDOT can respond quickly and effectively to developing sinkhole problem areas. The objective of the research was to develop guidelines for quick, economical remediation options for sinkholes. The focus of the work was on sinkholes affecting structures and pavements, but may be applicable to other voids, including those related to mining. As part of this objective, several sites were chosen for remediation as field studies.					
<b>17. Key Words</b> Karst, sinkhole, void, excavation, grout, remediation, pavements, structures			<b>18. Distribution Statement</b> No restrictions. This document is available from the National Technical Information Service, Springfield, VA 22161		
<b>19. Security Classif. (of this report)</b> Unclassified	<b>20. Security Classif. (of this page)</b> Unclassified		<b>21. No. of Pages</b> 120	<b>22. Price</b>	



# SINKHOLE VOID GROUT TREATMENT

## FINAL REPORT

Work Order No. PSU-001  
Intergovernmental Agreement No. 510602

Prepared for

Bureau of Planning and Research  
Commonwealth of Pennsylvania  
Department of Transportation

By

Dr. Andrea Schokker, Principal Investigator  
Dr. Jeff Laman, co-Principal Investigator  
Ashutosh Srivistava, Graduate Research Assistant

The Thomas D. Larson Pennsylvania Transportation Institute  
The Pennsylvania State University  
Transportation Research Building  
University Park, PA 16802-4710

October 10, 2008

PTI 2009-02

This work was sponsored by the Pennsylvania Department of Transportation and the U.S. Department of Transportation, Federal Highway Administration. The contents of this report reflect the views of the authors, who are responsible for the facts and the accuracy of the data presented herein. The contents do not necessarily reflect the official views or policies of either the Federal Highway Administration, U.S. Department of Transportation, or the Commonwealth of Pennsylvania at the time of publication. This report does not constitute a standard, specification, or regulation.



# TABLE OF CONTENTS

<b>EXECUTIVE SUMMARY .....</b>	<b>xi</b>
<b>CHAPTER 1 - INTRODUCTION.....</b>	<b>1</b>
1.1 Background.....	1
1.2 Engineering Geophysics .....	1
1.2.1 Seismic Wave Propagation .....	3
1.2.2 Crosshole Testing.....	5
1.2.3 Refraction and Reflection .....	5
1.2.4 Surface Wave Methods .....	6
1.2.5 Electrical Resistivity .....	7
1.2.5.1 Traditional Four-Electrode Systems .....	8
1.2.5.2 Multi-Electrode Systems.....	9
1.3 Objective and Scope of Research .....	10
1.4 Organization of Report .....	11
<b>CHAPTER 2 - LITERATURE REVIEW.....</b>	<b>13</b>
2.1 Elastic Wave Propagation in Homogeneous, Isotropic Half-space .....	13
2.1.2 Seismic Wave Methods.....	14
2.1.2.1 Refraction Method .....	15
2.1.2.2 Reflection Method .....	16
2.1.2.3 Surface Wave Methods .....	17
2.2 Multichannel analysis of surface waves – General Information.....	18
2.2.1 Forward and Inverse modeling .....	20
2.2.2 Analysis of Experimental Data .....	22
2.3 Applicability of MASW in Void/Sinkhole Detection.....	24
2.4 Sinkhole Remediation.....	26
<b>CHAPTER 3 - EQUIPMENT AND SOFTWARE .....</b>	<b>28</b>
3.1 Introduction.....	28
3.2 Data Acquisition System.....	28
3.2.1 Signal Analyzer.....	28
3.2.2 Geophones.....	30
3.2.3 Energy Source.....	32
3.3 Software .....	33
3.3.1 Data Acquisition .....	33
3.3.2 Data Processing.....	34
3.3.2.1 SeisImager2D refraction package.....	34
3.3.2.2 SurfSeis 2.0.....	34
<b>CHAPTER 4 - TEST SETUP AND PROCEDURE .....</b>	<b>35</b>
4.1 Introduction.....	35
4.2 Multi-channel Analysis of Surface Waves (MASW) .....	35
4.2.1 Field Test Setup .....	36
4.2.2 Interval of Source-Receiver Configuration (SRC) Movement .....	37

4.2.3 Data Acquisition Parameters.....	38
4.2.4 Test Procedure .....	38
4.3 Refraction Survey .....	38
4.3.1 P-wave Refraction Survey .....	39
4.3.1.1 P-Wave Refraction Test Procedure.....	40
4.3.2 SH-wave Refraction survey .....	41
4.3.3 Data Acquisition Parameters.....	43
4.4 Summary .....	43
<b>CHAPTER 5 - DATA PROCESSING .....</b>	<b>44</b>
5.1 Introduction.....	44
5.2 SignalCalc® 620.....	44
5.2.1 Step 1: Start New Test .....	44
5.2.2 Step 2: Setting the Input Channel Control Parameters .....	46
5.2.3 Step 3: Setting the Sampling Parameters .....	50
5.2.4 Step 4: Setting the Measurement Parameters.....	50
5.2.5 Step 5: Perform Test .....	52
5.2.6 Step 6: Exporting Data .....	52
5.3 SurfSeis 2.0.....	54
5.3.1 Step 1: Formatting.....	54
5.3.2 Step 2: Field Setup.....	55
5.3.3 Step 3: Generation of Overtone (OT) Records .....	57
5.3.4 Step 4: Inversion for 2-D vs. Profile.....	59
5.4 Seisimager 2D.....	61
5.4.1 STEP 1: Picking First Breaks .....	62
5.4.2 STEP 2: Inversion of Travel-Time curves .....	65
<b>CHAPTER 6 - DISCUSSION OF RESULTS .....</b>	<b>72</b>
6.1 Introduction.....	72
6.2 Penn State Golf Course Site.....	72
6.2.1 Source-Receiver Configuration (SRC) Movement.....	74
6.2.2 Field Geometry .....	74
6.2.3 Energy Source Offset.....	74
6.2.4 Test Line Setup .....	75
6.2.5 Test Organization.....	75
6.2.6 File Organization .....	78
6.2.7 Source-Receiver Array Configuration Management .....	78
6.3 Metzgar Field (Lafayette College) Site.....	78
6.3.1 Source-Receiver Configuration Movement .....	81
6.3.2 Field Geometry .....	81
6.3.3 Energy Source Offset.....	82
6.3.4 Test Line Setup .....	82
6.3.5 Test Organization.....	82
6.3.6 File Organization .....	83
6.3.7 Source-Receiver Array Configuration Management .....	83
6.4 Route 220 and Harrison Road .....	87

<b>CHAPTER 7 - TEST SITE DESCRIPTION AND RESULTS</b> .....	90
7.1 Introduction.....	90
7.2 Penn State Golf Course Test Site and Setup.....	90
7.2.1 Finding and Discussion of Tomography of Penn State Golf Course Site.....	92
7.2.1.1 Test Line 1 .....	92
7.2.1.2 Test Line 2 .....	92
7.2.2 Penn State Golf Course Test Summary .....	93
7.3 Metzger Field (Lafayette College) Test Site and Setup.....	100
7.3.1 Findings and Discussion of Tomography of Metzger Field Site .....	100
7.3.2 Metzger Field Test Summary.....	101
7.4 US 220 N Test Site and Setup.....	105
7.4.1 Finding and Discussion of Tomography of US 220 N Test Site .....	105
7.4.2 US 220 N Site Test Summary .....	106
 <b>CHAPTER 8 - SUMMARY AND CONCLUSIONS</b> .....	 109
8.1 Summary .....	109
8.2 Conclusions.....	110
8.3 Implementation Plan .....	110

## LIST OF FIGURES

Figure 2.1 P, S and R-waves in Elastic Isotropic Homogenous Half-space .....	14
Figure 2.2 Seismic Refraction Geometry.....	16
Figure 2.3 Seismic Reflection Geometry.....	17
Figure 2.4 Layered $V_s$ Profile .....	19
Figure 2.5 Test Setup .....	20
Figure 2.6 Dispersion Curve .....	20
Figure 2.7 Forward and Inverse Problem Associated with MASW .....	21
Figure 3.1 Signal Analyzer .....	29
Figure 3.2 General Layout of the Test Setup.....	30
Figure 3.3 Horizontal and Vertical Geophones .....	32
Figure 3.4 Shear Wave Device .....	33
Figure 4.1 MASW Test Setup.....	35
Figure 4.2 Steel Impact Plate .....	36
Figure 4.3 Seismic Refraction Geometry (Courtesy: Enviroscan Inc) .....	39
Figure 4.4 Geophone Array Setup .....	41
Figure 4.5 Refraction Test Procedure .....	41
Figure 4.6 SH-Wave Refraction Survey .....	43
Figure 5.1 Refresh VXI Resource Manager .....	45
Figure 5.2 SignalCalc <sup>®</sup> 620 Configure Hardware Dialog Box .....	45
Figure 5.3 SignalCalc <sup>®</sup> 620 Start New Test Dialog Box .....	46
Figure 5.4 SignalCalc <sup>®</sup> 620 Channel Control Box .....	47
Figure 5.5 SignalCalc <sup>®</sup> 620 Measurement Tab .....	48
Figure 5.6 SignalCalc <sup>®</sup> 620 Trigger Tab .....	48
Figure 5.7 SignalCalc <sup>®</sup> 620 Signal Conditioning Tab .....	49
Figure 5.8 SignalCalc <sup>®</sup> 620 Comment Tab.....	49
Figure 5.9 SignalCalc <sup>®</sup> 620 Sampling Parameters Window.....	50
Figure 5.10 SignalCalc <sup>®</sup> 620 Measurement Parameters Window .....	51
Figure 5.11 SignalCalc <sup>®</sup> 620 Signal Map.....	53
Figure 5.12 Formatting of Data .....	56
Figure 5.13 Survey Type.....	56
Figure 5.14 Field Setup.....	56
Figure 5.15 Field Geometry .....	57
Figure 5.16 Dispersion Analysis Controls and Record Display .....	58
Figure 5.17 OT Image and Dispersion Curve Generation Controlling Parameters .....	59
Figure 5.18 Controlling Parameters for Inversion Analysis .....	60
Figure 5.19 Control Tab.....	60
Figure 5.20 Final 2-D Shear Velocity Profile Obtain After Inversion Analysis .....	60
Figure 5.21 Seisimager <sup>®</sup> 2D Main Display Window.....	62
Figure 5.22 Seisimager <sup>®</sup> 2D Optimize Display Toolbar .....	62
Figure 5.23 Pick First Breaks for File 1000.dat.....	63
Figure 5.24 Travel-Time Curve for File 1000.dat .....	64
Figure 5.25 Travel-time Curves for All Data.....	65
Figure 5.26 Travel-Time Curves.....	66
Figure 5.27 Importing Elevation Model .....	67

Figure 5.28 Generating Initial Velocity Model.....	67
Figure 5.29 Initial Velocity Layer Model for Sample Data.....	68
Figure 5.30 Final Subsurface Wave Velocity Profile for Sample Data.....	69
Figure 5.31 Inversion Parameters For Tomography Method.....	70
Figure 6.1 (a) Penn State University Golf Course Satellite image .....	73
Figure 6.1 (b) Penn State University Golf Course Street locator map .....	73
Figure 6.2 (a) PENNDOT Site – I Pennsylvania State University Golf Course Site Layout 69 .....	76
Figure 6.2(b) Geophone Layout for Pennsylvania State University Golf Course Site.....	77
Figure 6.3 Receiver array configuration scheme .....	78
Figure 6.4 (a) Metzgar Athletic Field at Lafayette College Satellite Image.....	79
Figure 6.4 (b) Metzgar Athletic Field at Lafayette College Street Locator map .....	80
Figure 6.5 Metzgar Athletic Field Test Grid of 81m. ....	81
Figure 6.6 (a) PENNDOT Site – II Lafayette Athletic Field Layout .....	84
Figure 6.6 (b) PENNDOT Site – II Lafayette Athletic Field Layout (Control Line) .....	85
Figure 6.6 (c) PENNDOT Site – III Geophone Layout for Lafayette Athletic Field .....	86
Figure 6.7 Receiver Array Configuration Scheme .....	87
Figure 6.8 Location Map of Harrison Road Bridge over US220.....	88
Figure 6.9 (a) PENNDOT Site – III US 220/Harrison Road Intersection Site Layout.....	89
Figure 6.9 (b) PENNDOT Site – III Geophone Layout for US 220/Harrison Road Intersection Site .....	90
Figure 7.1 PSU Golf Course Site.....	92
Figure 7.2 (a) Shear Wave Profile of Test Line 1 (MASW Test) PENNDOT Site – I Pennsylvania State University Golf Course Site.....	95
Figure 7.2 (b) Shear Wave Profile of Test Line 1 (Refraction Test) PENNDOT Site – I Pennsylvania State University Golf Course Site.....	96
Figure 7.3 (a) Shear Wave Profile of Test Line 2 (MASW Test) PENNDOT Site – I Pennsylvania State University Golf Course Site.....	97
Figure 7.3 (b) Shear Wave Profile of Test Line 1 for span 100-128 feet (Refraction Test) PENNDOT Site – I Pennsylvania State University Golf Course Site...98	
Figure 7.3 (c) Shear Wave Profile of Test Line 1 for span 130-158 feet (Refraction Test) PENNDOT Site – I Pennsylvania State University Golf Course Site...99	
Figure 7.3 (d) Shear Wave Profile of Test Line 1 for span 160-188 feet (Refraction Test) PENNDOT Site – I Pennsylvania State University Golf Course Site...100	
Figure 7.4(a) Shear Wave Profile of Control Line (MASW TEST) PENNDOT SITE – II Metzger Field (Lafayette College) Test Site Layout.....	103
Figure 7.4(b) Shear Wave Profile of Test Line 1 (MASW TEST) PENNDOT SITE – II Metzger Field (Lafayette College) Test Site Layout .....	104
Figure 7.4(c) Shear Wave Profile of Test Line 2 (MASW TEST) PENNDOT SITE – II Metzger Field (Lafayette College) Test Site Layout.....	105
Figure 7.5 Shear Wave Profile of Test Line 1 (MASW Test) PENNDOT Site – III US 220/Harrison Road Intersection Site Layout.....	108
Figure 7.6 Shear Wave Profile of Test Line 1 (Refraction Test) PENNDOT Site – III US 220/Harrison Road Intersection Site Layout.....	109

## LIST OF TABLES

Table 3.1 Portable Computer Specifications .....	23
Table 3.2 SN4- 4.5 Hz Digital Grade Geophone Specifications .....	24

## EXECUTIVE SUMMARY

Pennsylvania has a significant number of active karst areas with sinkhole activity. When these areas threaten infrastructure, the Pennsylvania Department of Transportation needs to be able to respond quickly and to provide a solution. Rapid evaluation of the subsurface conditions of the site is crucial for this response. This work order focuses on the MASW (Multi-channel Analysis of Surface Waves) method. The method is well-established and the equipment is readily available, so implementation is feasible. However, research on the data processing techniques is ongoing and the associated software has changed significantly in recent years. The objective of this project is to provide the basis for future use of MASW by PennDOT personnel by focusing on the results from three specific Pennsylvania sites. All three sites have known sinkhole activity: 1) Penn State golf course property along West College Ave, 2) Lafayette College Athletic Field, and 3) Harrison Road (at Route 220). Site 1 was chosen as a baseline site with regular and easily accessible terrain that includes visual surface indications of sinkhole activity. Site 2 was chosen as a site with a previously mapped cave to use for validation of MASW compared to resistivity data. Site 3 was chosen as a currently active PennDOT site with visible indications of sinkhole activity at the surface near a bridge abutment that needed subsurface evaluation.

The MASW method proved to be efficient in this study for operators familiar with the equipment and software for data processing. Data can be collected rapidly and processed on site the same day. The output can be shown as a contour plot as a subsurface “slice” through the depth to visually delineate likely void/sinkhole areas. Multiple slices can be combined to allow interpretation over the three dimensional space.

In the case of the three sites chosen, the MASW method provided useful data for sites 1 and 3. In Site 2, the large void made by the cave along with multiple smaller sinkhole voids in the area made interpretation of the data difficult based on the layout chosen for the geophones and energy source. This site was originally intended to be the site for verification with existing resistivity data, but the MASW data was not clear enough to make meaningful comparisons. The MASW testing did show indications of voids and the cave, but standard approaches to geophone spacing and energy source distance may need to be refined to provide more meaningful results.

This report provides the details on how the MASW method is used in the field, including setup of the equipment and use of the processing software with typical output. Each site is thoroughly described with the locations of geophones and other key items so that the first-time user can use the report as a reference tool. The MASW method with current seismic wave analysis software showed excellent promise for use in rapid evaluation of sites of potential active sinkholes. The method in its present form provided inconclusive results in the presence of a cave with numerous sinkholes in the area.

# **Chapter 1 – Introduction**

## **1.1 Background**

Active karst areas in Pennsylvania are plagued by sinkhole activity, causing potential damage to the infrastructure and resulting in a public safety problem. A number of techniques such as full excavation and replacement, pin piles to bedrock, pressure grouting, polymer injection, and combinations of techniques are available for sinkhole remediation. These approaches may vary widely in cost, feasibility, speed, and effectiveness. Each of these approaches needs to be thoroughly investigated, with positives and negatives for various scenarios clearly defined so that the Pennsylvania Department of Transportation (PennDOT) can respond quickly and effectively to developing sinkhole problem areas. The first step in this process is finding a reliable method of detection and characterization of the sinkhole site.

Detection of obstacles, voids, cavities, subsurface rock profiles, or various types of utilities is also required for planning and designing of foundations. Therefore, determination of subsurface soil characteristics is not only important for sinkhole remediation but is also an essential part of the design process. Karst is characterized by unpredictable and variable rock depth and the possibility of rapid sinkhole formation. Active karst areas in Pennsylvania are characterized by sinkhole activity with the potential to cause significant damage to infrastructure, resulting in public safety concerns.

## **1.2 Engineering Geophysics**

Technologies generally categorized as engineering geophysical methods have been adapted from seismological and petroleum industry applications for characterization

of shallow (<100 ft) subsurface ground conditions. The methods are analogous to familiar medical techniques, e.g., X-ray, CAT scan, MRI, that enable “seeing” within a material using sensing devices located along the boundaries. Engineering parameters such as seismic wave velocity and electrical resistivity are highly determined by material type and condition. Geophysical measurement techniques can determine the variation of these significant parameters within the interior of a material, and thus infer subsurface characteristics without actually touching the material. Coupled with tomographic algorithms, a two-dimensional slice or a three-dimensional volume of the subsurface under study can be produced. Borehole geophysical methods typically provide the best accuracy and resolution, while surface-based techniques are typically more economical to implement but can suffer from depth of penetration and resolution problems.

There are a wide range of geophysical testing methodologies available for application, and based upon several physical principles. The broad categories of methodologies include seismic wave propagation, electromagnetic wave propagation, electricity, magnetics, and gravity. Each class of methods produces measurements that are sensitive to particular physical properties of the material under investigation. For example, seismic waves are primarily dependent on the elastic modulus and mass density of a material, while electromagnetic waves are primarily governed by the dielectric constant. While the broad categories of methodologies have been established for some time, specific applications are continually under development and improvement as sensing, data acquisition, computing, and other technologies evolve.

For characterization of geotechnical engineering sites, including the potential for subsurface anomalies such as sinkholes, methods based upon seismic waves,

electromagnetic waves, and electricity are of primary interest. Ground penetrating radar (GPR) is a very successful methodology for developing the two- and three-dimensional subsurface models desired in this research. Unfortunately, electromagnetic radar waves are highly damped in clayey soils, and thus have insufficient characterization distances to be practical in typical Pennsylvania karst terrane conditions. Thus, the following discussion will summarize some of the methods based upon seismic waves and electricity.

### **1.2.1 Seismic Wave Propagation**

Seismic wave propagation methods are among the most established geophysical exploration techniques available for geotechnical and civil engineering applications. These methods can be conducted nondestructively from cased boreholes, or non-intrusively and nondestructively from the ground surface. Seismic methods have wide application in all phases of the design and construction process. The methods most directly produce an in-situ determination of the depth and thickness of significant soil layers and the modulus of elasticity of a material. Modulus can be used directly in design, as a quality-control measure during construction, and as a diagnostic assessor after construction. The wave propagation velocities determined via seismic testing can also be used to infer other significant material parameters such as Poisson's ratio and the coefficient of lateral earth pressure.

The propagation of seismic waves occurs when a mechanical disturbance is created within or outside a medium. On a typical site composed of soil and rock, waves are assumed to travel through an elastic half space. Within an elastic half space two types of waves may be generated, body waves and surface waves. Waves that propagate

through the body of the medium are either compression or shear waves. Waves that are confined to travel in a zone near the boundary or surface of the half space are Rayleigh waves. Wave types are defined by the direction of particle motion with respect to the direction of wave motion as follows:

- Compression waves are distinguished by particle motion parallel to wave motion. A medium subjected to such a wave would experience compressions and dilatations as the wave propagates. Compression waves may also be referred to as “dilatational,” “primary,” “P-” and “irrotational” waves.
- Shear waves are identified by particle motion perpendicular to wave motion. Unlike the compression wave, the medium is distorted without volume change as the shear wave propagates. Shear waves are occasionally referred to as “distortional,” “secondary,” “S-” and “equivoluminal” waves. If the particle motion of a shear wave is purely confined to the vertical plane, the shear wave is referred to as a SV-wave or vertically polarized shear wave. Likewise, if the particle motion is purely confined to the horizontal plane, then the shear wave is referred to as an SH-wave or horizontally polarized shear wave.
- The Rayleigh wave motion is confined to the vertical plane and is characterized by particle movement that forms retrograde ellipses at the surface.

Using the theory of elasticity and Newton’s laws of motion, elastic moduli may be calculated from mass density and the respective propagation velocities of seismic waves. In addition to enabling the determination of moduli profiles with depth, wave velocities

obtained from seismic testing can also be used to calculate other material properties, such as coefficient of lateral earth pressure at rest and Poisson's ratio.

### **1.2.2 Crosshole Testing**

The crosshole test is an established technique for determining in-situ wave velocity profiles. The test consists of first establishing a series of cased boreholes along a common line a known distance apart. Testing can be conducted with a minimum of two boreholes, but the method is improved with the use of three cased holes. In one borehole a source is inserted to create a seismic wave. Receivers are placed in the remaining hole(s) to measure the arrival of the seismic wave. These receivers are usually some type of transducer, depending on the material being tested, and the receivers transfer the wave arrivals to a time recorder. The essential measurement of the crosshole test is travel time. Preferably, the interval for the wave to travel between two receiver boreholes is used as the travel time. The interval time eliminates the need for precise triggering of the source and recording equipment. Body wave velocities are then calculated by dividing the receiver borehole spacing by the interval travel time. The velocity of both compression and shear waves can be determined in this manner.

### **1.2.3 Refraction and Reflection**

Surface methods for measurement of seismic waves utilize sources and receivers located at the surface and therefore have an economic advantage over borehole methods since boreholes are not required. The surface refraction method consists of measuring the travel times of body waves from a surface source to a linear spread of receivers on the surface. The fastest paths of the seismic waves depend on the velocity distribution in the substructure, which is inferred from the time of first arrivals at each receiver.

Conceptually, the surface reflection is similar to the refraction method. A surface source and a linear spread of receivers are used. However, the receiver spread is much closer to the source because this method relies on measurement of first arrivals of direct arrivals and on later arrivals of waves reflected off the interfaces between layers rather than on measurement of only first arrivals as in the reflection method.

#### **1.2.4 Surface Wave Methods**

The spectral-analysis-of-surface-waves (e.g., SASW, MASW) method is a testing procedure for determining shear wave velocity profiles of soil systems in situ. The test is performed from the ground surface without boreholes. Current practice calls for locating two or more vertical receivers on the ground surface a known distance apart; a wave containing a large range of frequencies is then generated in the soil by means of a hammer, vibrator, or other energy source. Surface waves are detected by the receivers and are recorded using a Fourier spectrum analyzer or seismograph. The analyzer is used to transform the waveforms from the time to the frequency domain and then to perform necessary spectral analyses. Knowing the distance and spectral functions between the receivers for each frequency, the velocity of the surface wave associated with that frequency is calculated. This relationship is known as the dispersion curve. The final step is application of an inversion process that constructs the shear wave velocity profile from the dispersion information. Surface wave methods have proven to be a valuable tool for determining shear wave velocity profiles. The ability to determine a detailed profile entirely from surface measurements can result in substantial time and cost savings compared to other methods.

The seismic wave propagation methodologies have proven valuable in a number of applications, particularly for characterizing the vertical variation in shear modulus of natural soil deposits. Recent attention has been directed toward use of these methods for characterization of more problematic sites. For example, karst and mined terrane produce soil deposits with highly variable mechanical properties, and often contain voids and other anomalies that create very difficult design and construction conditions. Catastrophic failures in such terrane have been well documented. With the development of proper test protocols, crosshole, refraction, reflection, and surface techniques can be used to better characterize these troublesome subsurface environments.

### **1.2.5 Electrical Resistivity**

The electrical resistivity method has been used in site characterization for about a century. Most earth materials are either good insulators or dielectrics, i.e., they do not conduct electricity very well. Rather, electricity is conducted through the subsurface via interstitial water. Rock typically has a significantly higher resistivity than soil because it has a smaller primary porosity and fewer interconnected pore spaces. It is thus drier. Earth materials such as clay tend to hold more moisture and generally conduct electricity much better; their resistivity values are typically much lower than that of rock. Thus, resistivity methods typically work well in characterizing karst terrane because of the high contrast in resistivity values between carbonate rock and moist, clayey residual soil overlying it.

Resistivity measurements are made by introducing current into the subsurface through two current electrodes, and measuring the voltage difference with two potential electrodes. From the magnitude of the introduced current, measured voltage, and a factor

that accounts for the geometric arrangement of the electrodes, a resistivity value is calculated. The calculated resistivity value is not a true assessment of subsurface resistivity, but is instead an apparent value. Apparent resistivity is defined as the resistivity value that would be obtained if the subsurface were homogeneous. To obtain more accurate estimates for resistivities of inhomogeneous subsurface materials, measured values are compared with values calculated from an assumed model of the subsurface. This is typically an iterative procedure using inversion techniques in which the subsurface model is modified until a reasonable match is obtained.

#### **1.2.5.1 Traditional Four-Electrode Systems**

A traditional four-electrode system consists of a power source, current meter, voltage meter, and four electrodes. Two survey methods are commonly used. First, in a sounding survey, the spacing between electrodes is increased between measurements, while the centerline of the electrode group remains fixed. As the electrodes are spread further apart, resistivities of deeper subsurface materials are obtained. The data from a sounding survey are typically interpreted by comparing the measured results to results calculated using a one-dimensional model of a layered subsurface system. The depth of investigation is governed by array type (the geometrical arrangement of the electrodes), electrode spacing, and the specific subsurface materials present.

Second, in a profiling survey, the spacing between electrodes is fixed, and the electrode group is moved horizontally along a line between measurements. Resulting measurements can be used to locate variation in the subsurface along the measurement line. Interpretation of data obtained using this approach involves a simple plot of

measurements as a function of distance along the line, followed by observation of variations of interest.

### **1.2.5.2 Multi-Electrode Systems**

Recent development of multi-electrode earth resistivity testing has substantially improved investigation capabilities. Rather than moving equipment between data points, multi-electrode systems collect multiple data points with stationary equipment. These systems consist of multiple (usually 20 or more) electrodes connected to a switching device, a power source, a current meter, a voltage meter, and a data recorder. Electrodes are spaced at equal distances along a survey line, and the switching device is used to automatically select combinations of four electrodes for each measurement. In the most recent devices now available, it is possible to apply current to two electrodes, and then simultaneously measure voltages across multiple pairs of electrodes, significantly reducing test time still further. The resulting data set consists of a combination of soundings and profiles, resulting in a two-dimensional or three-dimensional survey of the subsurface materials. The depth of investigation using these methods is a function of line length, array type, and the subsurface materials present. Depths typically range from one-third to one-fifth of the length of the line.

A pseudo section is a simple plot of results from a multi-electrode test, where resistivity values are plotted at a horizontal location coinciding with the midpoint of the four electrodes responsible for the measurement, and at a depth proportional to the spread of the four electrodes. The process by which a geologic cross section of the subsurface is developed involves comparing pseudo sections of measured test data with pseudo sections of data calculated with an assumed model of the subsurface. This iterative

“inversion” process continues until an acceptable match is found between the measured and theoretical pseudo sections. Once a match is found, the subsurface model producing the match is accepted as the best representation of actual subsurface conditions. This inversion process is automated via commercial computer programs, allowing for observation of approximate site conditions shortly following completion of test measurements.

## **1.2 Objective and Scope of Research**

The objective of this project is to provide the basis for future use of MASW by PennDOT personnel by focusing on the results from three specific Pennsylvania sites with known sinkhole activity.

While the scope of this project is focused on sinkholes, the results are applicable to other voids, including caves and abandoned mines. Three sinkhole prone sites were chosen as a part of the field study for identification purposes. The three sites are 1) the Penn State Golf Course, a site of known sinkhole activity, 2) the Lafayette College Athletic Field, a site of measured and investigated sinkhole and void activity for proof testing, and 3) the site at Route 220 (future I-99) and Harrison Road. These sites are briefly discussed below:

The Penn State Golf Course site is located in an open field along West College Avenue on the property of the Penn State Golf Course. This site has known sinkhole activity in the field and near West College Avenue, but no prior testing has been done on this site. The Penn State Golf Course site has many depressions approximately 1 foot to 2 feet in diameter. The site is characterized by poor vegetation that is likely due to the

quick drainage of water through subsurface sinkholes. This site provides a “blind” test site for the equipment and method, with the possibility of multiple test arrays because of the close proximity to Penn State and the level terrain.

The Lafayette College Athletic Field is located near Braden Airpark, approximately 3.5 miles northwest of the Lafayette College campus. This site has been extensively mapped and includes a well-mapped cave that was investigated by Dr. Mary Roth in 2003 using the electrical resistivity method (Appendix A). The site provides a potentially valuable baseline evaluation of the proposed method.

The 220 site is located at the intersection of Route 220 (future I-99 to join I-80) and Harrison Road. The site has visible sinkhole activity along Route 220 under the Harrison Road overpass. This site has not been previously mapped for sinkholes, and the data acquired will be useful for District 2 in monitoring for potential problems in this area.

A laboratory test was conducted along with the sites at the Civil Infrastructure Testing and Evaluation Laboratory (CITEL) at Penn State. The laboratory test included the simulation of wave propagation phenomenon in stratified soil media. The laboratory test provides a better understanding of the dispersive nature associated with the wave propagation in layered media.

### **1.3 Organization of Report**

Chapter 2 provides the literature review of the relevant background information on the SASW and MASW tests. Testing and the data processing procedure will be

documented in brief in this chapter. Various remediation techniques will also be reviewed and compared for different site conditions.

Chapter 3 documents the details of the equipment and the software used for data acquisition and describes the data processing methods.

Chapters 4 and 5 give a general overview of the test setup for the MASW test, recording parameters, test procedure, and the data processing techniques of spectral analysis of surface waves through generation and inversion of overtone (OT) images.

Chapter 6 describes preliminary gravel box tests conducted under controlled laboratory conditions. This chapter also includes the details of the three field sites and test parameters for the field experiment.

Chapter 7 describes the test setup, data acquisition parameters, and results from each of the three sites.

Chapter 8 provides a summary, conclusions, and recommendations for further research.

## Chapter 2 – Literature Review

### 2.1 Elastic Wave Propagation in Homogeneous, Isotropic Half-space

In the three dimensional homogenous and isotropic medium, the equation of motion of an elastic wave is written as (Richart, et.al., 1970):

$$\rho \frac{\partial^2 \mathbf{u}_i}{\partial t^2} = (\lambda + G) \frac{\partial \bar{\epsilon}}{\partial x_i} + G \nabla^2 \mathbf{u}_i \quad (1)$$

where  $\rho$  is the density of the elastic medium,  $\mathbf{u}_i = (u, v, w)^T$ , is the displacement vector in the Cartesian Co-ordinates,  $x_i = (x, y, z)^T$ ,  $\bar{\epsilon}$  is the cubical dilation and is equal to the volume strain of the system,  $\lambda$  and  $G$  are the Lamé's constant, and  $\nabla$  is the Laplacian operator in the Cartesian Co-ordinates. For homogenous and isotropic elastic half-space, the above equation results in three solutions representing three types of waves (shown in Figure 2.1): 1) dilatational wave, 2) distortional wave and 3) surface wave. All the three types of waves are discussed in the following section (Richart, et. al., 1970):

- i. Dilatational wave (Primary wave, P-wave, pressure waves, compression waves)

P-waves result in the dilatation of the medium. In the region affected by P-waves, the medium particles vibrate along or parallel to the direction of travel of the wave energy. P-wave velocity is highest among all the wave types (P, S, and R). P-waves carry only 7 percent (approximately) of the total energy.

- ii. Distortional wave (Secondary wave, S-wave, shear waves)

S-waves result in the distortion of the medium. In the region affected by S-waves, the medium particles vibrate perpendicular to the direction of wave propagation. Wave velocity of the S-wave is higher than R-waves but is less than

P-waves, and 26 percent (approximately) of the total energy is carried by these waves.

iii. Surface wave (Rayleigh wave, R-wave)

A surface wave moves across a free surface and is confined to a zone near the free boundary of the half-space. As it passes, a surface particle moves in a circle or ellipse in the direction of propagation depending on the medium properties. The amplitude of the surface waves decrease rapidly with depth. The R-waves decay more slowly with distance than the body waves (P and S waves). Their velocity is slightly lower than that of S-waves. Surface waves carry approximately 67 percent of the total energy.

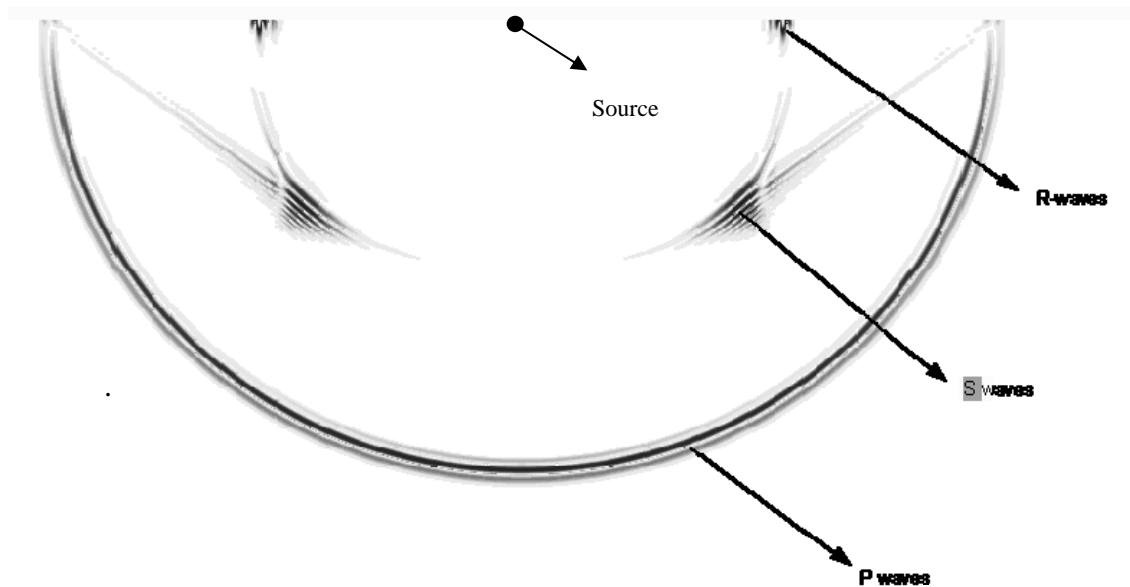


Figure 2.1. P, S, and R-waves in Elastic Isotropic Homogenous Half-space.

### 2.1.2 Seismic Wave Methods

In the conventional methods of determining soil properties such as the triaxial shear test, vane shear test, direct shear test uniaxial shear test, and cone penetration

method, it is difficult to determine in-situ properties below the uppermost layers. Seismic methods are advantageous in such cases because they are performed on the surface, and with the help of physics principles of wave propagation, important soil properties are determined at lower depths. Three types of seismic surveys conducted for subsurface soil profiling are discussed below.

#### **2.1.2.1 Refraction Method**

The seismic refraction survey requires measurement of the seismic energy component travel time where the P-wave or S-wave travels down to the top of the rock (or other distinct density contrast), is refracted along the top of the rock, and returns to the surface as a head wave along a wave front (Figure 2.2). The major limitation of seismic refraction occurs where a soil layer of low wave velocity underlies a soil layer of high wave velocity. In this circumstance, seismic refraction will fail to detect the underlying low velocity layer. In a seismic refraction survey, the depth of investigation depends on the spread of the geophone array and input energy. The geophone array spread is typically between four and five times the depth to the density contrast of interest, such as the top of the bedrock or the soil layer interface. Based on the typical energy sources used during the refraction test, the refraction survey is limited to mapping layers that occur at depths of less than 100 feet. If the seismic refraction survey is required for greater depth, then the geophone array spread is increased, but because of site dimension and input energy restriction, higher depth of investigation is not achieved. Recent advances in the inversion of seismic refraction data have made it possible to image relatively small targets such as foundation elements and to perform refraction profiling in the presence of localized low velocity zones such as developing sinkholes.

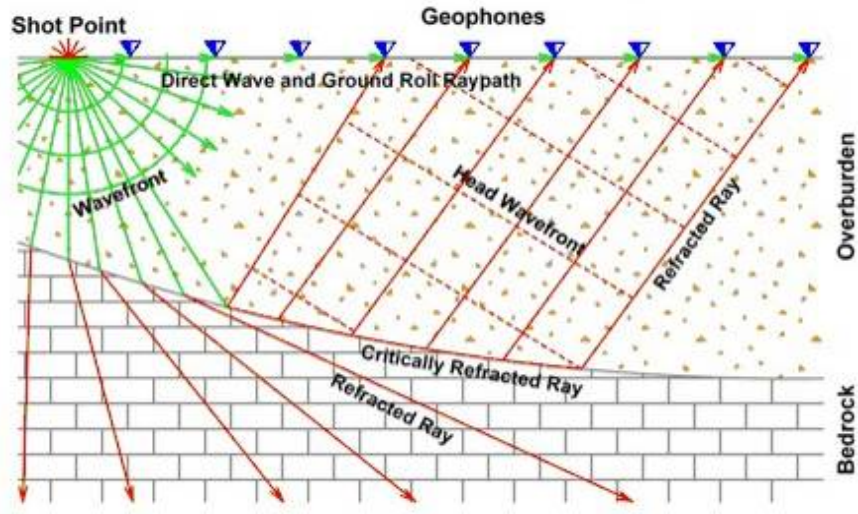


Figure 2.2. Seismic Refraction Geometry (Courtesy: Envirosan Inc.)

### 2.1.2.2 Reflection Method

The reflection survey requires the travel time measurement of the reflected seismic energy component of the P-wave from the desired subsurface density contrast, such as voids, layer interface, or bedrock (see Figure 2.3). The equipment used in seismic reflection surveys is similar to that used for seismic refraction, but field and data processing procedures employed in reflection methods are different. The reflection survey data processing procedures are intended to maximize the energy reflected along vertical ray paths by subsurface density contrast. In the reflection survey, the initial data at the geophones do not represent the reflected seismic energy. The reflected component of the seismic energy is identified by collecting and filtering multi-fold or highly redundant data from numerous shot points per geophone placement in a generally complex set of overlapping seismic arrival. The data and field processing for the reflection survey is highly complicated and requires more processing time than seismic refraction. The seismic reflection survey has several advantages over the seismic

refraction survey. The seismic reflection survey can be performed in the presence of low velocity zones or velocity inversions (low velocity layer under high velocity layer) and has better lateral resolution than seismic refraction. The main limitation of seismic reflection is the higher data processing cost compared to seismic refraction and the limitation in cutoff depths. At cutoff depths, reflections from subsurface density contrasts (bedrock, horizontal soil layer interfaces, voids, etc.) and the surface waves that carry most of the energy and air blast arrives approximately at the same time. Reflections from greater depths arrive at geophones after the surface waves and air blasts have passed, making these deeper subsurface density contrasts easier to detect and differentiate.

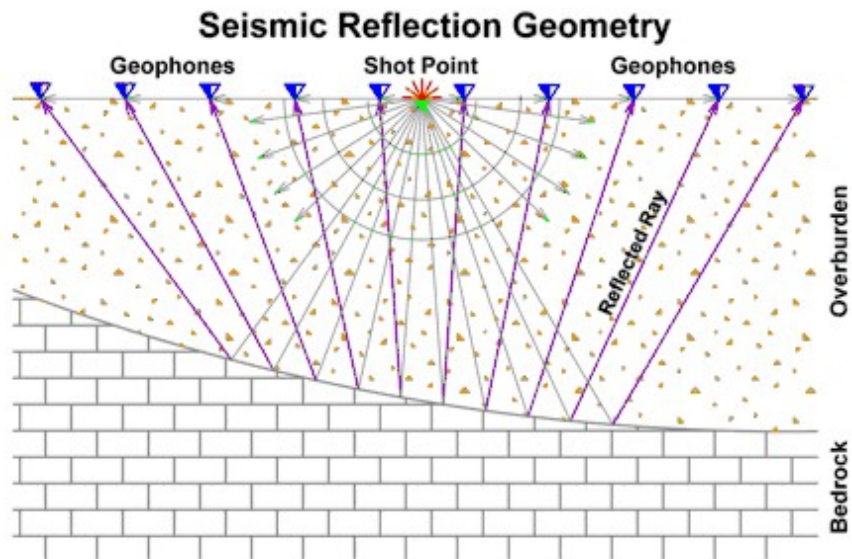


Figure 2.3. Seismic Reflection Geometry (Courtesy: Envirosan Inc.).

### 2.1.2.3 Surface Wave Methods

Surface waves are confined to a zone near the boundary of the half-space and carry a major portion of the input energy. If the material properties of the elastic media

are constant and independent of depth, then the surface wave velocity in the elastic media is constant and independent of frequency content of input excitation. However, if the properties of the elastic media are a function of depth, then surface wave velocity in the elastic media is the function of input excitation frequency content. This phenomenon is also known as dispersive behavior. All the techniques for processing surface wave data use this phenomenon to obtain information about the elastic properties of subsurface soil mass. The bulk of the surface wave energy is confined to a zone of the half-space about one wavelength deep related to the lowest excitation frequency. Therefore, the depth of investigation for surface wave methods is directly proportional to the longest wavelength or lowest frequency that can be analyzed. The depth of investigation is increased by increasing the wavelength of the input energy or lowering the frequency. In surface wave tests, an impact is used to deliver input energy. As the impact magnitude increases, a longer wavelength and increasing depth of investigation is possible; therefore, sledge hammers of different weights (for instance, 12 lb, 16 lb, or 20 lb) can be used to vary the depth of investigation.

## **2.2 Multichannel analysis of surface waves – General Information**

Multichannel analysis of surface waves (MASW) is an in-situ, non-intrusive seismic wave method to establish the shear wave velocity profile of subsurface soil media, allowing determination of the shear modulus of soil layers. Surface wave-based methods provide more accurate shear wave velocities of layered soil media than P or S wave-based methods (Turesson, 2007). This method utilizes dispersion characteristics of

stratified elastic soil media to determine the shear wave velocity profile of the soil media (Figure 2.4).

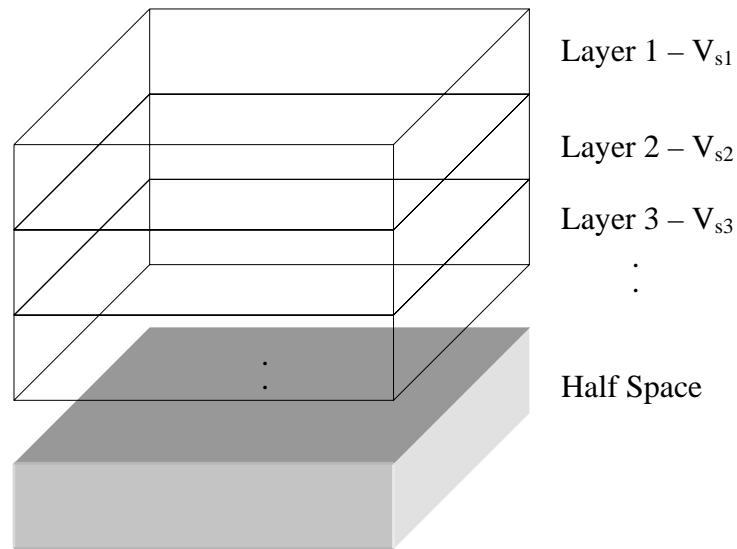


Figure 2.4. Layered  $V_s$  Profile.

In the MASW test (Stokoe, et. al., 1994), a series of vertical receivers is placed in a linear array on the ground surface to record vertical response at the surface created by an active source such as an impact hammer, vibrator, or any other source to produce energy. The response data are stored in a portable computer via a signal analyzer (Figure 2.5). Fourier transformation is then applied to convert the signal from the time to the frequency domain. From test measurements and Fourier analysis, phase velocities are calculated for each frequency and are plotted to obtain the experimental dispersion curve (Figure 2.6).

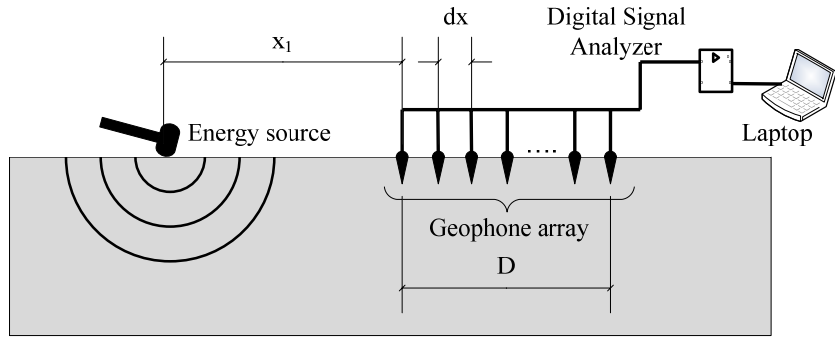


Figure 2.5. Test Setup.

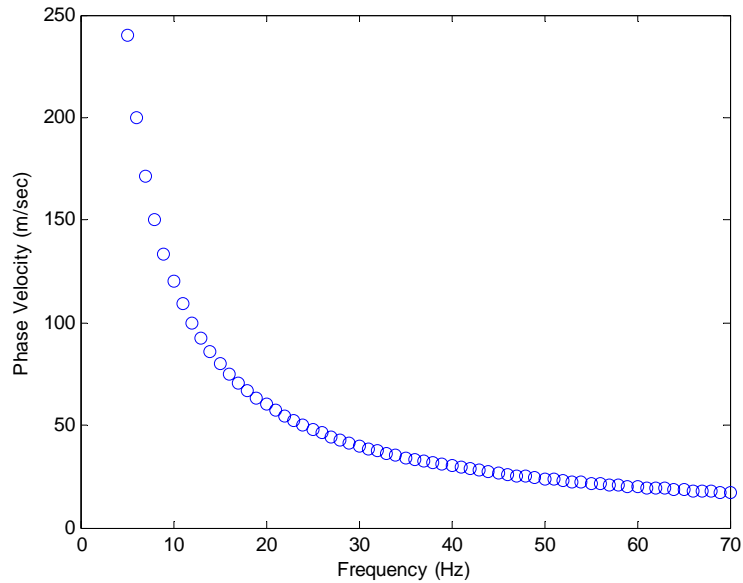


Figure 2.6. Dispersion Curve.

In the final step of MASW data processing, an inversion algorithm is utilized to construct the shear wave velocity profile under the geophone array from the information obtained from the experimental dispersion curve (Figure 2.7).

### 2.2.1 Forward and Inverse Modeling

Forward modeling is the process of predicting experimental or any measured data based on general principles of physics subjected to certain constraints and conditions (model parameters), whereas inverse modeling is the process of predicting model

parameters that are based on experiments or other measured data using general principles of physics. The forward problem associated with the MASW test consists of estimating the dispersion curve for a specific soil media consisting of certain specific model parameters using the principle of general wave-propagation theory, whereas inverse modeling deals with the estimation of model parameters that can explicitly define and represent soil media based on the experimental dispersion curve (Figure 2.7).

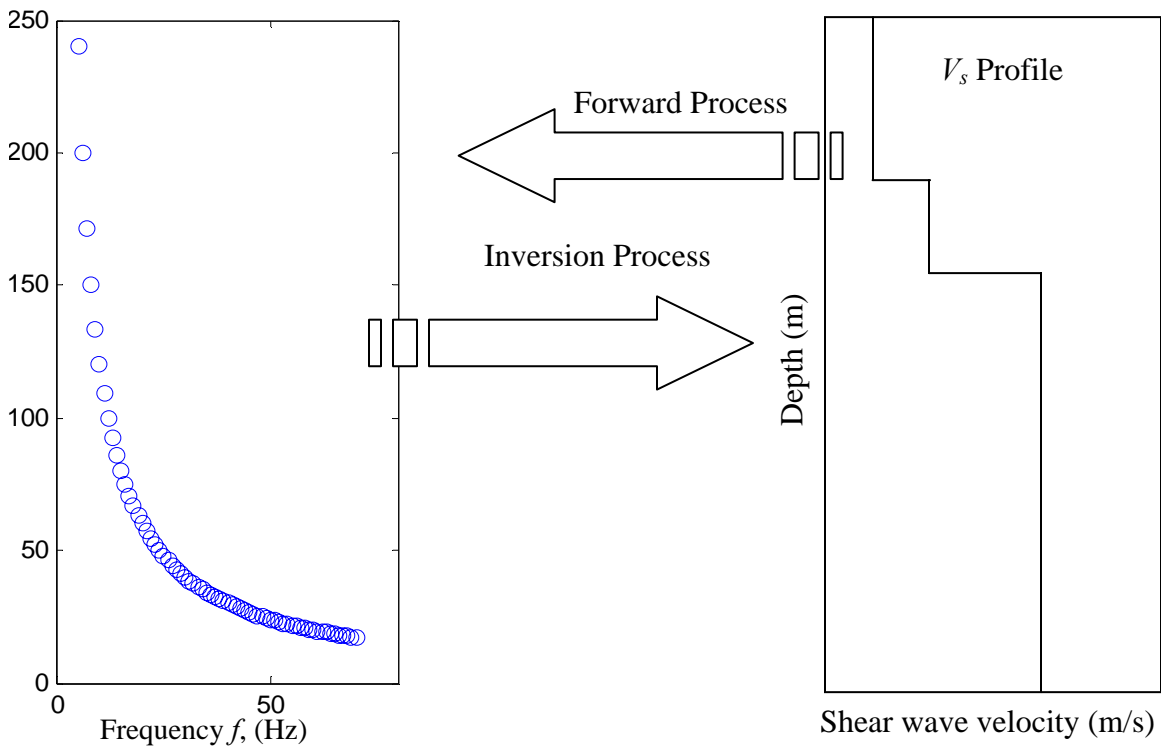


Figure 2.7. Forward and Inverse Problem Associated with MASW.

There are many algorithms currently available to solve the inverse problem associated with MASW. The simplest inversion algorithm consists of multiplying the phase velocities by the factor of 1.1 to construct a shear wave velocity profile from dispersion curve (Tokimatsu, 1995). Most of the inversion procedures are based on the general principle of wave propagation theory and are known as theoretical inversion. This

procedure tends to produce better results for a broader range of cases. There are two different approaches for theoretical inversion: (1) local search procedures (Tarantola, 1987; Menke, 1989) and (2) global search procedures (Tarantola, 1987; Sen and Stoffa, 1995).

Local search procedures are iterative. They require initial values for model parameters and minimize the error iteratively by finding the local minima in the neighborhood of the initial guess. In order to find the global minima, several iterations are run with different initial values of model parameters, and that solution is finalized, providing the minimum error. This procedure provides reasonable results in significantly less time if good initial estimates can be established for the model parameters.

Global search procedures look for the solution for model parameters randomly from a solution set, and each is then used for error calculation and minimization.

MASW includes a complex and highly non-linear inversion problem. In this case, application of global search procedures would take a significant amount of time and computing resources. Therefore, local search procedures are implemented with an appropriate initial guess of model parameters and constraints to arrive at a reasonable solution.

### **2.2.2 Analysis of Experimental Data**

The MASW method utilizes spectral analysis of the seismic wave dispersion phenomenon for shear velocity calculation. In the MASW test waves are generated by an impact source or steady state vibrator on the ground surface, and two or more vertical receivers are placed on the surface at fixed distances to collect the vertical response of the ground. In this section, the mathematics associated with MASW are explained with a

case of two receivers. The dynamic signal analyzer is used to record the signal in the real time domain  $x_1(t)$  and  $x_2(t)$  from the two receivers. The analyzer then converts these signals from the real time domain to the frequency domain  $X_1(f)$  and  $X_2(f)$ , and the cross-power spectrum ( $G_{X_1X_2}$ ) and coherence function ( $\gamma^2$ ) are calculated between them (Stokoe et.al [1994]). They are defined as follows:

$$\begin{aligned}
 G_{X_1X_2} &= X_1^*(f) X_2(f) \\
 G_{X_1X_1} &= X_1^*(f) X_1(f) \\
 G_{X_2X_2} &= X_2^*(f) X_2(f)
 \end{aligned} \tag{2}$$

where  $G_{X_1X_1}$  = auto-power spectrum of  $X_1(f)$ ,  $G_{X_2X_2}$  = auto-power spectrum of  $X_2(f)$ , and (\*) represents the complex conjugate of the quantity. The phase of the cross-power spectrum is defined as:

$$\phi(f) = \arctan\left(\frac{\text{Im}(G_{X_1X_2})}{\text{Re}(G_{X_1X_2})}\right) \tag{3}$$

The phase of the cross-power spectrum is also the phase difference between the two signals from two adjacent receivers. This phase difference is then used to determine the phase velocities for each frequency from the following relations:

$$\begin{aligned}
 t(f) &= \frac{\phi(f)}{2\pi f} \\
 V_R(f) &= \frac{D}{t(f)}
 \end{aligned} \tag{4}$$

where  $t(f)$  = time delay between the receivers,  $V_R$  = surface wave phase velocity, and  $D$  = distance between the two receivers. Phase velocities are then calculated against frequency to plot the experimental dispersion curve.

### **2.3 Applicability of MASW in Void/Sinkhole Detection**

Detection of obstacles, voids, cavities, or various types of utilities is required for planning and designing of foundations, to locate utility conduit before an excavation, or to examine the presence of abandoned mines. As discussed in Chapter 1, many techniques, such as ground penetrating radar, microgravity, electrical resistivity measurement, seismic wave refraction, and the reflection method have been used for void detection (Dobecki and Upchurch, 2006).

Seismic wave methods such as MASW have received attention because of the simple test procedure and relatively easy data analysis procedure. Seismic wave methods utilize wave propagation principles for elastic solids to study surface wave phenomena in stratified elastic media. Elastic waves carry significant information about the medium in which they travel like medium stiffness, elastic modulus, and Poisson's ratio, presence of anomalies like voids and cracks, which can be retrieved by wave propagation-based techniques, and are generally non-destructive (Richart, et.al, 1970). Seismic methods include both body and surface wave evaluation, which are based on spectral analysis and travel time-based techniques. In spectral analysis, data from receivers are analyzed in frequency domain, whereas in travel time-based techniques, arrival time of reflected and refracted waves from the layer interface or from any anomaly is measured at the

receivers. Therefore, travel time-based techniques can be used to detect anomalies such as subsurface voids and strata interfaces.

MASW is a micro-seismic method which uses properties of surface waves to study the material properties of stratified soil media. Past research has investigated the use of MASW to detect subsurface voids. The MASW method utilizes arrival time measurement of surface waves refracted from various interfaces of soil strata. Presence of any cavities or anomalies near the surface tends to increase arrival time, and thus voids can be detected using this phenomenon (Cooper and Ballard, 1988), but MASW may fail to detect soil or water filled cavities and rigid obstacles. MASW is also limited in the case of stratified soil profiles since the method cannot differentiate between signals arriving from an anomaly versus reflections from different layers of soil media (Belesky and Hardy, 1986).

Seismic surface methods like MASW have been proven both experimentally and via mathematical modeling to be effective in detecting near surface anomalies (Dravinski, 1983; Curro, 1983). The presence of voids or any other obstacle tends to influence amplitude of surface waves more than its arrival time. Thus, analyzing the signal in the frequency domain will be more effective than analyzing the signal in only the time domain. Cavity locations are determined by examining the attenuation of signal amplitude over time and distance (Belesky and Hardy, 1986). Discontinuities such as voids, rigid obstacles, or horizontal layers of soil in the wave path tend to produce fluctuations in the dispersion curve due to reflection of surface waves from these discontinuities (Gucunski, 1996). Thus, this phenomenon was examined to detect underground obstacles (Ganji, et. al., 1997).

The spectral analysis of MASW test data lack the information of spectrum variation in the time domain because of presence of cavities and layers of soil media. The travel time-based method, which is generally used in the case of reflection of seismic waves, does not supply any information regarding change in frequency content. However, if the data are analyzed in both the time and frequency domain, the waves reflected from anomalies can be taken into account. Gukunski, et. al., (2005) used wavelet transform to analyze data from finite element simulations of SASW tests in half-space to construct wavelet time-frequency maps. The researchers successfully detected the size, shape, and location of obstacles placed near the surface and proposed a void detection scheme based on the results.

## **2.4 Sinkhole Remediation**

If a sinkhole is detected by one of the methods discussed in the previous sections, considerable time may be available to evaluate remediation options. At other times, a sinkhole opens up, posing an immediate threat to public safety. In the case of the present study for PennDOT, the emergency response of interest will typically involve a sinkhole that has taken in a portion of a road or bridge or is encroaching on the structure.

Pennsylvania does not have a state agency division dealing with response, investigation, and remediation of sinkholes. The Pennsylvania Department of Environmental

Protection (PADEP) formed a committee to address this problem by compiling how different branches of PADEP and other state agencies address sinkholes (Hill, 2005).

The long-term goal for this committee is to develop a comprehensive policy regarding sinkhole prevention and response. While each site has specific conditions that need to be

addressed, guidance can be given in relation to specific variables (such as quarry dewatering, urbanization effects, vast swings from drought to heavy rainfall, etc.). In general, techniques for remediation include filling with rock and clay, grouting, and/or underpinning. The process order, gradation of fill material, and many other factors differ depending on the site characteristics.

Rapid response protocol was developed with PADEP during handling of several active sinkhole areas in Northampton County. This protocol includes a distinction of methods for remediation of sinkholes on land away from drainage areas and those in areas that receive drainage. These protocols are a good start for the types of documents needed but do not provide a comprehensive guide.

Funding is a critical issue for repairs, particularly in an emergency situation. No source of money is currently designated for emergency repairs. This must be addressed in order to effectively utilize any comprehensive remediation guide that is completed by PADEP.

## **Chapter 3 – Equipment and Software**

### **3.1 Introduction**

Seismic refraction surveys such as the MASW method require specialized electronic data acquisition and instrumentation that is common to seismic ground motion testing equipment. In addition, specialized data processing software is needed to process the acquired data. Each component of the equipment and each of the commercially available software packages used in this research is described in detail in this chapter. The data acquisition setup requires a portable computer, a signal analyzer, and a number of horizontal and vertical geophones. The software consists of SignalCalc for data acquisition and SeisImager2D and SurfSeis for data processing.

### **3.2 Data Acquisition System**

#### **3.2.1 Signal Analyzer**

An Agilent Technologies™ VXI mainframe E8408A signal analyzer from Data Physics was used in the present study (see Figure 3.1). This signal analyzer is a 4-slot, C-size mainframe that contains a one-slot E8491B with an IEEE-1394 PC Link, message-based VXI module. This module allows a direct connection from the portable computer to the VXI mainframe via standard IEEE-1394 bus. Contained in the VXI mainframe are two Agilent E1433B, 8 channel, 196 Ksa/sec digitizers plus DSP. The E1433B is a single slot, C-size, register-based VXI module that includes DSP, transducer signal conditioning, alias protection, digitization, and high-speed measurement computation. The general configuration for the test setup is shown in Figure 3.2.



Figure 3.1. Signal Analyzer.

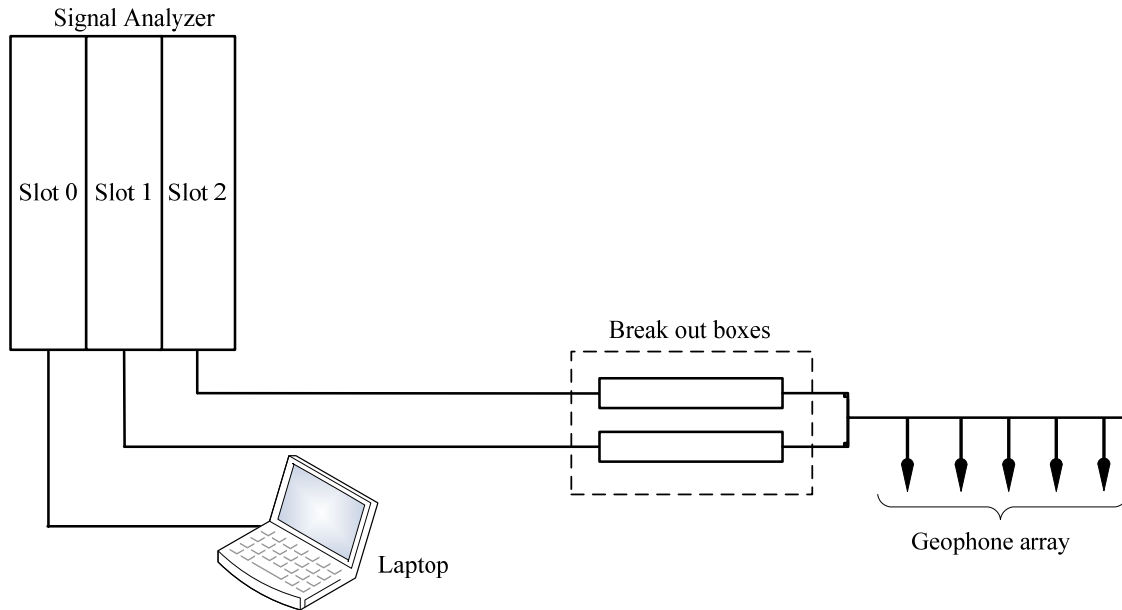


Figure 3.2. General Layout of the Test Setup.

The portable computer used for data acquisition and data processing is a standard notebook PC with the minimum specifications presented in Table 3.1.

Table 3.1 Portable Computer Specifications.

Specifications	Value
Model	Dell Inspiron 8000
Random access memory	256 MB
Hard disk capacity	20 GB
Processor	Intel Pentium
Operating system	Microsoft Windows 2000

### 3.2.2 Geophones

Geophones are highly sensitive instruments used to measure ground motions generated by ground disturbances. A geophone consists of a spring supported coil surrounded by a permanent magnet. When the geophone case is excited, the magnet mass, due to inertia effects, tends to remain at rest. The relative motion between the coil

and the magnet generates direct current in the coil due to magnetic induction as it moves through the magnetic field. The current is directly proportional to the velocity of motion. This direct current is measured and recorded using a digital signal analyzer.

In the present study, Gisco™ SN4 digital grade geophones were used (Figure 3.3). These are high sensitivity, low frequency geophones that are widely used in seismic tests. Both vertical and horizontal geophones are used to capture the response of ground particles for vertical and shear impact. A vertical impact is used for the P-wave refraction survey, and a shear impact result is used for the shear wave survey. The results from both tests are combined to determine the properties of the subsurface soil.. The technical specifications of these geophones are presented in Table 3.2. As the number of geophones is increased, the time required to acquire data in the field is reduced.

Table 3.2. SN4- 4.5 Hz Digital Grade Geophone Specifications.

<b>Specifications</b>	<b>Value</b>	<b>Tolerances</b>
Natural frequency	4.5 Hz $\pm$ 0.5 Hz	Max tilt angle 25 <sup>0</sup>
Coil frequency	375 $\Omega$	$\pm$ 5%
Open circuit damping	0.60	$\pm$ 10%
Sensitivity	28.8 v/m/s	$\pm$ 10%
Distortion	<0.3%	
Maximum coil excursion	4.0 mm	
Moving mass	11.30 mg	
Diameter	26.0 mm	
Height	37.0 mm	
Weight	77.0 g	
Operating temp. range	-40 <sup>0</sup> C to + 100 <sup>0</sup> C	



Figure 3.3. Horizontal and Vertical Geophones.

### 3.2.3 Energy Source

There are many different types of energy sources used to generate waves in a soil mass. Methods include: 1) a sledge hammer of varying weights, typically used in traditional MASW tests; 2) a heavy drop weight, able to generate lower frequency (high wavelength) surface waves; 3) a steady-state vibrator to generate single frequency waves; and 4) a shear wave device as shown in Figure 3.4.

The impact energy sources strike either a metallic or rubber plate that serves to engage the soil mass at the impact point and distribute the energy in order to create a body wave rather than localized distorted energy.

In a steady state survey, seismic waves of single frequency are generated by vertically oscillating vibrator. The displaced shape of the ground due to steady state vibration can be approximated by a sine curve that is captured by the array of vertical geophones. The wave length of a Raleigh wave can easily be estimated as the distance between two successive troughs and peaks. Once the wavelength is calculated, the velocity of the surface waves (approximately equal to shear wave velocity) is computed using basic wave mechanics. This shear velocity represents the average property of the

subsurface zone with a depth equivalent to the half wavelength of surface waves. By decreasing the frequency, the wavelength can be increased, thus increasing the depth of the survey. For a homogenous, isotropic, elastic half-space, the shear wave velocity is independent of depth, but for elastic half-space whose properties vary with depth, it is an effective method for finding the shear wave velocity distribution along depth.

A shear wave device is used to create horizontal disturbance in the ground for SH-wave survey. The shear wave device is a stiffened rectangular steel box of dimension 24 in by 6 in by 6 in, with triangular spikes at the bottom to fix the box rigidly to the ground as shown in Fig 3.4. Rubber pads are placed on either side of the box to dampen the sound from the impact of the hammer. To generate shear waves, the box is hit with a sledge hammer on its side; this results in horizontal movement of ground particles, thus creating a shear wave.



Figure 3.4. Shear Wave Device.

### 3.3 Software

#### 3.3.1 Data Acquisition

Signal Calc<sup>®</sup> 620 Dynamic Signal Analyzer was used as interface software between the signal analyzer and the portable computer. This software was developed by

Data Physics Corporation and is the part of the data physics signal analyzer equipment. Signal Calc<sup>®</sup> 620 can interface an unlimited number of input channels and can perform Fourier transform, real time order analysis, real time octave analysis, modal testing, amplitude domain measurements like histograms, probability density plots, modal testing, disk record and playback, and waterfall and spectrograms construction.

### **3.3.2 Data Processing**

#### **3.3.2.1 SeisImager2D Refraction Package**

SeisImager<sup>®</sup>2D is the data processing software from Geometrics, Inc., San Jose, CA, for analyzing data of refraction tests. SeisImager<sup>®</sup>2D can perform comprehensive refraction modeling using ray tracing for both P-wave and SH-wave refraction survey. It can perform comprehensive refraction modeling using ray tracing and includes three methods for refraction data analysis: 1) quick-look time-term inversion; 2) the reciprocal method; 3) tomography.

#### **3.3.2.2 SurfSeis 2.0**

SurfSeis 2.0 is the seismic-data processing software for shear-wave velocity profiling of subsurface soil. It can perform data processing for both active and passive MASW tests. SurfSeis 2.0 takes the seismic data obtained from active or passive tests, extracts Rayleigh surface waves from the data, and then uses surface wave information as an input to produce 1-D or 2-D shear velocity profiles through several steps: (1) Processing for dispersion image data, (2) Extraction of modal dispersion curve, (3) Inversion of the dispersion curve to construct 1-D shear velocity profile, and (4) construction of 2-D shear wave velocity profile from several 1-D shear wave velocity profiles.

A more detailed discussion of the data processing for the project is presented in Chapter 5.

## Chapter 4 – Test Setup and Procedure

### 4.1 Introduction

Multichannel analysis of surface waves (MASW) and refraction survey test setups require a well-planned instrumentation placement procedure and testing procedure. This chapter provides a detailed description of the test design and procedures for both methods of subsurface investigations. Both micro seismic wave tests are able to utilize the same test setup which significantly reduces the data collection effort for the two methods.

### 4.2 Multi-channel Analysis of Surface Waves (MASW)

Multi-channel analysis of surface waves (MASW) utilizes the properties of surface waves for subsurface tomography. Surface waves are confined to a zone near the boundary of the half-space, and they carry a major portion of the input energy. This method utilizes dispersion characteristics of stratified soil media, i.e., surface wave travel with different velocities in different layers of soil, to determine shear wave velocity of layered soil media. A generalized test setup schematic is presented in Figure 4.1. The general test setup consists of a geophone array, an energy source to produce waves, digital signal analyzer to record signals from the geophones, and a portable computer for data storage and processing. The test setup is explained in detail in the following sections:

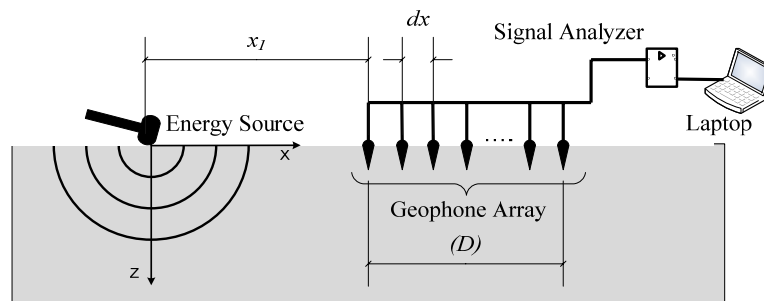


Figure 4.1. MASW Test Setup.

### 4.2.1 Field Test Setup

A MASW field test setup consists of a geophone array configuration and an energy source and location. The receiver-array dimension  $D$  is proportional to the longest wavelength that can be analyzed and thus is related to the maximum depth of investigation  $z_{max}$ , whereas geophone spacing  $dx$  is proportional to the shortest wavelength that can be analyzed and thus is related to the minimum depth of investigation and resolution of velocity profile.

An impact is used to deliver input energy. As the impact magnitude increases, a longer wavelength and increasing depth of investigation is possible; therefore, sledge hammers of different weights (12 lb, 16 lb, or 20 lb) are used to vary the depth of investigation. A steel impact plate (Figure 4.2) distributes the energy from the sledge hammer, reducing the penetration of the hammer into the soil, thus dispersing the impact energy smoothly into the ground.



Figure 4.2. Steel Impact Plate.

The distance between the first geophone and the source,  $x_1$ , controls the contamination from the near field effects. Generally, the source offset is maintained at approximately 20 percent of the receiver-array dimension,  $D$ .  $D$  varies with site conditions and other parameters such as number of channels, number of geophones, and

depth of investigation. The source offset should be increased in regular increments and data collected for each source location. The source offset that generates data providing the maximum energy distribution in the fundamental mode with minimized near field effects is accepted for the subsequent testing and analysis.

#### **4.2.2 Interval of Source-Receiver Configuration (SRC) Movement**

In MASW, one test with a single geophone array provides the wave velocity profile of the middle section of that array. Therefore, testing of a single array provides the wave velocity profile a distance equal to one-half  $D$  from the first geophone. To construct a two-dimensional velocity profile of the subsurface section under the geophone array, the entire source-receiver configuration is moved along the array by the distance  $ndx$  where  $n$  is generally taken between 1 and 4. From each source-receiver configuration movement, a one-dimensional wave profile under the midsection of each array is generated. Finally, wave velocity in the space between each section is interpolated to construct a 2-D velocity profile.

Where a testing site is located near significant vehicular traffic, particularly trucks, or other interference, the collected signals may be contaminated, either by energy generated by traffic or electrical interference. To reduce the signal contamination at each source location, three to four data records are stacked, or superimposed. If the contamination is invariant, then the contamination may be due to a localized electrical or other continuous frequency source. If the contamination can be confidently identified, then the noise is removed using a banded filter during the data processing.

### 4.2.3 Data Acquisition Parameters

Data acquisition parameters include sampling duration and frequency. The sampling time for MASW tests is usually established between 10 and 12 seconds so that enough data are collected for the best spectral resolution during Fourier transformation. Sampling frequency for MASW test is typically between 500 and 1000 samples/sec. If the sampling rate is too high, the data file size will be large, and unnecessary higher modes will be captured that are not required for the data processing.

### 4.2.4 Test Procedure

The MASW test is explained step by step in this section. The MASW test procedure consists of four main steps:

**Step 1:** Arrange the geophones in a linear array and place the energy source at  $x_1$  distance from the first geophone.

**Step 2:** Generate waves by making an impact at the energy source location.

**Step 3:** Collect the data using a digital signal analyzer.

**Step 4:** Move the whole configuration by some distance along the longitudinal direction of the array, and repeat steps 1 to 3.

## 4.3 Refraction Survey

A refraction survey utilizes the properties of body waves (compression and shear waves) for subsurface profiling. There are two types of refraction surveys based on the type of body wave used in the analysis: P-wave refraction and SH-wave refraction. Both types of refraction surveys are explained in the following sections:

### 4.3.1 P-wave Refraction Survey

P-wave refraction survey utilizes a compression wave to survey the site. P-wave refraction requires measurement of the seismic energy component travel time where the P-wave travels down to the top of rock (or other distinct density contrast), is refracted along the top of rock, and returns to the surface as a head wave along a wave front (Figure 4.3). During the data processing, the wave path can be traced from the energy source to all geophones. Regions of low wave velocity can be identified with P-wave refraction because the wave will take the path of least resistance (regions with high wave velocity). Thus, the regions where no or very few wave paths are present are potentially the low velocity regions or voids.

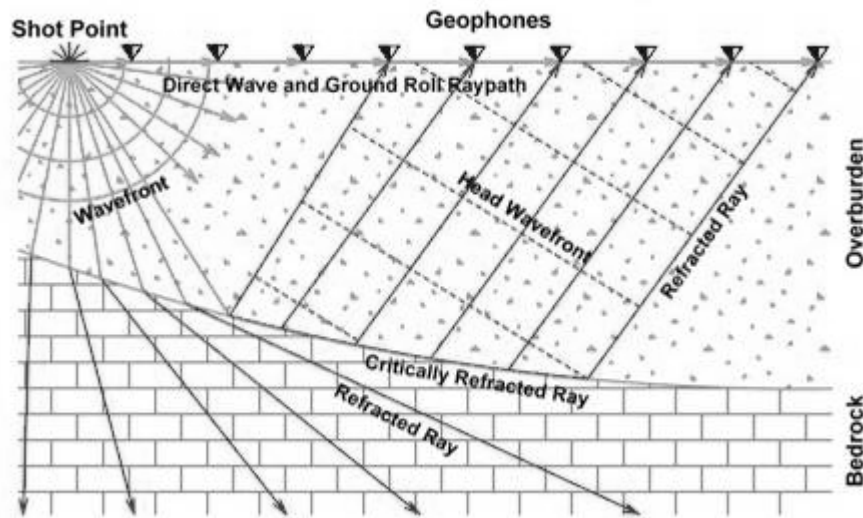


Figure 4.3. Seismic Refraction Geometry (Courtesy: Envirosan, Inc).

The major advantage of P-wave refraction is that the procedure is time efficient and returns the velocity profile underneath the whole array of geophones in one setup; thus more area can be covered in less time. The other advantage of this P-wave refraction is that no separate setup is necessary for this method; it can be completed with the same instrument setup used for an SH-wave survey and MASW.

The major disadvantage of P-wave refraction occurs where a soil layer of low wave velocity underlies a soil layer of high wave velocity. In this circumstance, P-wave refraction will fail to detect the underlying low velocity layer. Another disadvantage is that the resolution depends largely on the number of geophones in an array; therefore, P-wave refraction should be conducted with a large number of channels.

#### **4.3.1.1 P-Wave Refraction Test Procedure**

The P-wave refraction test procedure is explained step by step in this section and consists of the same setup as the MASW test. The P-wave refraction test procedure consists of three main steps:

**Step 1:** Position a linear array of geophones with periodic spacing (see Figure 4.4). The determination of spacing depends on the number of geophones, extent of region to be surveyed, and desired velocity profile resolution.

**Step 2:** After the geophone array is positioned, the energy source is positioned at points along the array with some initial offset and is continued along the array line with some final offset (see Figure 4.5).

**Step 3:** Collect the data using a digital signal analyzer.

**Step 4:** Move the whole configuration by one Geophone Array spread  $D$  along the longitudinal direction of the array and repeat steps 1 to 3.



Figure 4.4. Geophone Array Setup.

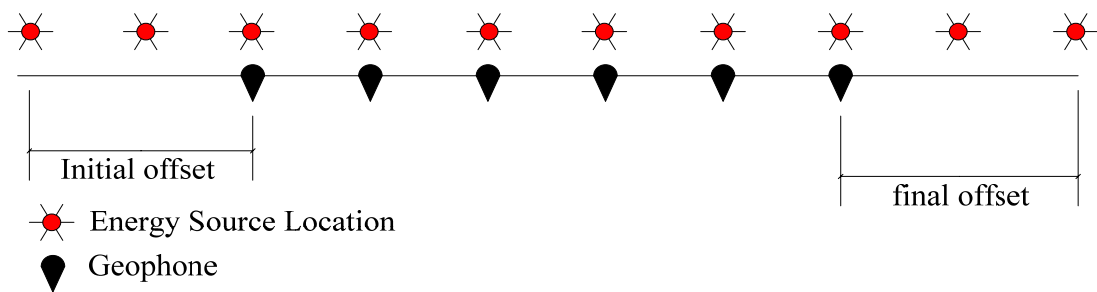
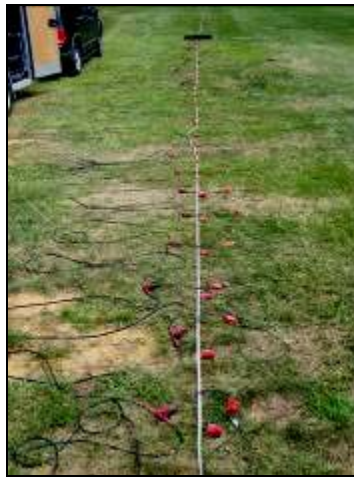


Figure 4.5. Refraction Test Procedure.

### 4.3.2 SH-Wave Refraction Survey

SH-wave refraction survey utilizes Love waves (surface shear waves) to survey the site. The same data acquisition equipment, data processing, and field geometry parameters as the P-wave refraction survey are used for the SH-Wave Refraction survey. In an SH-wave refraction survey, horizontal geophones are used instead of vertical

geophones for measuring the horizontal response of the ground (Figure 4.6). The SH-wave refraction test provides the shear wave velocity profile of the region under consideration. By combining the results of the P-wave refraction test and the SH-wave refraction tests, all important properties of subsurface soil can be determined.



(a) Horizontal Geophone Array Setup.

(b) Generation of Shear Waves.

Figure 4.6. SH-Wave Refraction Survey.



(c) Shear Wave Generating Device.

Figure 4.6. SH-Wave Refraction Survey (continued).

### 4.3.3 Data Acquisition Parameters

Refraction test acquisition parameters include sampling duration and frequency. The sampling time for the refraction test is typically kept between three to four seconds. This sampling time is sufficient to obtain the first breaks in the signals required for refraction analysis. The sampling frequency for a refraction survey is typically between 900 and 1200 samples/second to achieve a high time resolution, and the signal's first breaks are precisely selected.

### 4.4 Summary

This chapter summarizes the detailed test setup description and procedures for the MASW method and the refraction and reflection surveys. The procedure for micro-seismic wave tests is straightforward but requires a carefully planned procedure. All three micro-seismic wave tests are able to utilize the same test setup, which significantly reduces the data collection effort. Organized file management during testing is critical.

## Chapter 5 – Data Processing

### 5.1 Introduction

This research project requires the use of three proprietary, commercially available software packages. SignalCalc<sup>®</sup> 620 interfaces between the computer and the signal analyzer during field data collection. Surfseis<sup>®</sup> 2.0 and Seisimager<sup>®</sup> 2D process the field data for interpretation. Surfseis<sup>®</sup> 2.0 is used to process data for surface wave tests, and Seisimager<sup>®</sup> 2D is used to process refraction survey data. The use of this software for data analysis is discussed in detail in this chapter.

### 5.2 SignalCalc<sup>®</sup> 620

SignalCalc<sup>®</sup> 620 Dynamic Signal Analyzer is the interface software for the high-speed, industry standard HP VXI digital signal processing hardware and was developed by Data Physics Corporation. This software can interface with an unlimited number of input channels and can perform Fourier transforms, real-time order analysis, real-time octave analysis, modal testing, amplitude domain measurements like histograms, probability density plots, modal testing, disk record and playback, and waterfall and spectrogram construction. A step-by-step data acquisition procedure is detailed in this section.

#### 5.2.1 Step 1: Start New Test

Before starting a new test, all connections between the signal analyzer and the computer must be completed. To start a new test, turn on the VXI instrument and boot up the computer. When the computer is properly booted, refresh the VXI resource manager by clicking the icon *IO Control* on the task bar (Figure 5.1). This will confirm that a

proper connection is established between the VXI hardware and computer. Next, start the “Soft Front Panel” from Windows: *start* → *all programs* → *vxipnp* → *VT1432 – 36 SFP*. This step initializes the VXI hardware. Start the Signalcalc® 620 software and configure the hardware by selecting “Configure Hardware” from the pull-down menu (see Figure 5.2). This initializes and configures the VXI hardware for a new test using Signalcalc® 620. Click on the “New” button or select “Test → New” from the menu bar. A dialog box as shown in Figure 5.3 will open. Select the appropriate test type. Signalcalc® 620 will automatically set the default parameters for that test type. The default parameters for the tests are stored in the ‘Default.620’ folder within the main SignalCalc folder.

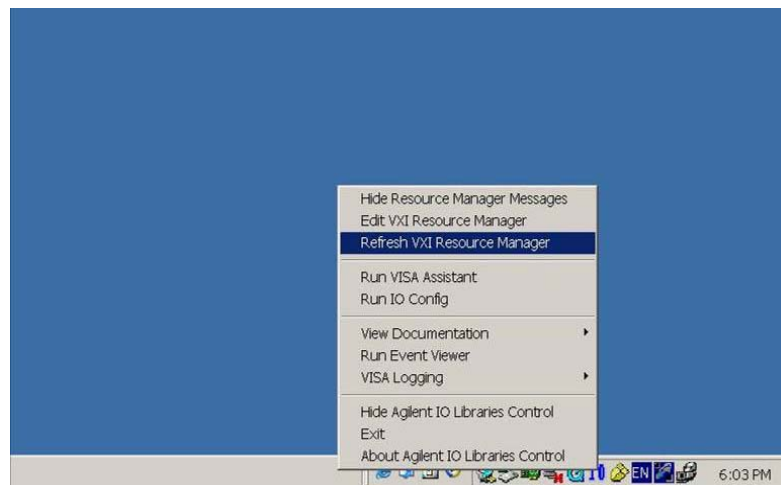


Figure 5.1. Refresh VXI Resource Manager.

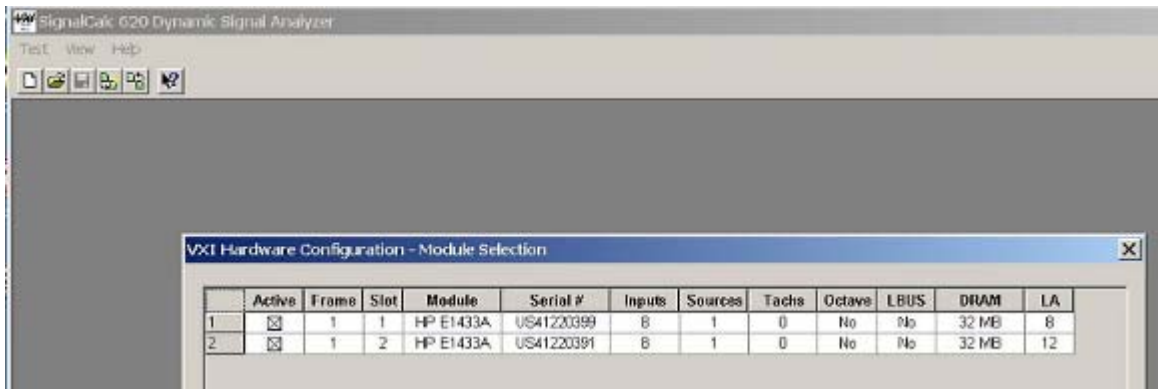


Figure 5.2. SignalCalc® 620 Configure Hardware Dialog Box.

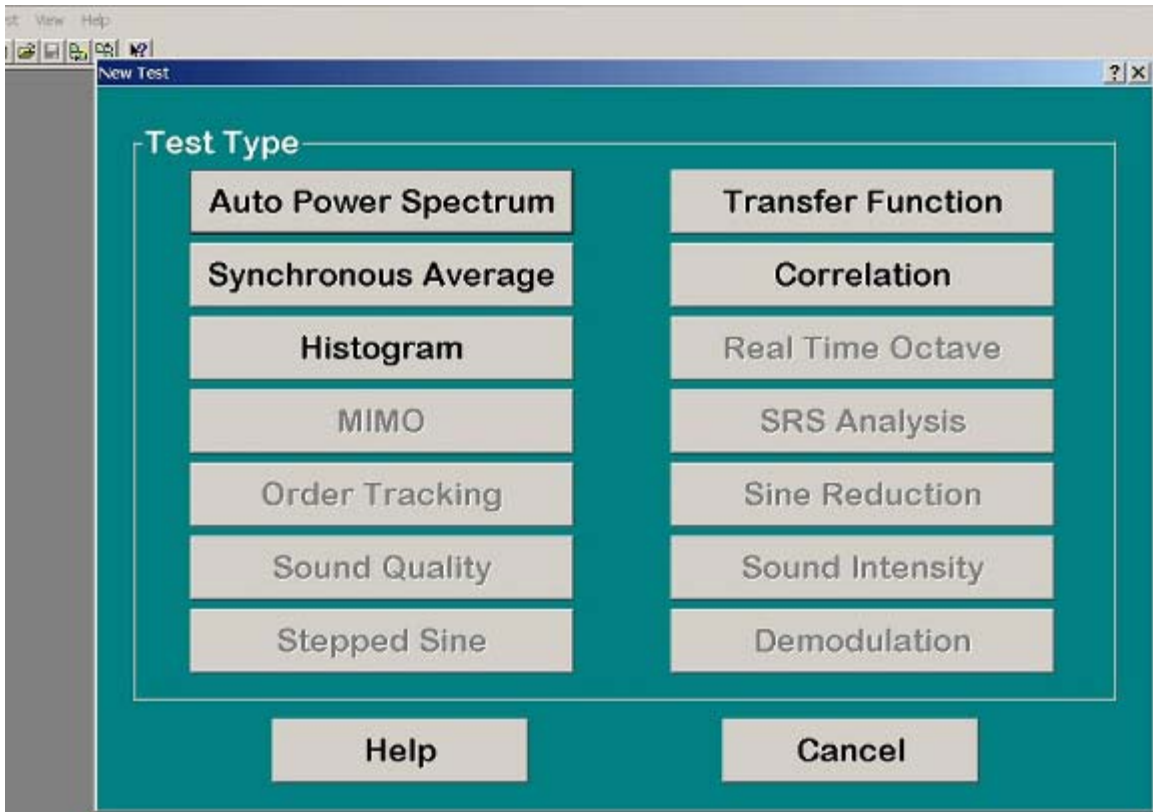


Figure 5.3. SignalCalc® 620 Start New Test Dialog Box.

### 5.2.2 Step 2: Setting the Input Channel Control Parameters

Input channel control settings adjust the various parameters associated with data acquisition that are explained later in this chapter. For setting the input channel control parameters, click on the “View → channels” from the main menu bar. A dialogue box as shown in Figure 5.4 will appear. The input channel parameters are controlled by six tabs: “Front End,” “Measurement,” “Info,” “Trigger,” “Signal Conditioning,” and “Comment” as shown in the dialogue box (Figure 5.4).

The “Front End” tab as shown in Figure 5.4 is used to activate or deactivate the channel, setting the full-scale input range, the AC or DC coupling of each channel, and the sensitivity of the sensor feeding the channel.

Ch#	Active	Range (EU)	mV/EU	EU	Coupling	HPF (Hz)	DC Offset(V)
1	<input checked="" type="checkbox"/>	1.000	1.000 K	V	DC	1.000	0.000
2	<input checked="" type="checkbox"/>	1.000	1.000 K	V	DC	1.000	0.000
3	<input checked="" type="checkbox"/>	1.000	1.000 K	V	DC	1.000	0.000
4	<input checked="" type="checkbox"/>	1.000	1.000 K	V	DC	1.000	0.000
5	<input checked="" type="checkbox"/>	1.000	1.000 K	V	DC	1.000	0.000
6	<input checked="" type="checkbox"/>	1.000	1.000 K	V	DC	1.000	0.000
7	<input checked="" type="checkbox"/>	1.000	1.000 K	V	DC	1.000	0.000
8	<input checked="" type="checkbox"/>	1.000	1.000 K	V	DC	1.000	0.000
9	<input checked="" type="checkbox"/>	1.000	1.000 K	V	DC	1.000	0.000
10	<input checked="" type="checkbox"/>	1.000	1.000 K	V	DC	1.000	0.000
11	<input checked="" type="checkbox"/>	1.000	1.000 K	V	DC	1.000	0.000
12	<input checked="" type="checkbox"/>	1.000	1.000 K	V	DC	1.000	0.000
13	<input checked="" type="checkbox"/>	1.000	1.000 K	V	DC	1.000	0.000
14	<input checked="" type="checkbox"/>	1.000	1.000 K	V	DC	1.000	0.000
15	<input checked="" type="checkbox"/>	1.000	1.000 K	V	DC	1.000	0.000
16	<input checked="" type="checkbox"/>	1.000	1.000 K	V	DC	1.000	0.000

Front End Measurement Info Trigger Signal Conditioning Cd  
View Active Input

Figure 5.4. SignalCalc<sup>®</sup> 620 Channel Control Box.

The “Measurement” tab shown in Figure 5.5 is used for modifying the signal processing parameters such as setting the reference channel, the “Window” or “Weighing Function” used in Fourier analysis, the “Autorange” option, and the “Input Wgt” that determines the frequency-dependent acoustic weighting applied to each channel.

The “Trigger” tab shown in Figure 5.6 is used for modifying the parameters associated with transient and signal-triggered analysis. This tab sets the channel as an active trigger source or selects the “Trigger Mode.” This tab is also utilized for setting the trigger slope and the delay between the recognition of the specified trigger conditions and the issuance of the trigger signal.

Channels			
Input		Generator	Tachometer
Ch#	Window	Autorange	
1	Hann	Up	
2	Hann	Up	
3	Hann	Up	
4	Hann	Up	
5	Hann	Up	
6	Hann	Up	
7	Hann	Up	
8	Hann	Up	
9	Hann	Up	
10	Hann	Up	
11	Hann	Up	
12	Hann	Up	
13	Hann	Up	
14	Hann	Up	
15	Hann	Up	
16	Hann	Up	

Front End \ Measurement \ Info \ Trigger \ Signal Conditioning \ Cd

iew Active Input

Figure 5.5. SignalCalc® 620 Measurement Tab.

Channels									
Input		Generator	Tachometer						
Ch#	Active	Mode	Slope	MaxVolts	Level-	Level+	Level Unit	Delay	
1	<input checked="" type="checkbox"/>	Level	Rising	1.000	25.000		%ADC	0.000	
2	<input type="checkbox"/>	Level	Rising	1.000	25.000		%ADC	0.000	
3	<input type="checkbox"/>	Level	Rising	1.000	25.000		%ADC	0.000	
4	<input type="checkbox"/>	Level	Rising	1.000	25.000		%ADC	0.000	
5	<input type="checkbox"/>	Level	Rising	1.000	25.000		%ADC	0.000	
6	<input type="checkbox"/>	Level	Rising	1.000	25.000		%ADC	0.000	
7	<input type="checkbox"/>	Level	Rising	1.000	25.000		%ADC	0.000	
8	<input type="checkbox"/>	Level	Rising	1.000	25.000		%ADC	0.000	
9	<input type="checkbox"/>	Level	Rising	1.000	25.000		%ADC	0.000	
10	<input type="checkbox"/>	Level	Rising	1.000	25.000		%ADC	0.000	
11	<input type="checkbox"/>	Level	Rising	1.000	25.000		%ADC	0.000	
12	<input type="checkbox"/>	Level	Rising	1.000	25.000		%ADC	0.000	
13	<input type="checkbox"/>	Level	Rising	1.000	25.000		%ADC	0.000	
14	<input type="checkbox"/>	Level	Rising	1.000	25.000		%ADC	0.000	
15	<input type="checkbox"/>	Level	Rising	1.000	25.000		%ADC	0.000	
16	<input type="checkbox"/>	Level	Rising	1.000	25.000		%ADC	0.000	

Front End \ Measurement \ Info \ **Trigger** \ Signal Conditioning \ Cd

iew Active Input

Figure 5.6. SignalCalc® 620 Trigger Tab.

The “Signal Conditioning” tab shown in Figure 5.7 controls the features of the various HP breakout boxes that are attached to the system. The “Comment” tab shown in Figure 5.8 is used to provide a typed description of each channel input.

Channels				
Input   Generator   Tachometer				
Ch#	Cond Type	Gain (dB)	LPF (Hz)	Connection
1	Direct	0.0	0.0	Ground
2	Direct	0.0	0.0	Ground
3	Direct	0.0	0.0	Ground
4	Direct	0.0	0.0	Ground
5	Direct	0.0	0.0	Ground
6	Direct	0.0	0.0	Ground
7	Direct	0.0	0.0	Ground
8	Direct	0.0	0.0	Ground
9	Direct	0.0	0.0	Ground
10	Direct	0.0	0.0	Ground
11	Direct	0.0	0.0	Ground
12	Direct	0.0	0.0	Ground
13	Direct	0.0	0.0	Ground
14	Direct	0.0	0.0	Ground
15	Direct	0.0	0.0	Ground
16	Direct	0.0	0.0	Ground

Front End | Measurement | Info | Trigger | **Signal Conditioning** | Cd

View Active Input

Figure 5.7. SignalCalc® 620 Signal Conditioning Tab.

Channels	
Input   Generator   Tachometer	
Ch#	Comments
1	Channel #1
2	Channel #2
3	Channel #3
4	Channel #4
5	Channel #5
6	Channel #6
7	Channel #7
8	Channel #8
9	Channel #9
10	Channel #10
11	Channel #11
12	Channel #12
13	Channel #13
14	Channel #14
15	Channel #15
16	Channel #16

Measurement | Info | Trigger | Signal Conditioning | **Comment** |

View Active Input

Figure 5.8. SignalCalc® 620 Comment Tab.

### 5.2.3 Step 3: Setting the Sampling Parameters

The “Sampling Parameters” window shown in Figure 5.9 sets the time/frequency span and resolution of analysis. The sampling frequency and data collection time can be adjusted through “Sampling Parameters.” This window provides the option for either time domain or frequency domain. The controls can be switched between frequency domain and time domain parameters using the  $F$  and  $T$  radio buttons in the window. If  $F$  is selected, the slider controls the frequency domain parameter ( $Fspan$  and  $Lines$ ), and when  $T$  is selected, the slider controls the time domain parameters ( $Tspan$  and  $Blocksize$ ).  $Fspan$  is the upper frequency of all computed spectra and is equal to the product of  $Lines$  and  $df$ , where  $df$  is the nominal frequency resolution.  $Tspan$  is the time duration for each capture or acquisition, which is equal to the product of  $Blocksize$  and  $dt$ , where  $dt$  is the time resolution.

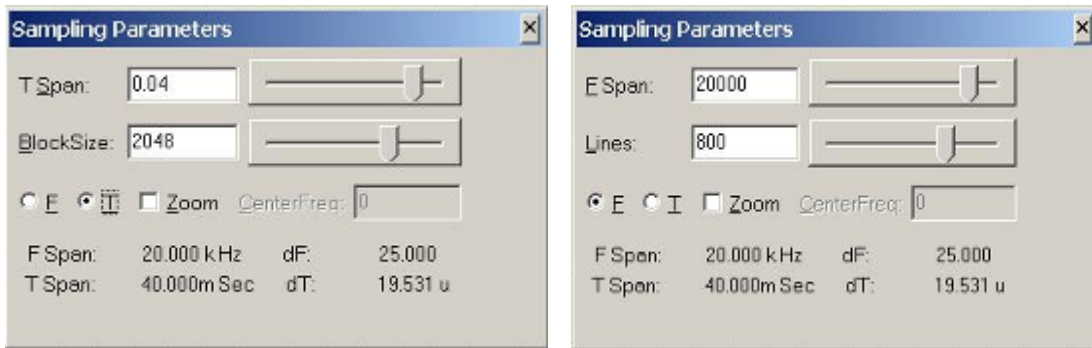


Figure 5.9. SignalCalc<sup>®</sup>620 Sampling Parameters Window.

### 5.2.4 Step 4: Setting the Measurement Parameters

The “Measuring Parameters” window shown in Figure 5.10 is used to control four basic aspects of signal processing: 1) trigger, 2) averaging, 3) autoranging, and 4) pacing.

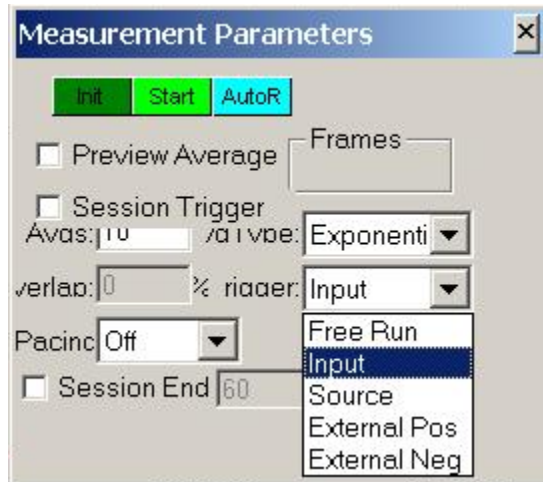


Figure 5.10. SignalCalc® 620 Measurement Parameters Window.

The “Trigger” pull-down menu is used to define the trigger source and enable the trigger operation. There are three choices available to set the trigger:

1) FreeRun. This option is used to collect data continuously as soon as the test is started without waiting for a trigger signal;

2) Input. This option causes the system to wait for the input signal trigger conditions to be satisfied as specified in the “Trigger” tab of the “Input Channels” dialogue box. This option is generally used for all transient analysis and synchronous average tests; and

3) Source. This option is generally used in the experiments with pseudo-random, burst random, thump signals. When the trigger option is set at “Source,” the start of each acquisition is synchronized with a signal.

The “Session Trigger” check box is used to modify the use of the trigger. If this check box is enabled, then the first run is activated by an input trigger, and the remaining data acquisition process utilizes the “Free Run” option.

The “Preview Average” check box is generally used when multiple test data must be averaged. When this option is enabled, each data capture can be viewed for its quality before it is included in the main data.

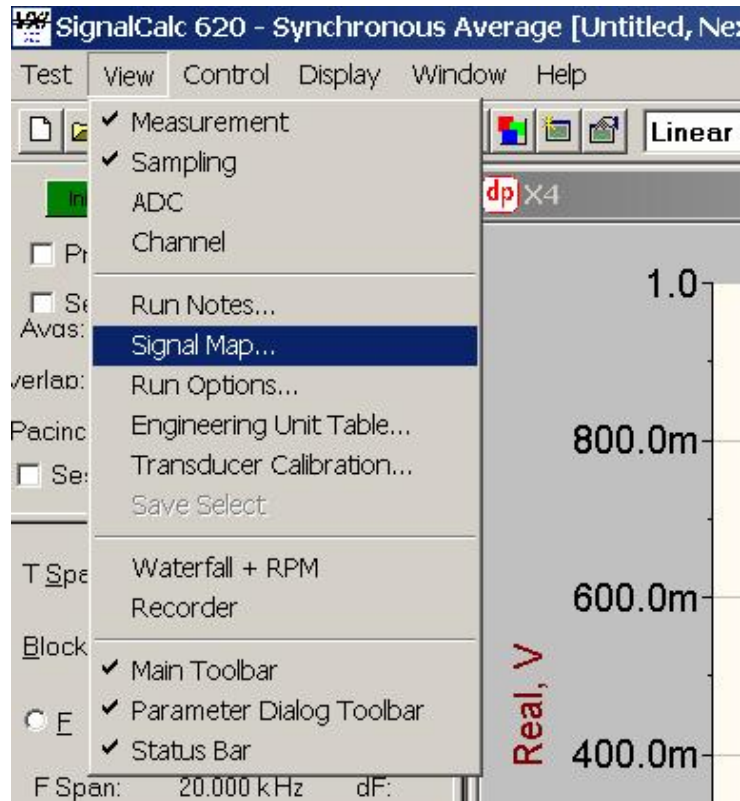
The “Init” button (see Figure 5.10) is used to initialize the hardware associated with the SignalCalc<sup>®</sup> 620 software (generally VXI modules).

### **5.2.5 Step 5: Perform Test**

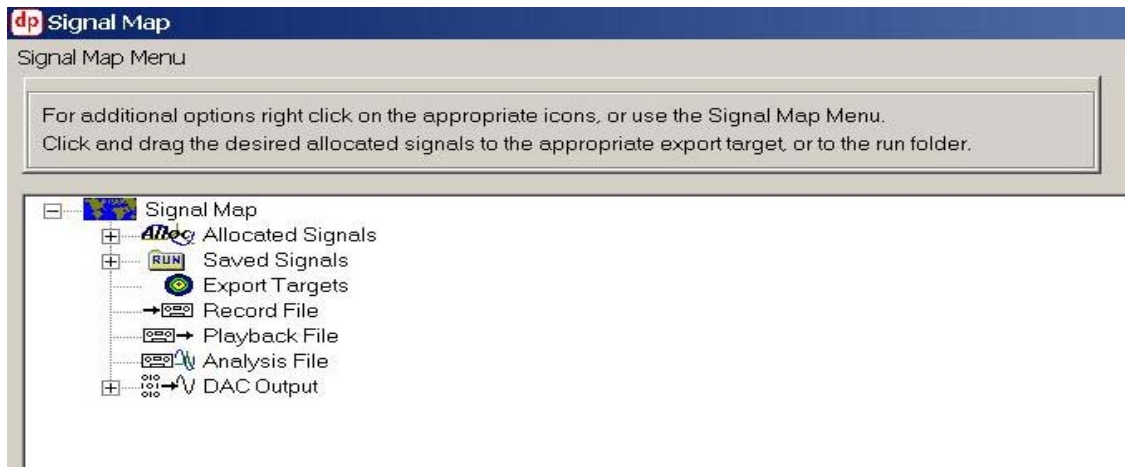
After all the input channels, measurements, and sampling parameters are properly set according to the test requirements, the “Start” button on the “Measurement Parameters” window shown in Figure 5.10 is clicked to initiate the measurement . If the trigger is set for the test session, a message will appear at the bottom of the window, “waiting for input trigger,” to start the test. When the trigger conditions are satisfied, data will be collected according to the sampling and measurement parameters.

### **5.2.6 Step 6: Exporting Data**

Signalcalc<sup>®</sup> 620 can export data in various formats via a powerful tool called “Signal Map.” “Signal Map” can be viewed by selecting “View → Signal Map” as shown in Figure 5.11. “Signal Map” provides a graphical overview of all the signals available for exporting and the formats in which they can be saved or exported. The formats available in Signalcalc<sup>®</sup> 620 for exporting are ASCII text file, Universal File format, ME Scope File, SMS Star Files, VEC Modal Files, SDF Files, and Matlab<sup>®</sup> (MAT) Files.



(a) Signal Map Pull-Down Menu.



b) Signal Map Graphical User Interface.

Figure 5.11. SignalCalc<sup>®</sup> 620 Signal Map.

### 5.3 SurfSeis<sup>®</sup> 2.0

SurfSeis<sup>®</sup>2.0 is seismic data processing software for subsurface shear-wave velocity profiling. It can perform data processing for both active and passive MASW tests. SurfSeis<sup>®</sup>2.0 reads the seismic data obtained from active or passive tests in SEG-2 format, extracts Rayleigh surface waves from the data, and then uses the surface wave information as an input to produce 1-D or 2-D shear velocity profiles. The signal analyzer exports data in ASCII format, which is converted to SEG-2 format using data conversion software “IXSeg2Segy,” which is the general format for seismic data analysis software such as SurfSeis<sup>®</sup>2.0 and Seisimager<sup>®</sup>2D.

In this section, a step-by-step procedure to process an active set of data is explained by using a sample set of data stored in ..\Surfseis20\SampleData\Active of the computer where Surfseis 2.0 is installed. This data folder consists of 20 field records (named as 1011.dat to 1030.dat) collected from a 24-channel data acquisition system. The data were collected with a source offset ( $x_l$ ) of 1.22 m, a receiver array spacing ( $dx$ ) of 1.22 m, and a source-receiver configuration of  $5dx$ , all constant for each record. These tests were performed with a sampling frequency of 1000 samples/sec and a sampling duration of 1 second. To reduce noise and signal contamination, three test impacts were conducted at each location and subsequently stacked. The data were processed with SurfSeis<sup>®</sup>2.0 and is explained in the following sections as a step-by-step procedure.

#### 5.3.1 Step 1: Formatting

Most seismographs and digital signal analyzers store data either in ASCII or SEG-2 format; however, SurfSeis<sup>®</sup>2.0 requires input seismic data in SEG-Y format. Thus, the seismic data must be converted into SEG-Y or standard KGS format. In order to convert

the data, click on “Utility→Format,” select all 20 records, specify the output file name “test.dat,” and then click the “Run Format” button (Figure 5.12).

### **5.3.2 Step 2: Field Setup**

In this step, the location of source, receivers, receiver-array spacing, and SRC is entered. To input the required information, select “Utility → Field Setup,” and open the formatted data file created in the previous step, “test.dat” and select the “Active Radio” button in the “Survey Type” dialogue box as shown in Figure 5.13. A graphical user interface will appear as shown in Figure 5.14. Assign ‘1001’ and ‘1002’ as the station numbers for the first two stations. The station numbers used here are for reference only and can be selected arbitrarily; however, it is recommended for tracking purposes that station numbers be sequential. After station numbers are entered, details for the source offset,  $x_l$ , and receiver-array spacing,  $dx$ , are filled, and the appropriate measuring unit is chosen using the “unit” radio button in the bottom right corner of the dialogue box. The sample data were collected using the SI system. In the “Source/Receiver” move tab, type 1005 for the next source location. Apply the settings for all records from 1011.dat to 1030.dat. One record/move and moving direction is now selected. Click on the “Run Field Setup” button to start the field setup process. A prompt window will appear that will ask to save the formatted \*.dat file created during the field setup process. Click “ok,” and save the file as “test(Field setup).dat”. After the process is complete, a window will appear with the encoded field geometry as shown in Figure 5.15.

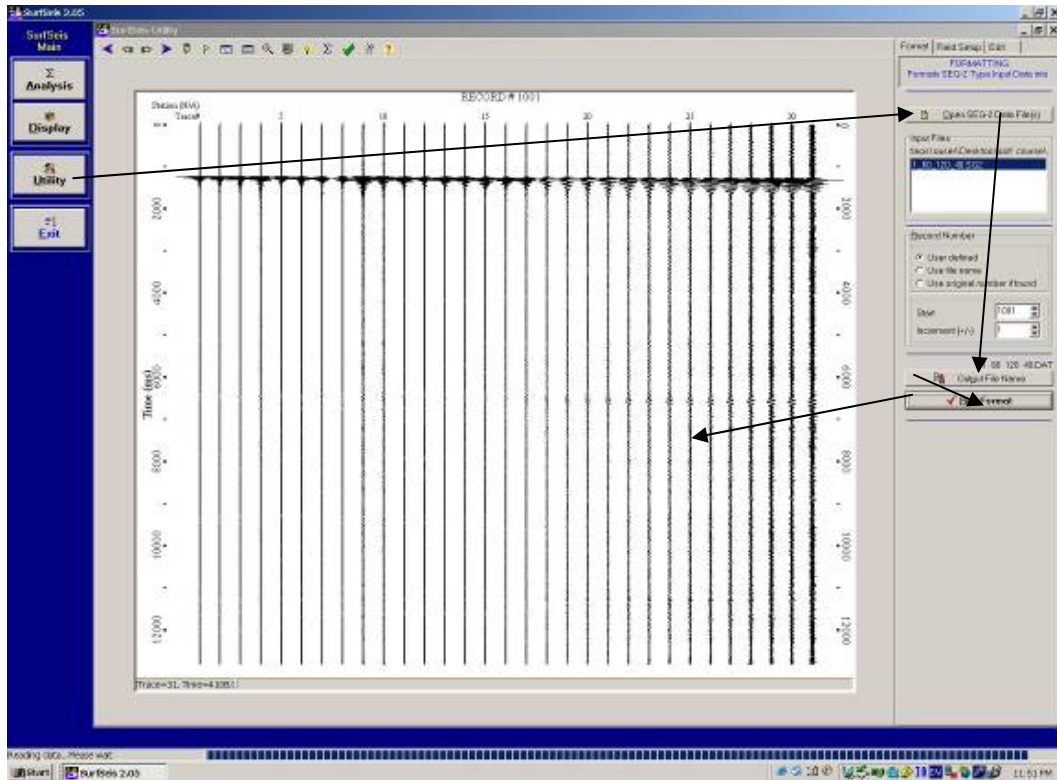


Figure 5.12. Formatting of Data.

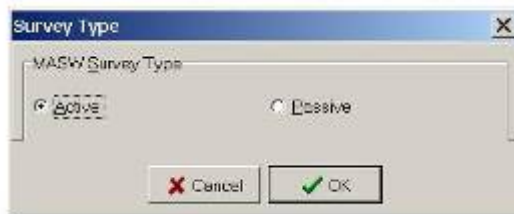


Figure 5.13. Survey Type.

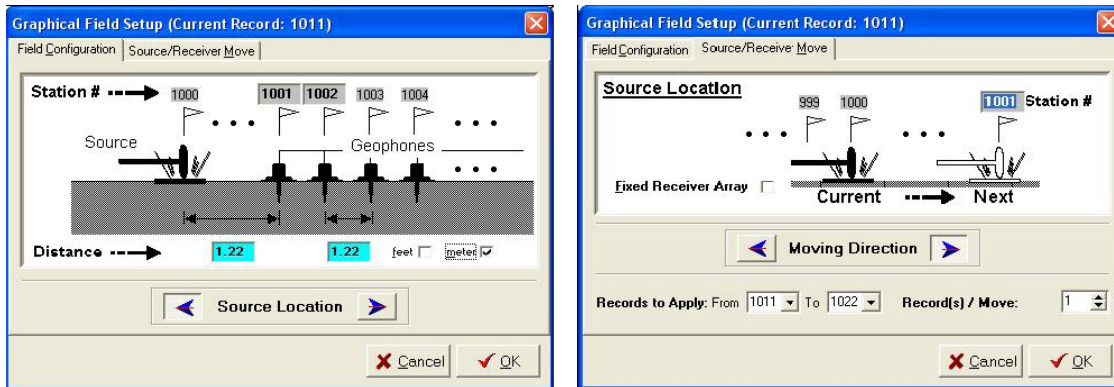


Figure 5.14. Field Setup.

RCD#\STA#	1000	1001	1002	1003	1004	1005	1006	1007	1008	1009	1010	1011	1012	1013	1014	1015	1016	1017
1011	[X]	1	2	3	4	5	6	7	8	9	10	11	12	13	14	15	16	17
1012		[X]	1	2	3	4	5	6	7	8	9	10	11	12	13	14	15	16
1013			[X]	1	2	3	4	5	6	7	8	9	10	11	12	13	14	15
1014				[X]	1	2	3	4	5	6	7	8	9	10	11	12	13	14
1015					[X]	1	2	3	4	5	6	7	8	9	10	11	12	13
1016						[X]	1	2	3	4	5	6	7	8	9	10	11	12
1017							[X]	1	2	3	4	5	6	7	8	9	10	11
1018								[X]	1	2	3	4	5	6	7	8	9	10
1019									[X]	1	2	3	4	5	6	7	8	9
1020										[X]	1	2	3	4	5	6	7	8
1021											[X]	1	2	3	4	5	6	7
1022												[X]	1	2	3	4	5	6

Figure 5.15. Field Geometry.

### 5.3.3 Step 3: Generation of Overtone (OT) Records

After all data are formatted and the field setup is encoded with the data, the next step is to process the dispersion information from each record that is also the first step in the dispersion analysis. This step consists of the generation of the dispersion image or the overtone image and extraction of the dispersion curve from the overtone images. Click on the “Analysis → Dispersion” button, and open the field geometry encoded data file “test(Fieldsetup).dat” created in the previous step. When the data file is selected, the first data set is ready to process. On the left side of the screen, the tool bar shown in Figure 5.16 will appear. Extraction of the dispersion curve from the seismic data is a three-step procedure:

- 1) Click “Preprocess.”
- 2) Set controls for the dispersion curve generation using the “Controls” button on the dispersion manual side bar, and then click the “Run” button on the dispersion manual side bar. A dispersion curve will appear on the OT image. The best

dispersion curve lies over the orange portion of the OT image, indicating the maximum accumulation of energy as shown in Figure 5.17.

3) Click “Save” to save the picked dispersion curve.

When all dispersion curves have been processed and saved, then they can be opened for inversion analysis.

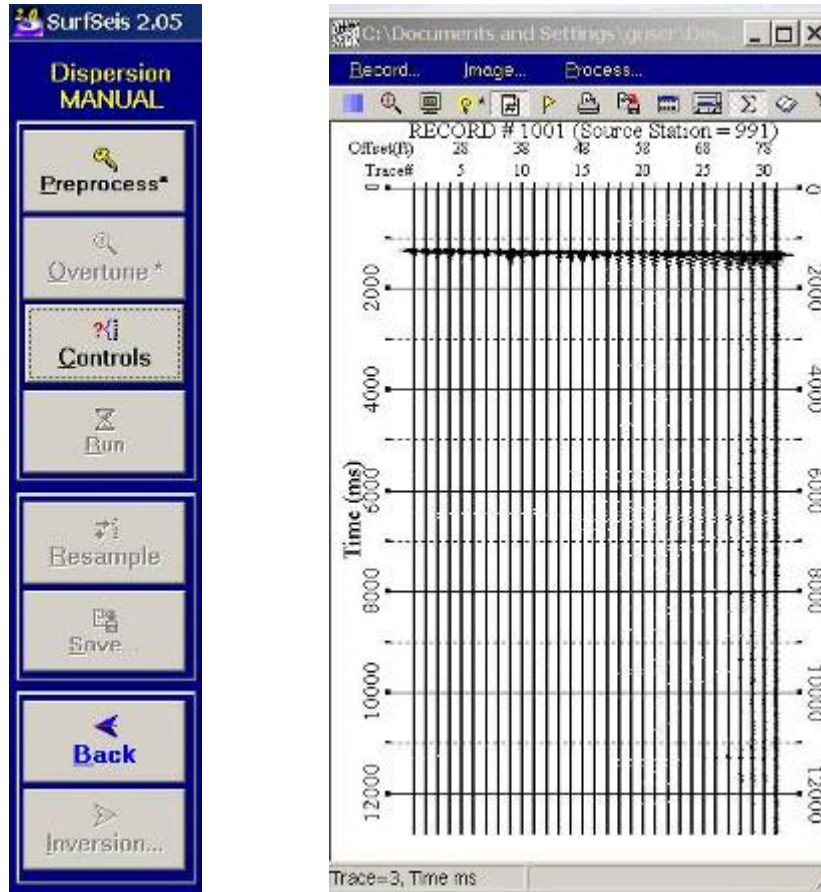


Figure 5.16. Dispersion Analysis Controls and Record Display.

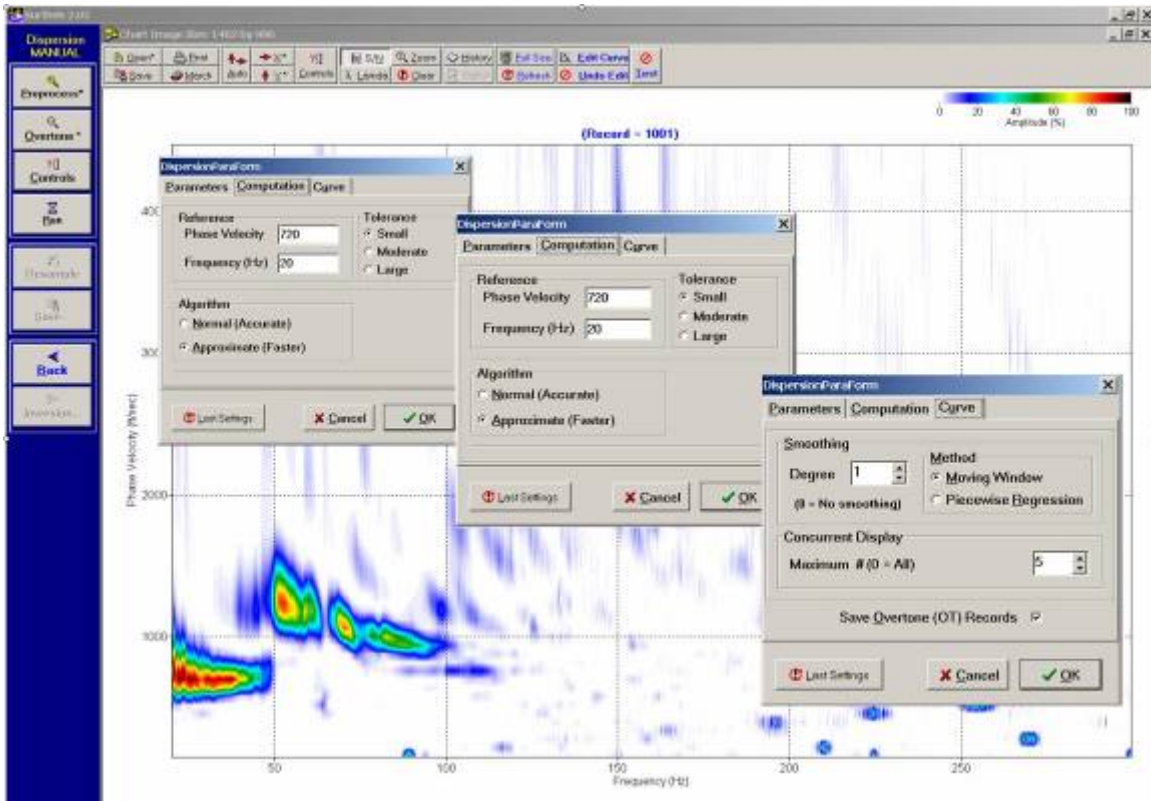


Figure 5.17. OT Image and Dispersion Curve Generation Controlling Parameters.

### 5.3.4 Step 4: Inversion for 2-D vs. Profile

Inversion of the dispersion curves extracted in the previous step is the last step in the data processing. In this step, either a 1-D or 2-D shear velocity profile is constructed by the inversion of single or multiple dispersion curves. Two different types of inversion analyses are possible in SurfSeis<sup>®</sup> 2.0: analysis of extracted and saved dispersion curves or analysis of the OT image using the Monte Carlo method that randomly searches for a shear wave velocity model whose dispersion trend best matches with the trends of the OT image.

To initiate the inversion process, click the “Analysis → Inversion” button. Select all the dispersion curves extracted in step 3 and saved during the dispersion analysis. The

parameters for this step include stopping criteria, initial  $V_s$  layer setup, and weight applied to data sets, all set using the “Control” tab shown in Figure 5.18. After selecting all analysis parameters, click the “Run” button to start the inversion analysis (Figure 5.19). Finally, a 2-D velocity profile is obtained as shown in Figure 5.20 after all the dispersion curves are inverted.

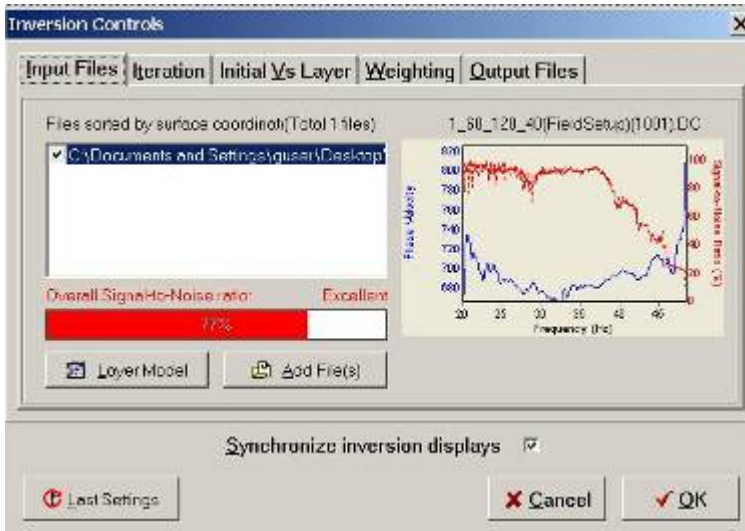


Figure 5.18. Controlling Parameters for Inversion Analysis. Figure 5.19. Control Tab.

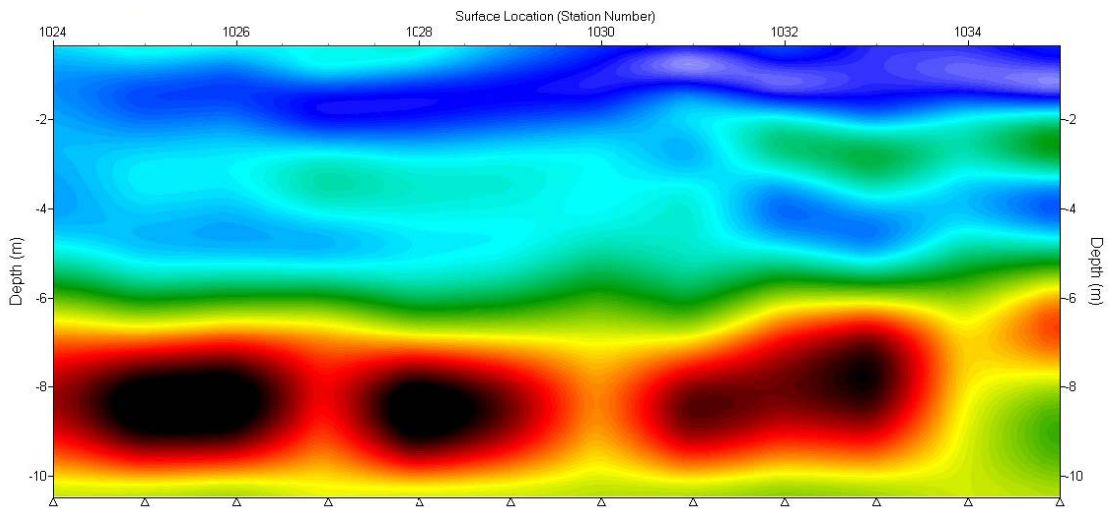


Figure 5.20. Final 2-D Shear Velocity Profile Obtain After Inversion Analysis.

## 5.4 Seisimager<sup>®</sup>2D

SeisImager<sup>®</sup>2D analyzes refraction test data and performs comprehensive refraction modeling using ray tracing for both P-wave and SH-wave refraction surveys. SeisImager<sup>®</sup>2D reads the seismic trace data obtained from refraction survey tests in the SEG-2 or SEG-Y format. The signal analyzer exports data in ASCII format that must be converted to SEG-2 format using data conversion software “IXSeg2Segy,” which is the general format for the seismic data analysis software such as Surfseis<sup>®</sup>2.0 and Seisimager<sup>®</sup>2D.

In this section, a step-by-step procedure for processing P-wave refraction data is explained by using a sample data set stored in ...\\seisimager\_e\\sample\_data2(Refraction) of the computer on which Seisimager<sup>®</sup>2D is installed. This data folder contains seven field records named 1000.dat, 1002.dat, 1003.dat, 1004.dat, 1005.dat, 1006.dat, and 1008.dat collected from a 24-channel data acquisition system. The first geophone was located at the 100 ft, and the last geophone was located at 146 ft, with uniform receiver-array spacing,  $dx$ , equal to 2 ft. The energy impact coordinates for eight tests are 98 ft, 70 ft, 109 ft, 123 ft, 135 ft, 148 ft, and 176 ft, respectively, for each of the eight listed data files. Data analysis of the refraction test involves two main steps:

- 1) Obtain the first breaks from all traces and plot travel time curves for each location.
- 2) Invert the travel time curves to obtain reasonable sub-surface wave velocity profiles.

The first step in obtaining the first breaks is performed using the “Pickwin” package and the second step of inverting the travel time curve is done by “Plotrefra.”

These are the two main packages of Seisimager<sup>®</sup>2D. The full process of the refraction data analysis is explained in the following sections as a step-by-step procedure:

### 5.4.1 Step 1: Picking First Breaks

In this step, the first breaks are obtained using the “Pickwin” package of Seisimager<sup>®</sup>2D. Start the “Pickwin” module by double clicking on its icon on the desktop. Open the first trace file from the “File→open” pull-down menu, and select the first \*.dat file, 1000.dat, as shown in Figure 5.21. In “Pickwin,” the display of the data can be optimized using the main tool bar shown in Figure 5.22.

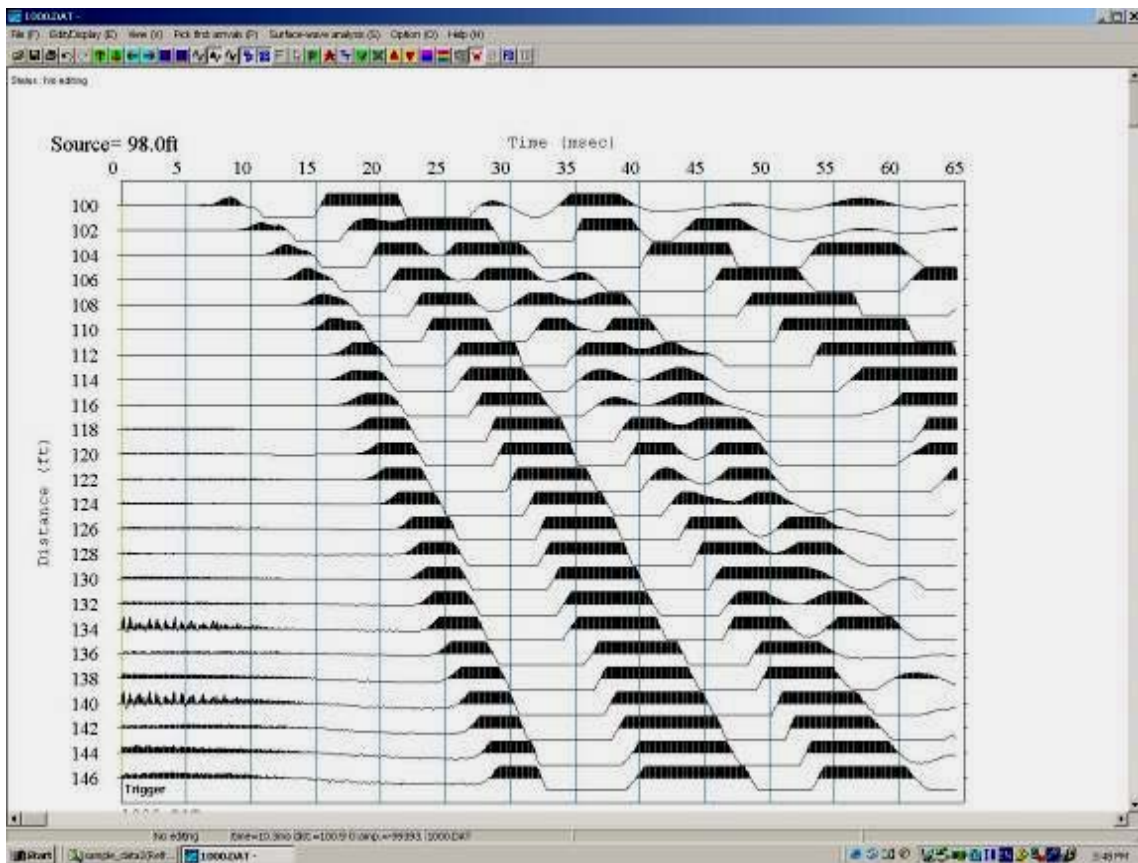


Figure 5.21. Seisimager<sup>®</sup>2D Main Display Window.



Figure 5.22. Seisimager<sup>®</sup>2D Optimize Display Toolbar.

The “Pickwin” module can automatically obtain the first break through an internal algorithm by clicking the  button on the main menu bar. The first breaks are shown by a small vertical line on each trace (see Figure 5.23).

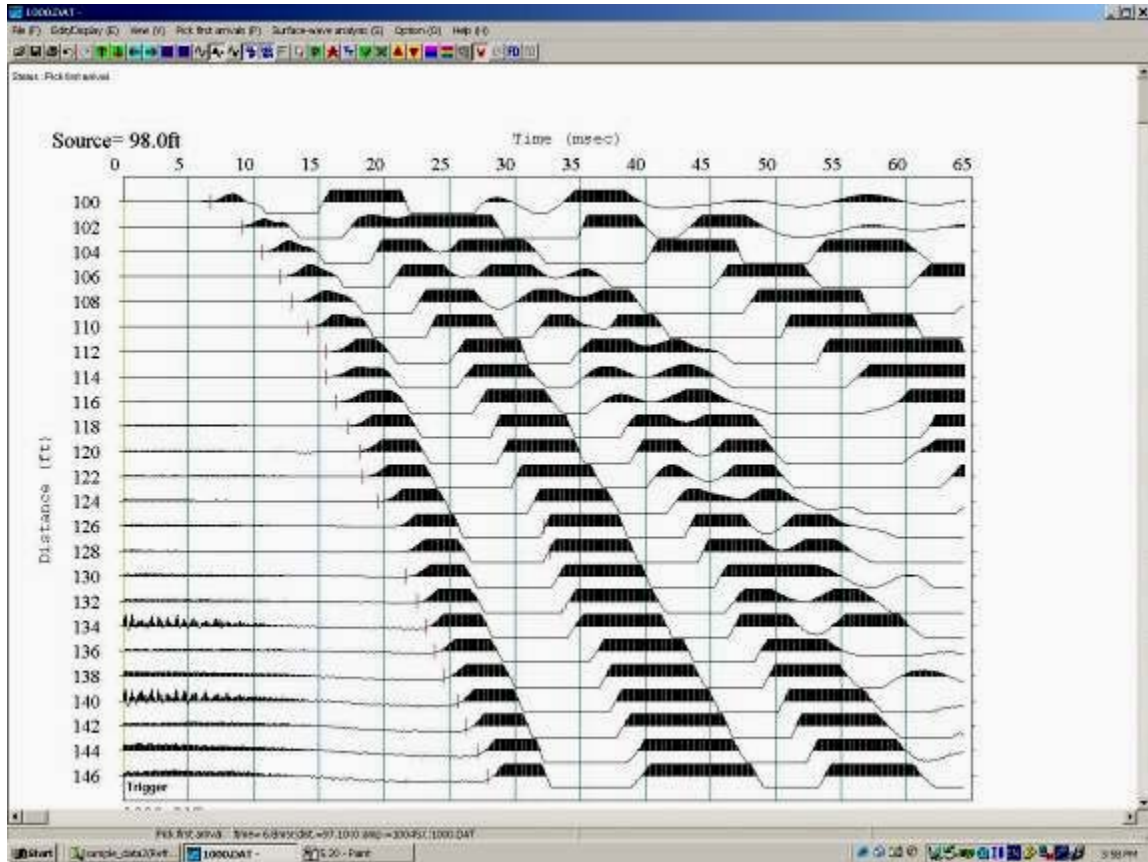


Figure 5.23. Pick First Breaks for File 1000.dat.

The automated procedure of picking the first breaks from the traces is not always correct or precise and sometimes must be manually adjusted. To manually adjust the picks, click on the appropriate point of the trace, and the small vertical red line will move to that point. Finally, click on  button on the main menu bar to connect all of the first breaks to construct the travel-time curve for the data (see Figure 5.24).

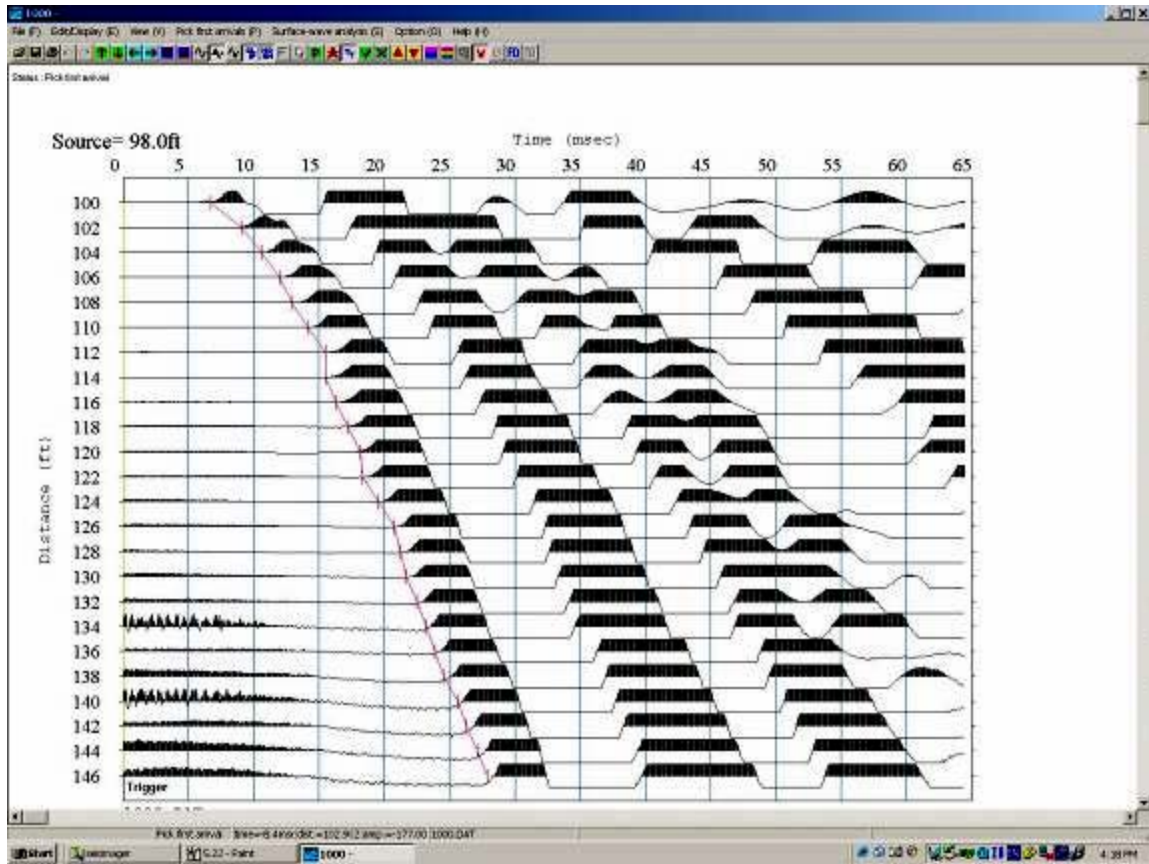


Figure 5.24. Travel-Time Curve for File 1000.dat.

Read the remaining files in a similar manner by opening them as new files and extracting the travel-time curve from each file (see Figure 5.25). When all data files have been processed for first breaks and the travel-time curve, the first break picks file can be saved using the “File→save pick file” pull-down menu. This saved pick file is used as an input file for the “Plotrefra” package that is used to run the inversion analysis to obtain a wave velocity profile by minimizing the root mean square error for the travel time between the source and the receiver.

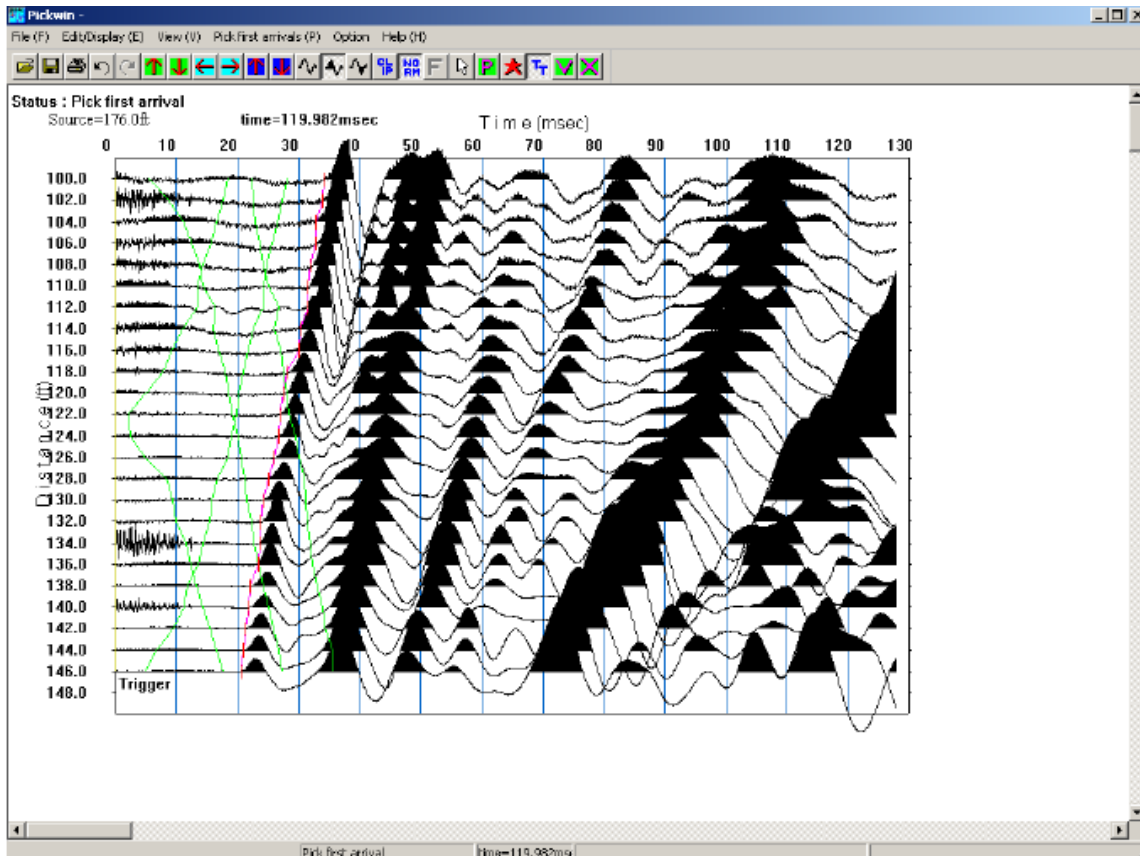


Figure 5.25. Travel-Time Curves for All Data.

#### 5.4.2 Step 2: Inversion of Travel-Time Curves

The Seisimager<sup>®</sup>2D performs comprehensive refraction modeling using ray tracing. The Seisimager<sup>®</sup>2D package includes three methods for refraction data analysis: 1) quick-look time-term inversion, 2) the reciprocal method, and 3) tomography.

The tomography method is the most recently developed method and involves complicated mathematical concepts. Seisimager<sup>®</sup>2D offers a partially automated inversion facility with the tomography method. The tomography method involves the creation of an initial velocity model, iteratively traces rays through the model, compares

calculated travel times to measured, modifies the model, and then repeats the process until the difference between calculated and measured travel time is minimized.

To start the inversion process, initiate the “Plotrefra” module by double clicking on its icon on the desktop, and open the first break pick file from the “File→Open Plotrefra file” pull-down menu and select the first break pick file created in the previous step. All the travel time curves will appear as shown in Figure 5.26

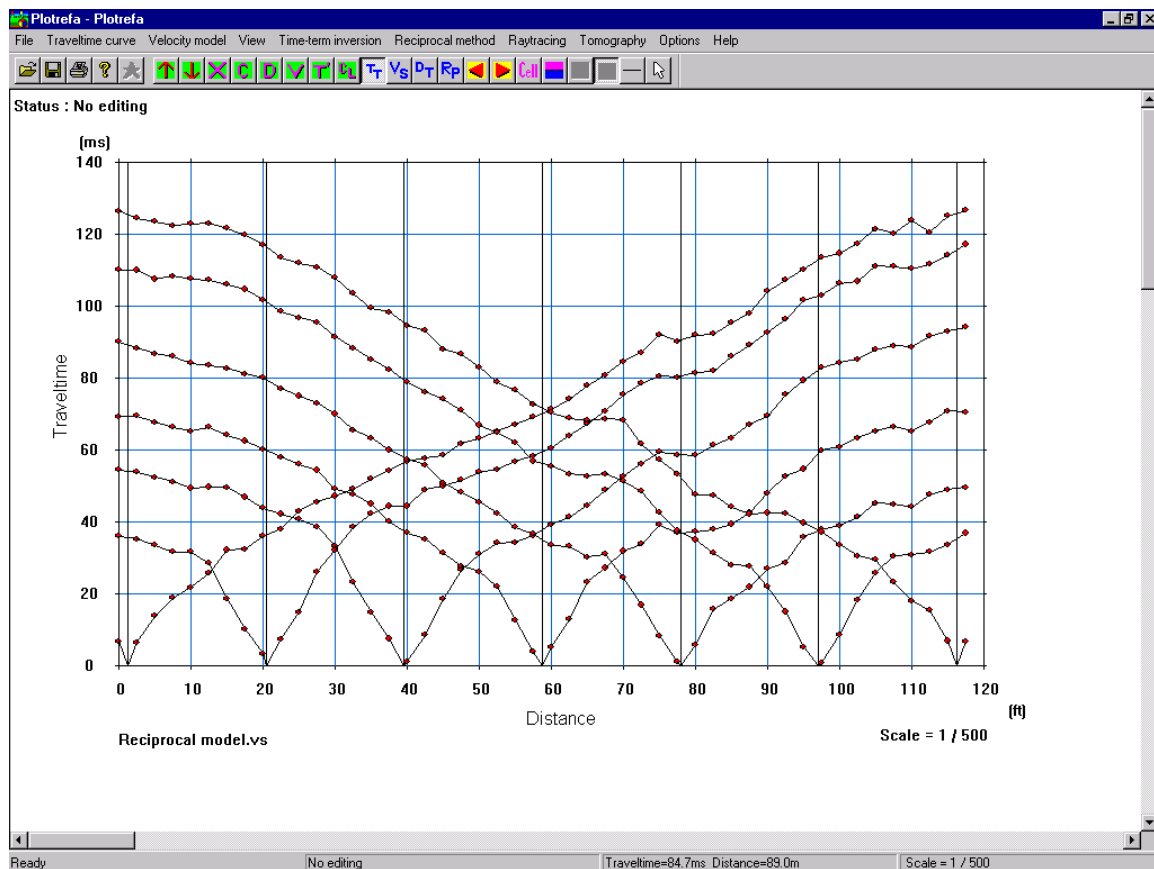


Figure 5.26. Travel-Time Curves.

After opening the first break pick file, import the elevation file for the array (see Figure 5.27). For the sample data set, the elevation file is in the same folder as the data. The “Tomography” method requires an initial velocity model to initiate the inversion process. To generate the initial velocity model, select “Tomography → Generate initial

model” from the “Tomography” pull-down menu on the main menu bar. A dialogue box as shown in Figure 5.28 will appear.

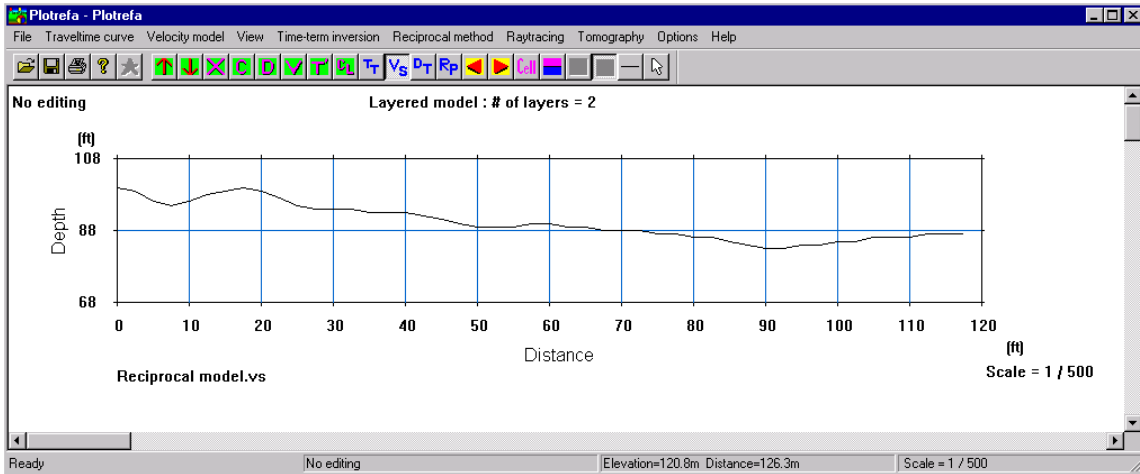


Figure 5.27. Importing Elevation Model.

Figure 5.28. Generating Initial Velocity Model.

An initial layer model can also be generated by performing a “quick look time-travel inversion” and use the resulting layer model as the initial velocity model. When all

parameters are set, click the “ok” button (see Figure 5.28). The initial velocity layer model will appear as shown in Figure 5.29.

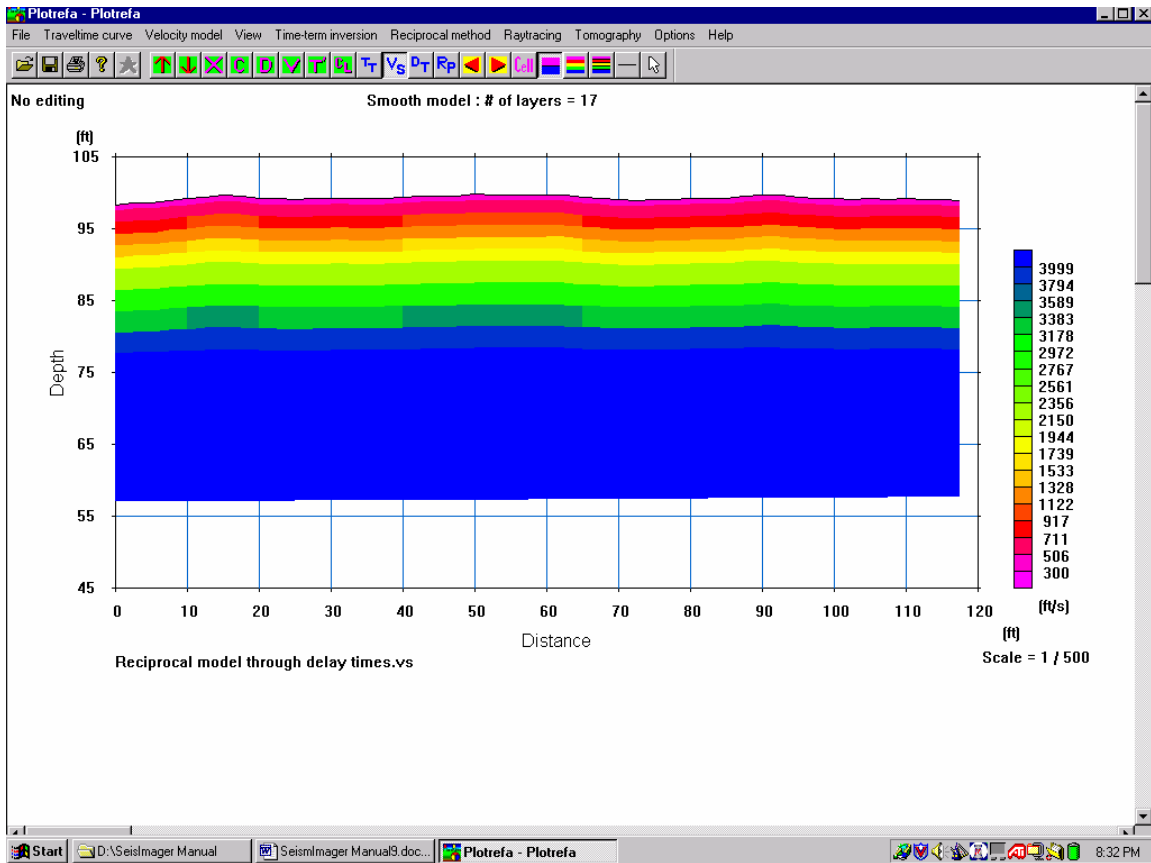


Figure 5.29. Initial Velocity Layer Model for Sample Data.

In the tomography method, the inversion process offers two choices: 1) inversion with default parameters and 2) inversion with manually adjusted parameters. To initiate the inversion process with default parameters, select “Tomography → Inversion (with default parameters)” from the “Tomography” pull-down menu on the main menu bar. This will initiate the inversion process with default settings, which takes several minutes to complete depending on the size of the problem. After the inversion process is completed, a final velocity model is displayed as shown in Figure 5.30. To evaluate the agreement between observed travel-time and calculated travel-time curves, select

“Raytracing→Execute” from the “Raytacing” pull-down menu on the main menu bar. This will perform ray tracing from the source to each receiver, and the RMS error is calculated using observed and calculated travel-time curves. The final objective of the inversion process is to minimize the RMS error. The velocity profile provided with the least RMS error is accepted as the final velocity profile.

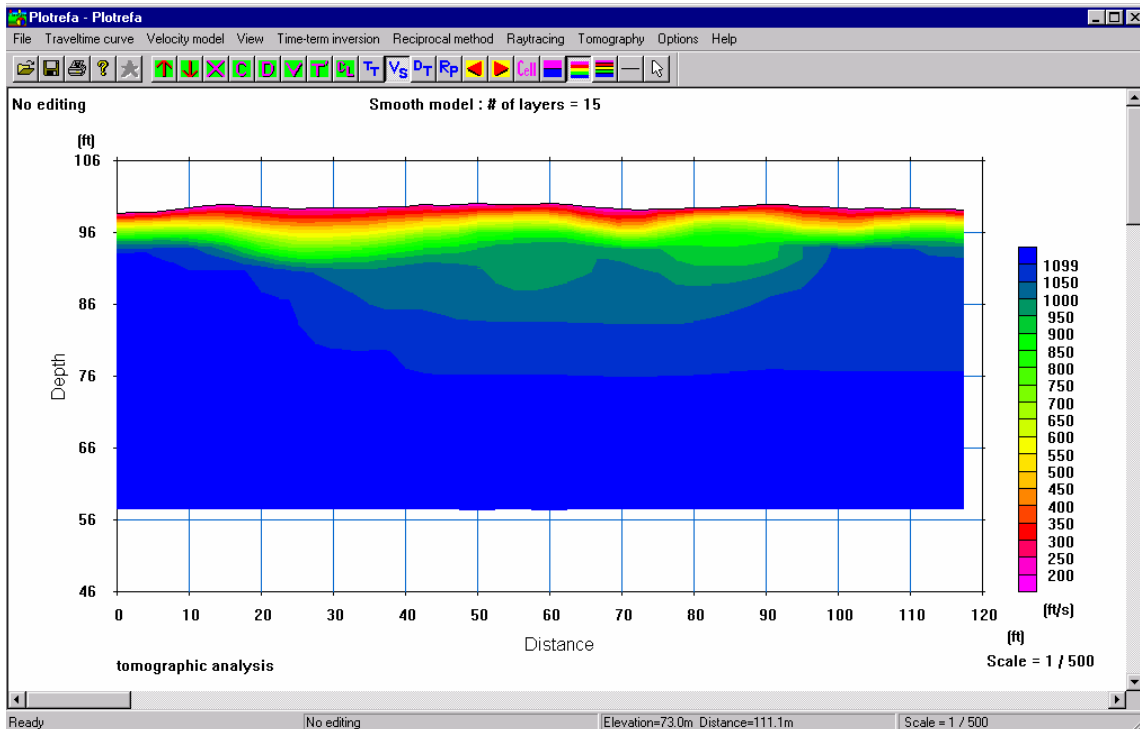


Figure 5.30. Final Subsurface Wave Velocity Profile for Sample Data.

Inversion with the default parameters is a safe choice for an inexperienced user. If the user is familiar with the procedure, inversion with manually adjusted parameters can produce more accurate results. To initiate inversion with manually adjusted parameters, select the “Tomography → Inversion (set parameters manually)” from the “Tomography” pull-down menu on the main menu bar. A dialogue box as shown in Figure 5.31 will appear displaying all adjustable parameters for the inversion process. There are ten parameters that can be adjusted manually in this option.

The “Number of iterations” default value is 10. If the initial model is accurate, fewer iterations are required to arrive at a reliable solution; however, if the quality of the initial velocity model is uncertain, the number of iterations can be increased to arrive at an acceptable solution.

The image shows a software dialog box titled "Automatic reconstruction". It contains several input fields and checkboxes for configuring the tomography method. The "Number of iterations" is set to 3. The "Option" section is currently empty. The "Number of nodes" is set to 5. The "Horizontal smoothing" section includes "Number of smoothing passes" set to 1 and "Smoothing weight" set to 0.5 (with a range of 0.3 to 1.00). The "Vertical smoothing" section includes "Number of smoothing passes" set to 0, "Smoothing weight" set to 0.5 (with a range of 0.3 to 1.00), and "Number of layers to be smoothed" set to 5. The "Minimum velocity" is set to 500 ft /sec and the "Maximum velocity" is set to 2500 ft /sec. There is an unchecked checkbox labeled "Velocity does not increase with depth". "OK" and "Cancel" buttons are located on the right side of the dialog.

Parameter	Value	Range/Unit
Number of iterations	3	
Number of nodes	5	
Horizontal smoothing - Number of smoothing passes	1	
Horizontal smoothing - Smoothing weight	0.5	(0.3 to 1.00)
Vertical smoothing - Number of smoothing passes	0	
Vertical smoothing - Smoothing weight	0.5	(0.3 to 1.00)
Vertical smoothing - Number of layers to be smoothed	5	
Minimum velocity	500	ft /sec
Maximum velocity	2500	ft /sec
Velocity does not increase with depth	<input type="checkbox"/>	

Figure 5.31. Inversion Parameters For Tomography Method.

In the tomography method, the velocity model is divided into cells of constant velocity, and then rays are traced through the model. The “Number of nodes” defines the density of the rays in a cell. The default value is three. If the number of nodes per side is

increased, the time taken for inversion will also increase. This parameter is also sensitive to accuracy of the initial model. “Horizontal/Vertical smoothing” is adjusted to apply the smoothing of cell velocities that results in acceptable velocity plots and removal of small-scale velocity objects. “Number of smoothing passes” controls the number of times the smoothing process is applied in the specific direction. Increasing the value of this parameter results in more smoothing of the final velocity plot, but it may also obscure the small-scale variations that might be essential for the objective of the refraction survey. “Smoothing weight” weights the velocity at the central node at a side. This parameter also controls the extent of smoothing applied in a specified direction. The larger the smoothing weight, the less the model will be smoothed. “Number of layers to be smoothed” applies to the vertical direction only. This parameter determines the number of layers to be smoothed in a vertical direction that is counted from the last layer. “Minimum/Maximum velocity” sets the bounds for velocity in the velocity profile model. If there is significant uncertainty regarding the distribution of wave velocity in the vertical direction, check the “Velocity vs depth” box.

## **Chapter 6 – Test Site Descriptions and Test Setup**

### **6.1 Introduction**

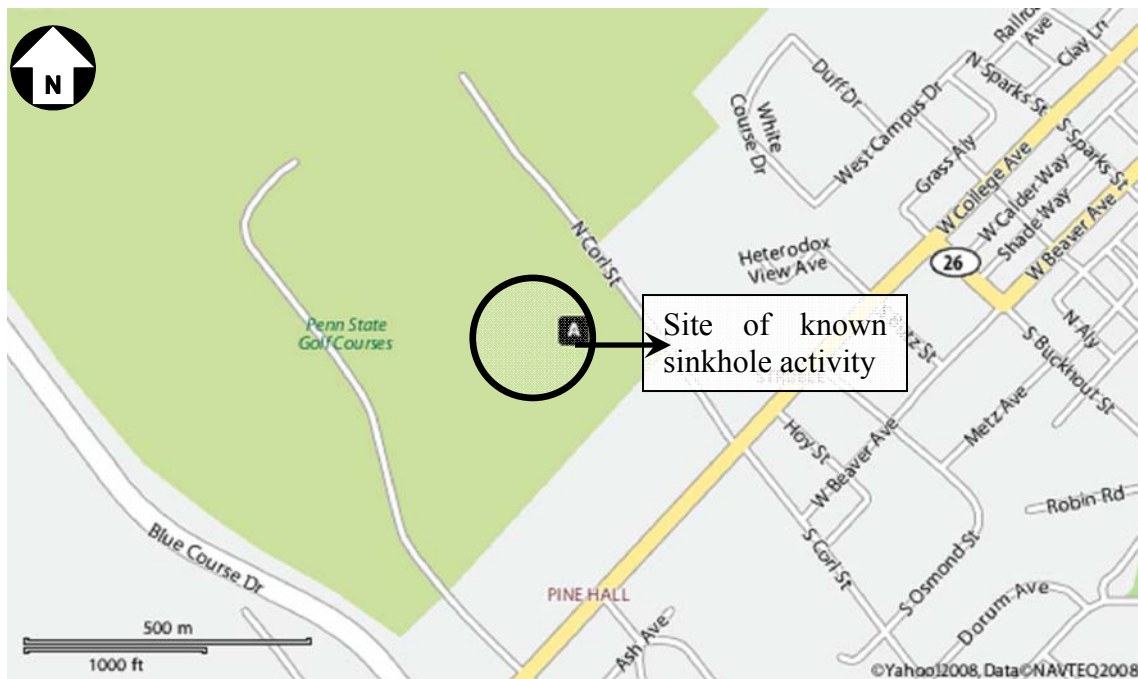
This chapter describes the three sinkhole-prone sites that were chosen as a part of the field study for this project. The three sites are 1) the Penn State Golf Course, a site of known sinkhole activity, 2) the Lafayette College Athletic Field, a site of measured and investigated sinkhole and void activity for proof testing, and 3) a site at the intersection of Route 220 (SR6026: future I-99) and Harrison Road in Benner Township. Characteristics of all three sites are described in detail in the following sections.

### **6.2 Penn State Golf Course Site**

The Penn State Golf Course site is located in an open field along West College Avenue on the property of the Penn State Golf Course in State College, PA as shown in Figure 6.1. It has known sinkhole activity in the field near College Avenue, but no prior testing has been completed on this site. The site has many depressions approximately 1 ft to 2 ft in diameter and provides a blind test site for the equipment and method with the possibility of multiple test arrays due to the close proximity to Penn State and the level terrain. The sinkhole activities were further confirmed from the results of the micro seismic tests conducted in August 2007; thus, more intensive testing is required to map the area tomographically.



(a) Penn State Golf Course Satellite Image (Courtesy map.yahoo.com).



(b) Penn State Golf Course Street Locator Map (Courtesy map.yahoo.com).

Figure 6.1. Penn State Golf Course Site.

Two arrays of 100 ft were tested on April 8 and April 18, 2008. The array for the experimentation is shown in Figure 6.2. All the parameters of the test setups are discussed in detail in the sections below:

### **6.2.1 Source-Receiver Configuration (SRC) Movement**

From the results of preliminary tests conducted in August 2007, it was concluded that a spatial resolution of 6 ft is adequate to distinguish between the tomographical features. Thus, the source-receiver configuration (SRC) movement was repeated at 6 ft.

### **6.2.2 Field Geometry**

The geophone array dimension,  $D$ , is directly related to the longest wavelength that can be analyzed and is directly proportional to the maximum depth of investigation. From the tests conducted in August 2007, it was concluded that a spacing of 30 ft was adequate to capture the sinkhole activity; therefore, the inter-receiver spacing was kept at two ft, and with 15 channels, a geophone array dimension  $D$  of 30 ft was established.

### **6.2.3 Energy Source Offset**

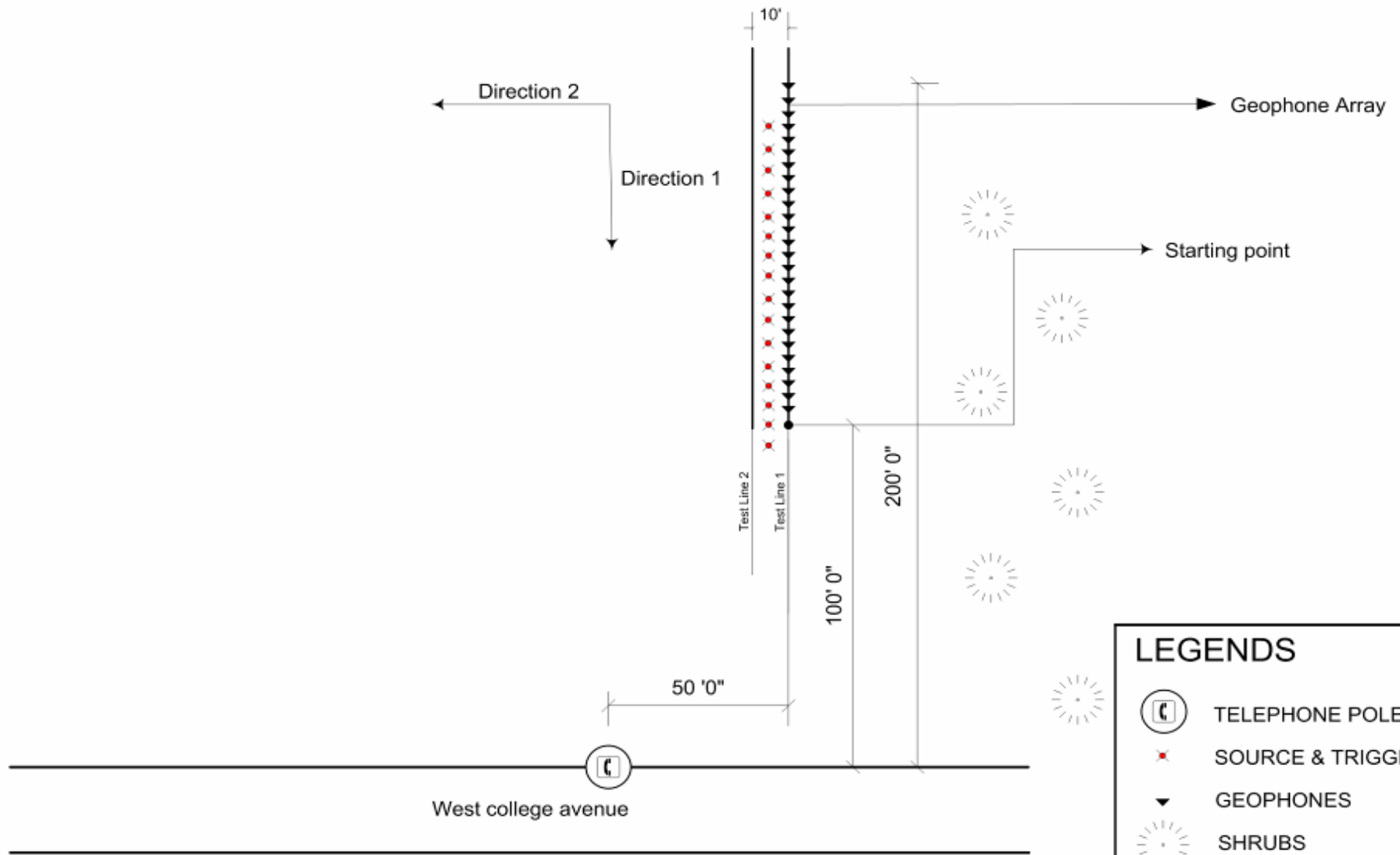
The energy source offset determines the intensity of contamination by near field effects and the participation of higher modes in the vibration, thus reducing the energy content in the fundamental mode. To eliminate the contamination of data, the source offset is set at approximately 30 percent of the geophone array dimension  $D$ . During the preliminary test, it was observed that an energy source offset of 10 ft provided acceptable results. The source offset was maintained at 10 ft and was varied in each test from 10 ft to 20 ft to verify the preliminary results. The data that provided maximum energy content in the fundamental mode and minimum near field effect intensity were chosen for the final analysis.

#### **6.2.4 Test Line Setup**

Tests were conducted over the surface depression at the northeastern edge of the grass area as indicated in the aerial view (Figure 6.1a). The test setup consists of two lines of 100 ft in length separated by 10 ft as shown in Figure 6.2.

#### **6.2.5 Test Organization**

The test was started from point “A” shown in Figure 6.2 along direction 1. The location of the energy source is marked by  sign in the figure. To cover a 100-ft test line length, 14 tests were conducted to complete one line. After completing the one full line in direction 1, the test setup was shifted 10 ft in direction 2, and the whole test procedure was repeated.



**LEGENDS**

-  TELEPHONE POLE
-  SOURCE & TRIGGER
-  GEOPHONES
-  SHRUBS



Figure 6.2 (a) PENNDOT SITE – I Pennsylvania State University Golf Course Site Layout  
 PROJECT: Sinkhole Void Grout Treatment

Drawing By: Ashutosh Srivastava  
 Date: 05/30/2008



### 6.2.6 File Organization

Tests were initiated from the point nearest to West College Avenue in the test line, and data were stored with the file name protocol as: *Line#\_test#s'location,'* for example, Line1\_test1\_s90, Line1\_test2\_s96, Line1\_test3\_s102 etc.

### 6.2.7 Source-Receiver Array Configuration Management

There are a total 15 channels available in the current signal digitalizer. The source receiver configuration (SRC) movement was maintained at 6 ft; therefore, the first three geophones at the end of the array were relocated after each test as shown in Figure 6.3. There are 24 channels available in the seismic cable; therefore, four tests were conducted before the testing trailer was moved to a new location.

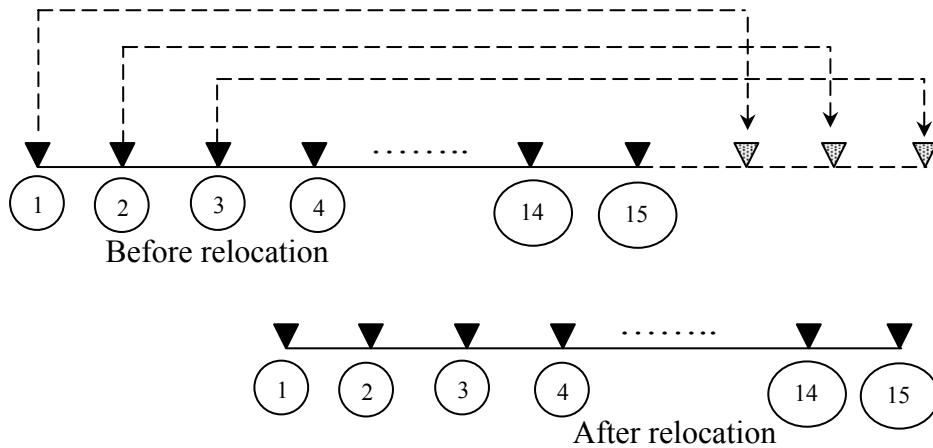


Figure 6.3. Receiver Array Configuration Scheme.

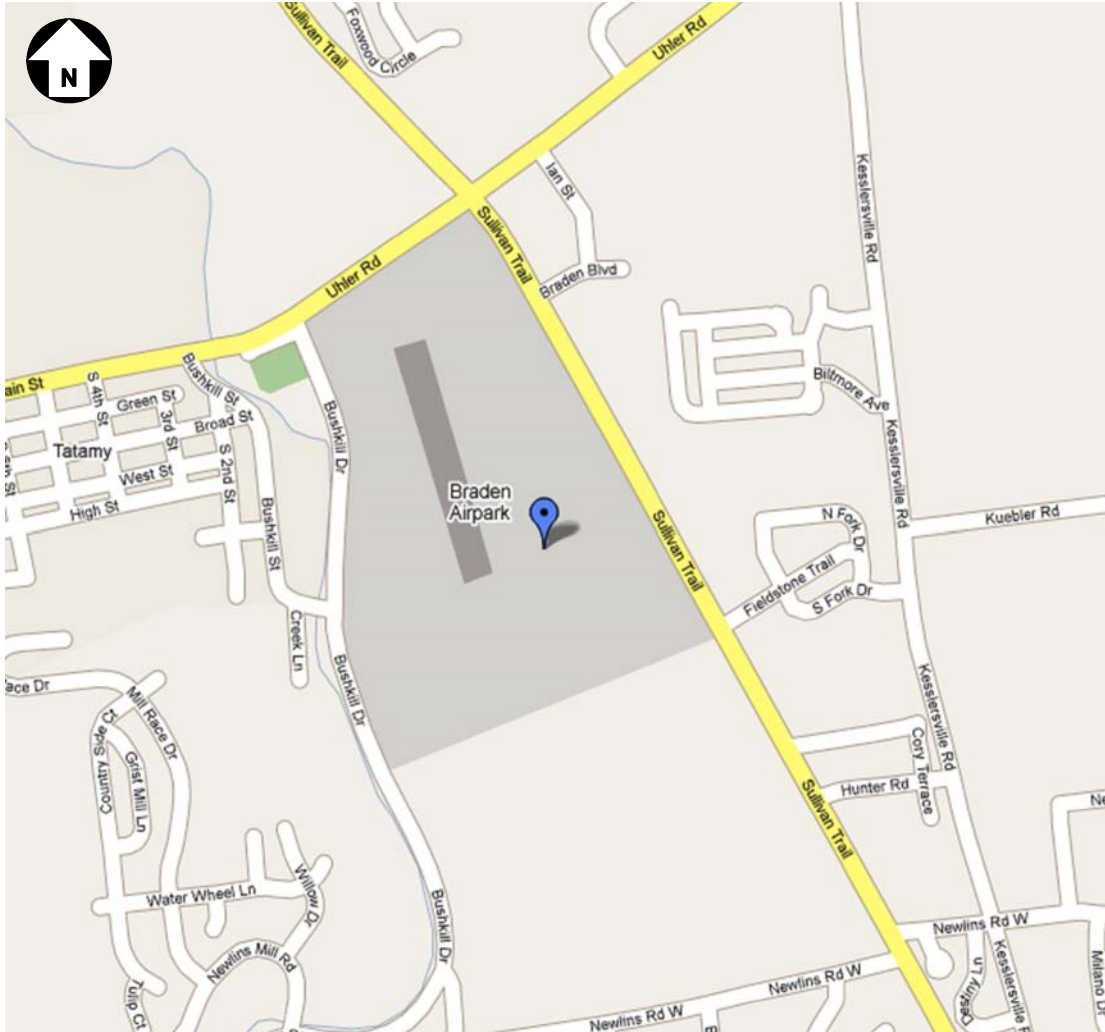
### 6.3 Metzgar Field (Lafayette College) Site

Metzgar Athletic Field at Lafayette College is located near Braden Airpark (Figure 6.4), approximately 3.5 miles northwest of the Lafayette College campus on Sullivan Trail at Uhler Road. Metzgar Athletic Field has been extensively mapped and

includes a known and mapped cave that was investigated by Dr Mary Roth in 2003 using the electrical resistivity method (Appendix A). The site provides a valuable baseline evaluation of the proposed method.



(a) Metzgar Athletic Field at Lafayette College Satellite Image (Courtesy map.google.com).



(b) Metzgar Athletic Field at Lafayette College Street Locator map (Courtesy map.google.com).

Figure 6.4. Metzgar Athletic Field at Lafayette College Site.

Figure 6.5 presents the 3-m grid used for the resistivity test conducted at Metzgar Athletic Field. The grid is 81 m long and 81 m wide and runs from the north-south and east-west directions.

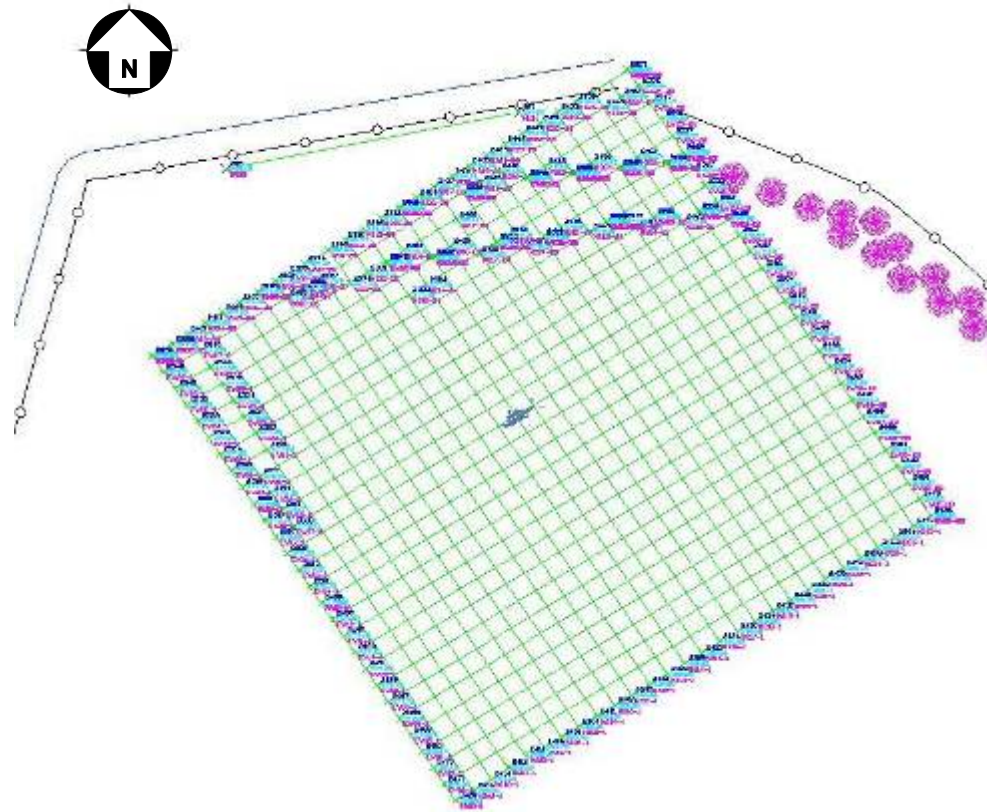


Figure 6.5. Metzgar Athletic Field Test Grid of 81 m.

From the results of the electrical resistivity test conducted in 2003, it was concluded that the cave is aligned in an east-west direction; therefore, the test was conducted on May 19-20, 2008, in the north-south direction.

### 6.3.1 Source-Receiver Configuration Movement

From the results of the electrical resistivity tests, it can be concluded that the spatial resolution of 6 ft is adequate to distinguish tomographical features. Thus, the source receiver configuration (SRC) movement was kept at 6 ft.

### 6.3.2 Field Geometry

The geophone array dimension  $D$  is directly related to the longest wavelength that can be analyzed and is directly proportional to the maximum depth of investigation. From

the electrical resistivity test results, it can be concluded that a spacing of 45 ft was adequate to capture the cave; therefore the inter-receiver spacing was kept at three ft, and with 15 channels, the geophone array dimension  $D$  of 45 ft was established.

### **6.3.3 Energy Source Offset**

The energy source offset determines the intensity of contamination by near field effects and the participation of higher modes in the vibration, thus reducing the energy content in the fundamental mode. To eliminate the contamination of the data, the source offset is set approximately 30 percent of the geophone array dimension  $D$  that gives the source offset of 15 ft. During the preliminary test, it was observed that an energy source offset of 12 ft provided acceptable results. The source offset was varied in each test from 6 ft to 12 ft to verify the preliminary results. The data that provided maximum energy content in the fundamental mode and minimum near field effect intensity were chosen for the final analysis.

### **6.3.4 Test Line Setup**

Two tests were conducted over the leveled surface at the northeastern edge of the fenced area as indicated in the aerial view. The test setup consisted of two lines of 100 ft separated by 19.7 ft. One control line test was conducted south of the two main lines to study the general tomography of the region that is not affected by the cave in Figure 6.6.

### **6.3.5 Test Organization**

The test was started from the point “A” as shown in Figure 6.6 along direction 1. The location of the energy source is marked by  sign in the figure. To cover the length of 100 ft in one array, 14 tests were conducted. A total of two arrays of 100 ft in length were tested along direction 1 separated by 19.75 ft as shown in the Figure 6.6. One

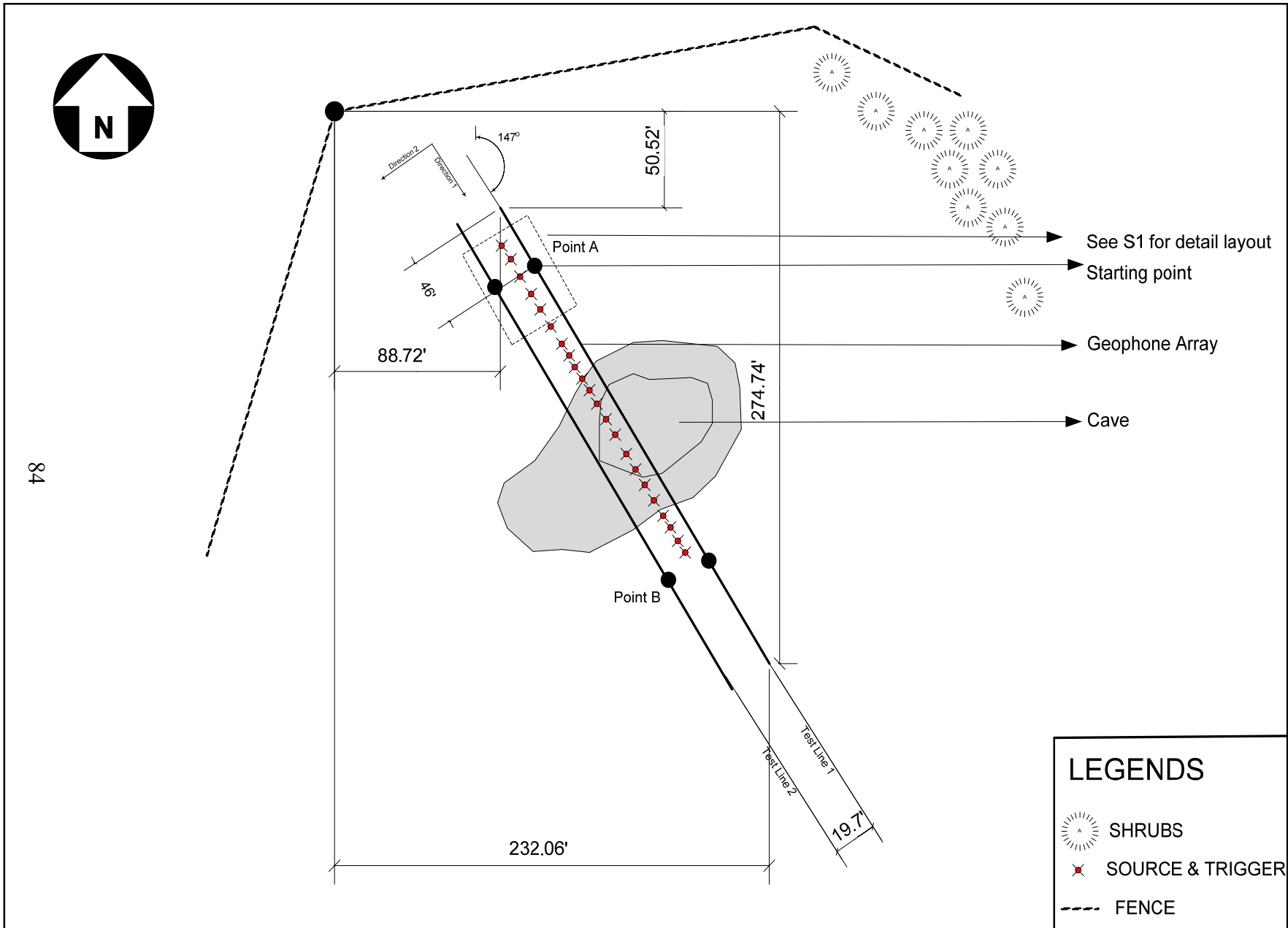
control line experiment was conducted to study the subsurface soil profile not affected by the cave. A total of 43 tests were conducted.

### **6.3.6 File Organization**

Tests were initiated from the northernmost point in the test line, and the data were stored with the file name protocol as: *Line#\_test#s'location'* for example, Line1\_test1\_s34, Line1\_test2\_s40, Line1\_test3\_s46 etc.

### **6.3.7 Source-Receiver Array Configuration Management**

There are a total 15 channels available in the current signal digitalizer. The SRC movement was maintained at 6 ft; therefore, the first two geophones at the end of the array were relocated after each test as shown in Figure 6.7. There are 24 channels available in the seismic cable; therefore, five tests were conducted before the testing trailer was moved to a new location.

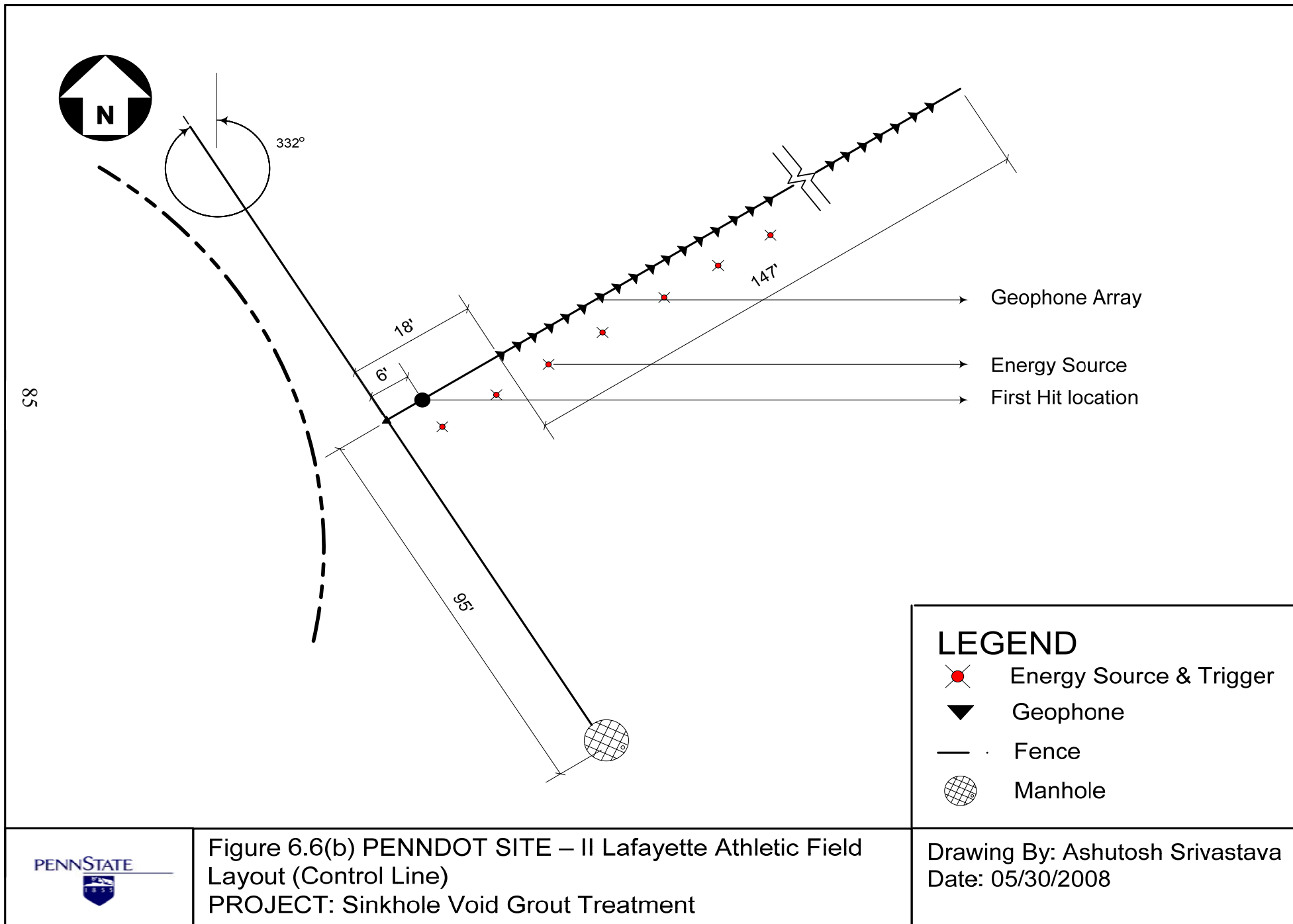


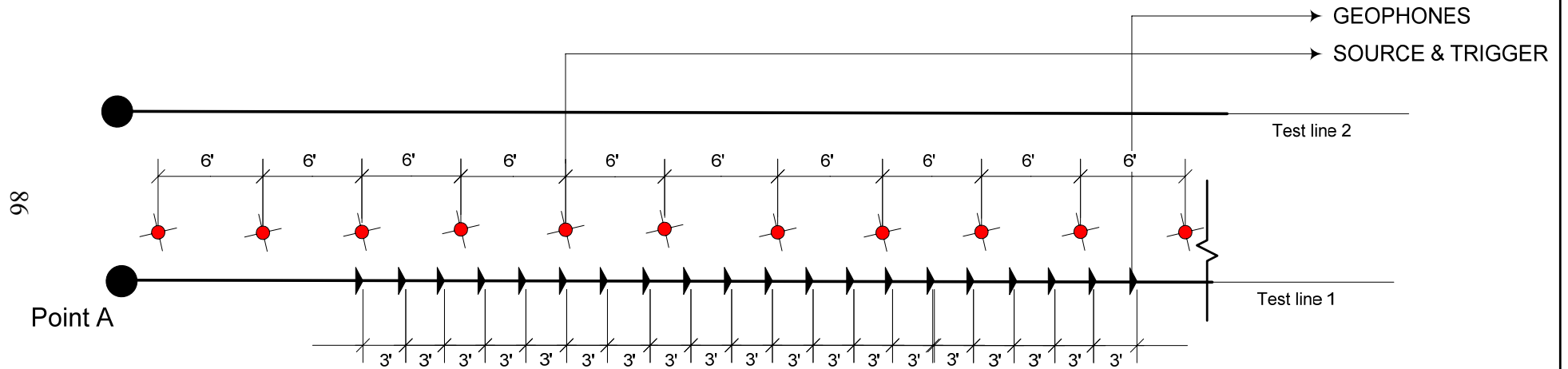
84



Figure 6.6(a) PENNDOT SITE – II Lafayette Athletic Field  
 Layout  
 PROJECT: Sinkhole Void Grout Treatment

Drawing By: Ashutosh Srivastava  
 Date: 05/30/2008





**LEGEND**

- ★ SOURCE & TRIGGER
- ▼ GEOPHONES



Figure 6.6(c) PENNDOT SITE – II Geophone Layout for Lafayette Athletic Field  
 PROJECT: Sinkhole Void Grout Treatment

Drawing By: Ashutosh Srivastava  
 Date: 05/30/2008

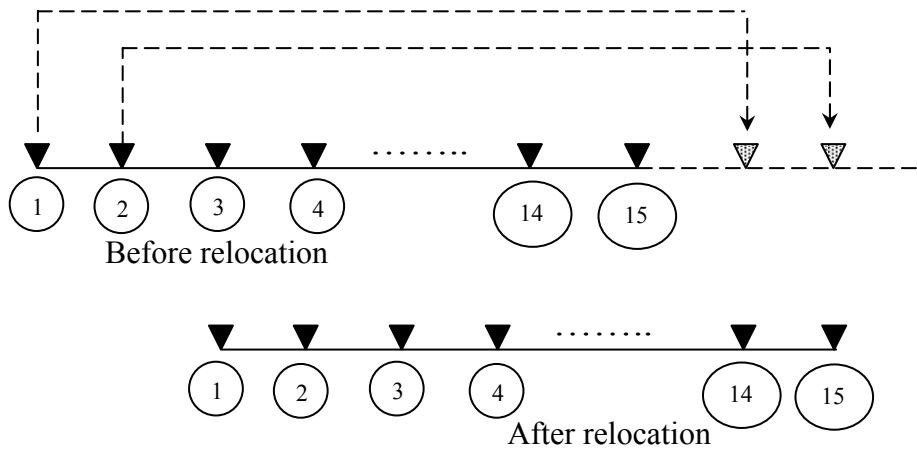


Figure 6.7. Receiver Array Configuration Scheme.

#### 6.4 Route 220 and Harrison Road

The third site is located along the new I-99 extension (Route 220) to I-80 in Benner Township, PA (Figure 6.8). Surface indications of sinkhole activity are present at this site. District 2-0 proposed the site for mapping with seismic methods to determine the scale of the activity in the area of the bridge abutment and to map potential problem areas located under the surface. Figure 6.9(a) shows the test line parallel to the bridge abutment. Figure 6.9(b) shows the geophones layout.

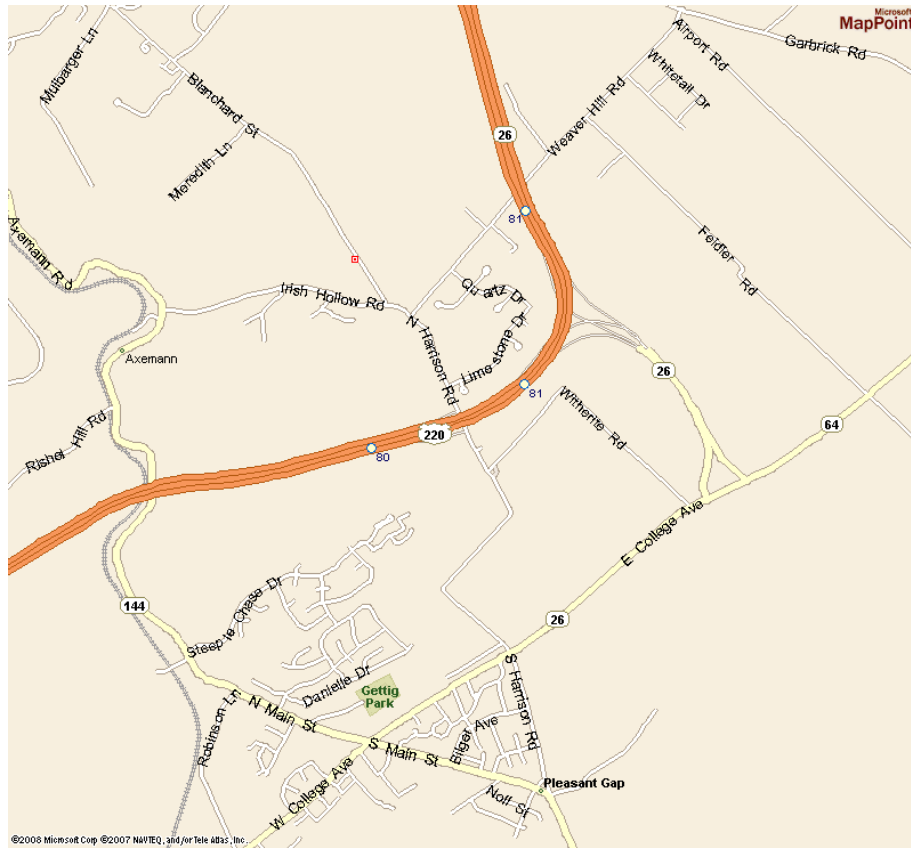
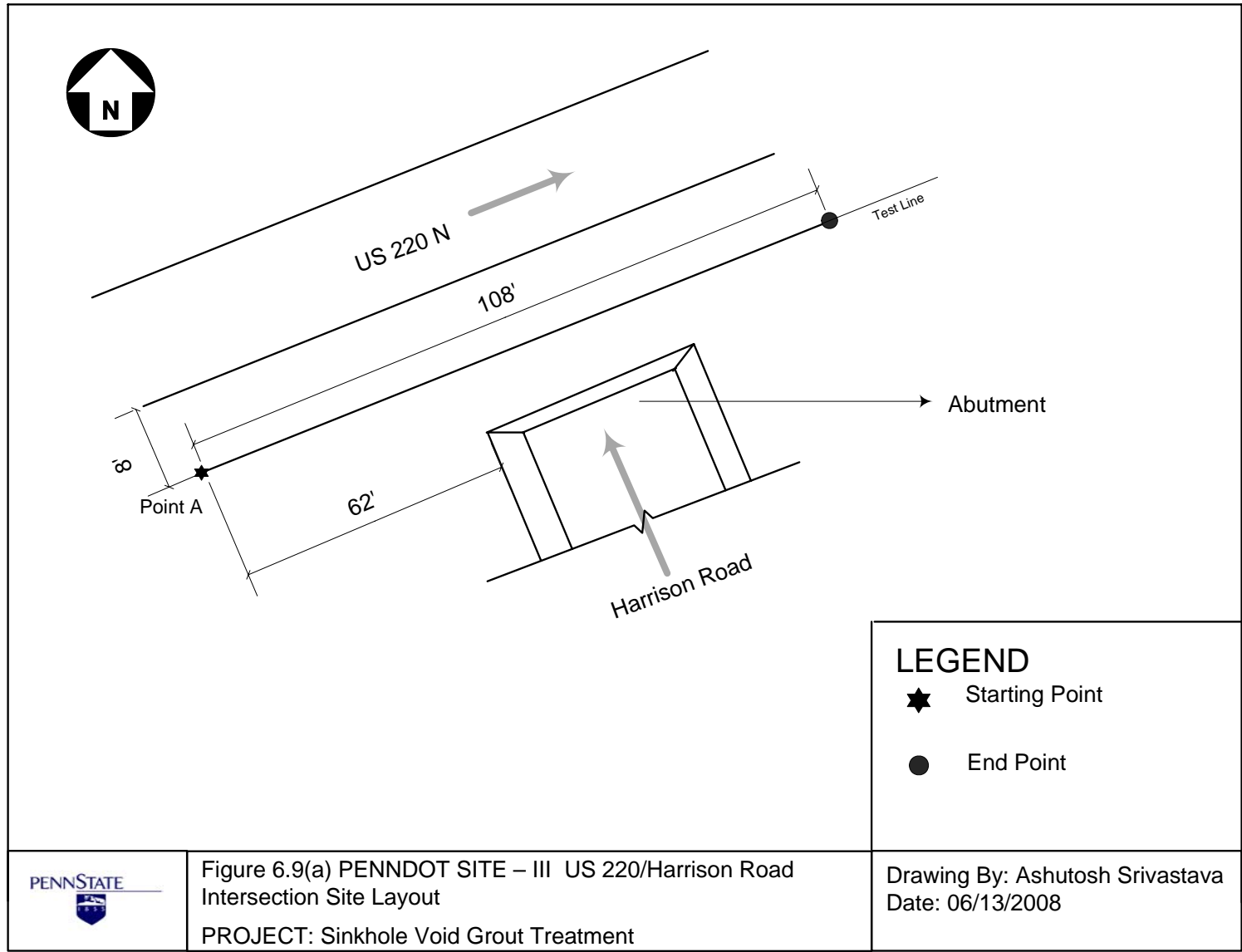
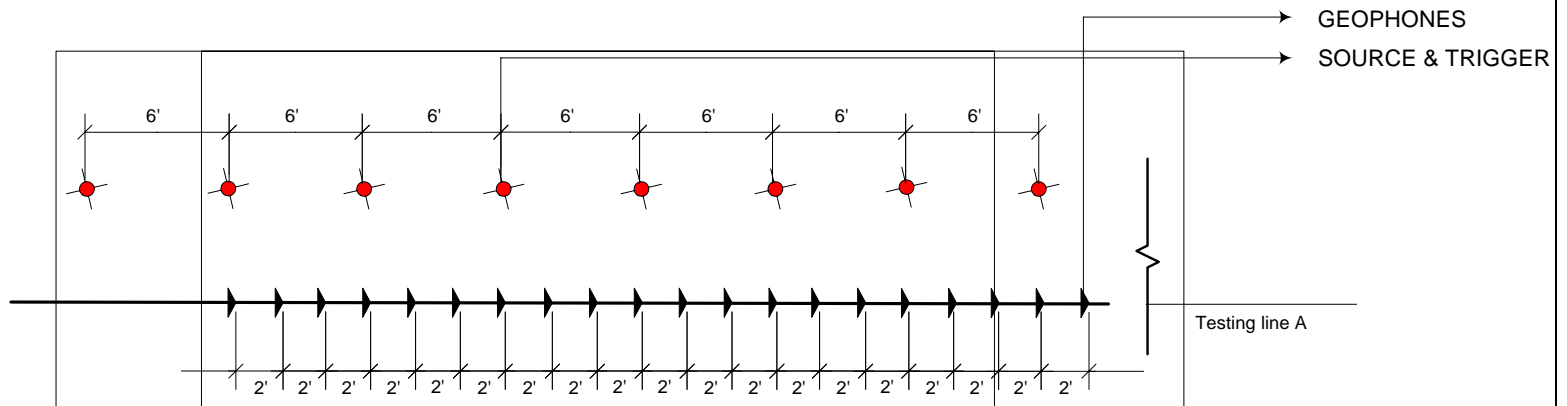


Figure 6.8. Location Map of Harrison Road Bridge over US 220.





**LEGEND**

- ✘ SOURCE & TRIGGER
- ▼ GEOPHONES



Figure 6.9 (b) PENNDOT SITE – III Geophone Layout for US 220/Harrison Road Intersection Site  
PROJECT: Sinkhole Void Grout Treatment

Drawing By: Ashutosh Srivastava  
Date: 06/13/2008

## **Chapter 7 – Test Site Description and Results**

### **7.1 Introduction**

MASW testing and the seismic refraction surveys were conducted between April 2008 and June 2008 at the three trial sites: 1) the Penn State Golf Course in State College, 2) Metzger field (Lafayette College) in Easton, and 3) US 220N near Harrison Road. Testing at the three sites was focused on improving the current schemes for the detection of anomalies in stratified soil media by refining the current seismic tomography methods and developing a time-efficient and economical protocol for these current seismic techniques that will aid in quick, safe, and environmentally responsible remediation of anomalies. The description of test sites and the results of MASW and the refraction survey are discussed in the sections below.

### **7.2 Penn State Golf Course Test Site and Setup**

An MASW test and seismic refraction survey were conducted on April 8 and April 18, 2008, on the Penn State Golf Course site located in an open field along West College Avenue. The survey consisted of a series of two test lines 10 ft apart, perpendicular to West College Avenue at a distance of 100 ft from the road (Figure 7.1).



Figure 7.1. Penn State Golf Course Site.

Both seismic tests were conducted along the same 100-ft test line with the same geophone spacing. The MASW test was conducted with a 2-ft geophone spacing, a geophone array dimension  $D$  of 30 ft, and two energy source offsets of 10 ft and 20 ft. A total of 15 MASW tests were conducted on each test line with a source receiver configuration (SRC) movement of 6 ft. The refraction test was conducted with the same instrument setup used for MASW. The geophone spacing was maintained at 2 ft. Initial and final offsets for the refraction tests were maintained at 20 ft for each geophone array spread. The dynamic field data collected using parameters described in Chapter 6 and the data were processed using the protocol described in Chapter 5.

## **7.2.1 Findings and Discussion of Tomography of Penn State Golf Course Site**

The subsurface shear wave velocity profile for the two test lines is shown in Figure 7.2 and Figure 7.3. This site is characterized by a low velocity region in two layers and several localized wave velocity variations in bedrock. These variations are possibly a solution cavity, a developing sinkhole, or voids as marked in the figures. Results for both test lines are discussed in the sections below.

### **7.2.1.1 Test Line 1**

Test line 1 results indicate a rapid variation in the tomography (Figure 7.2). As expected, the refraction survey was not able to detect the rapid variation of the tomography, but the MASW data were able to characterize all the tomographical features of the subsurface terrain such as the bedrock depth, top soil, weathering characteristics, anomalies like voids, and localized solution cavities. The depth of bedrock under test line 1 varies from 30 ft to 50 ft from the ground surface and is highly undulated (as a result of enhanced weathering). The shear wave velocity profile under test line 1 shows a possible solution cavity that may be a developing sinkhole. The subsurface shear wave velocity profile is also marked with a few low velocity layers and localized low velocity regions that indicate voids.

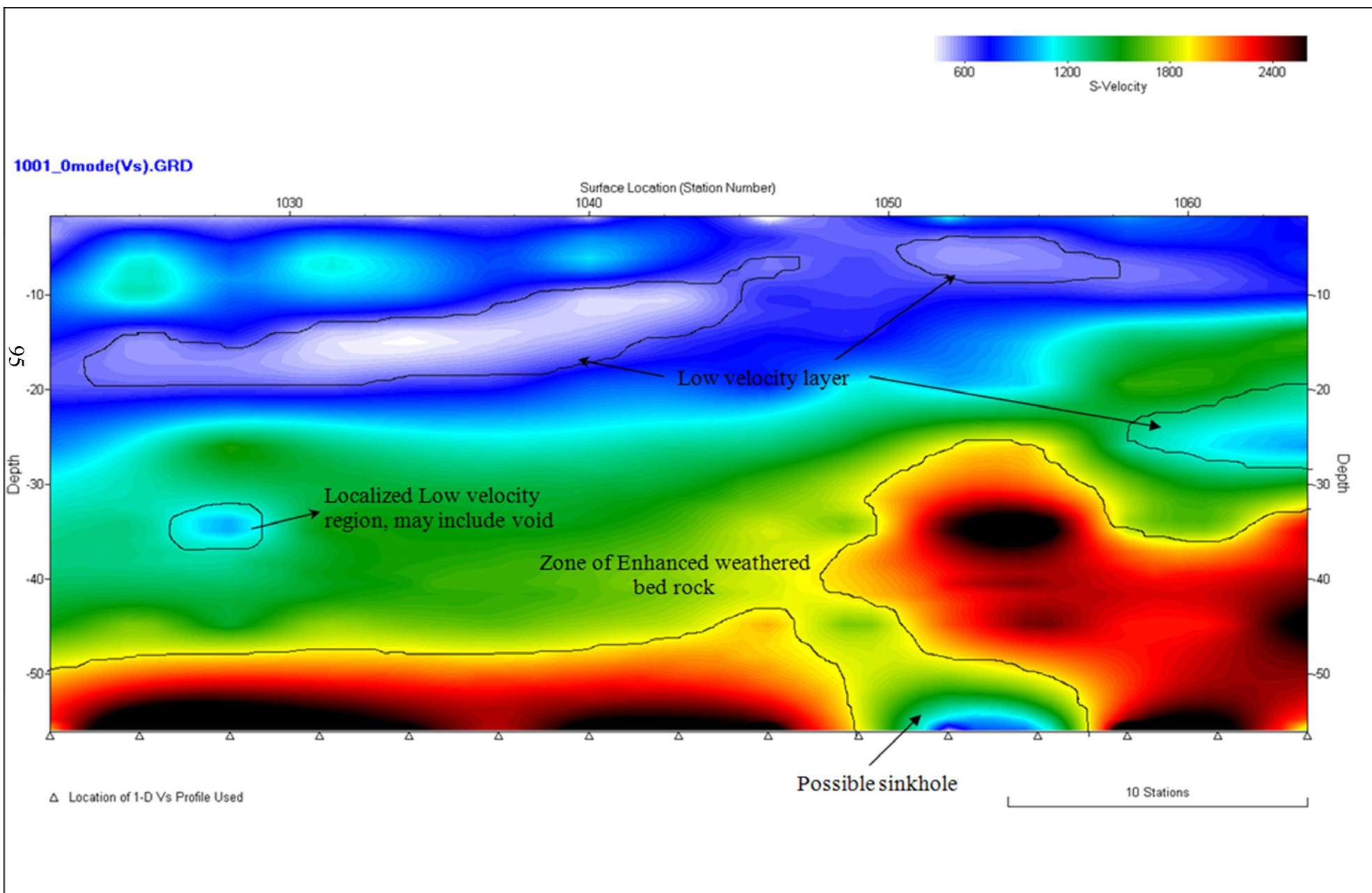
### **7.2.1.2 Test Line 2**

Test line 2 is situated to the east of test line 1. The shear wave velocity profile under test line 2 shows a zone of weathering, but the intensity of weathering is less than that under test line 1. The subsurface topographic features under test line 2 are shown in Figure 7.3. The depth of bedrock under test line 2 is uniform at 30 ft. The bedrock region also has a localized low velocity region that could be an extension of the possible

solution cavity observed under test line 1 at the same location. The subsurface is also marked with a low velocity region and localized low velocity regions, which indicate voids.

### **7.2.2 Penn State Golf Course Test Summary**

The indication of potential voids from test data coincides with surface indications of patches of sinkhole activity (reduced vegetation and some subsidence). In particular, a potential sinkhole is indicated that extends over both of the test lines.



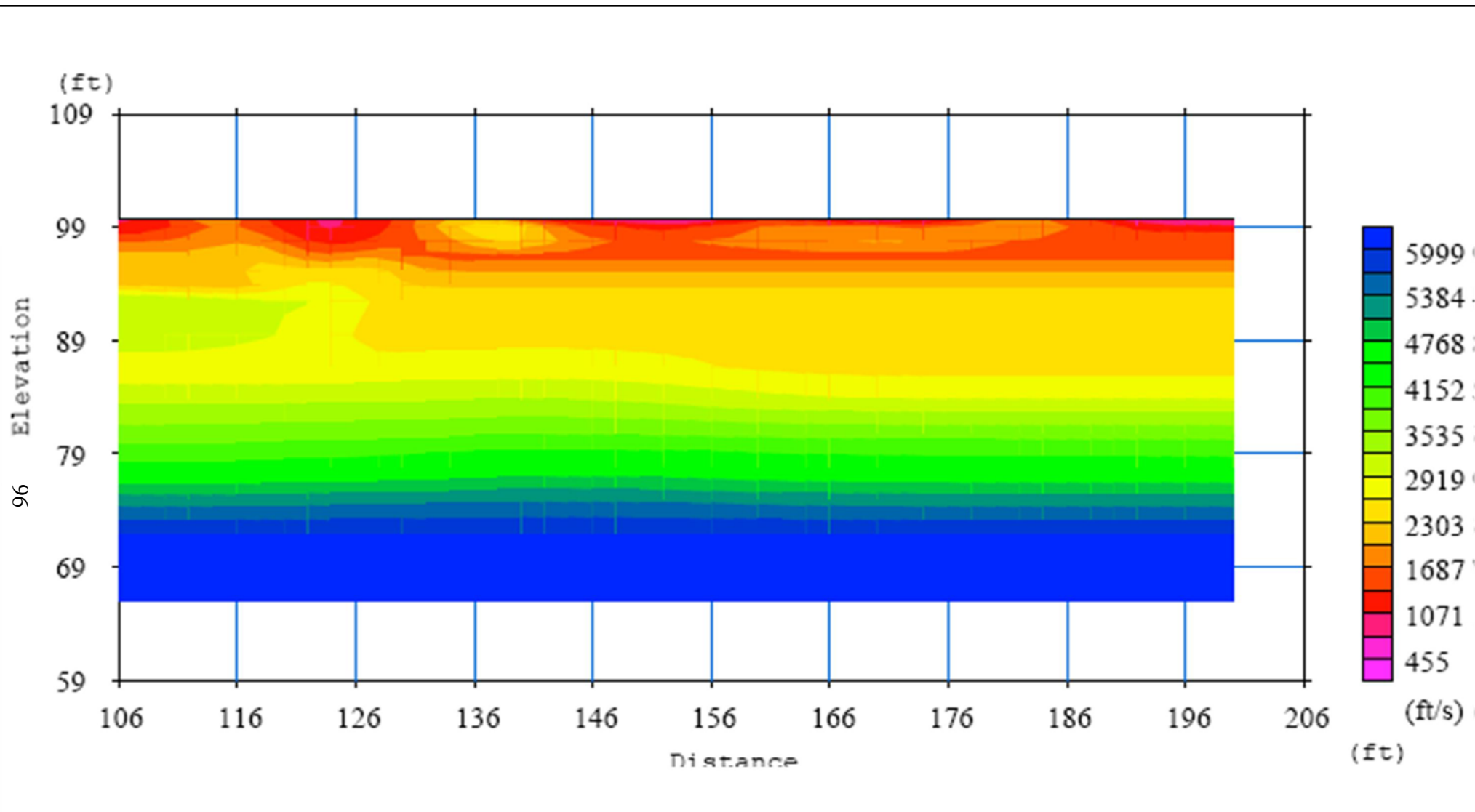


Figure 7.2 (b) Shear wave profile of Test Line 1 (Refraction Test)  
 PENNDOT SITE – I Pennsylvania State University Golf Course Site

Drawing By: Ashutosh Srivastava  
 Date: 04/24/2008

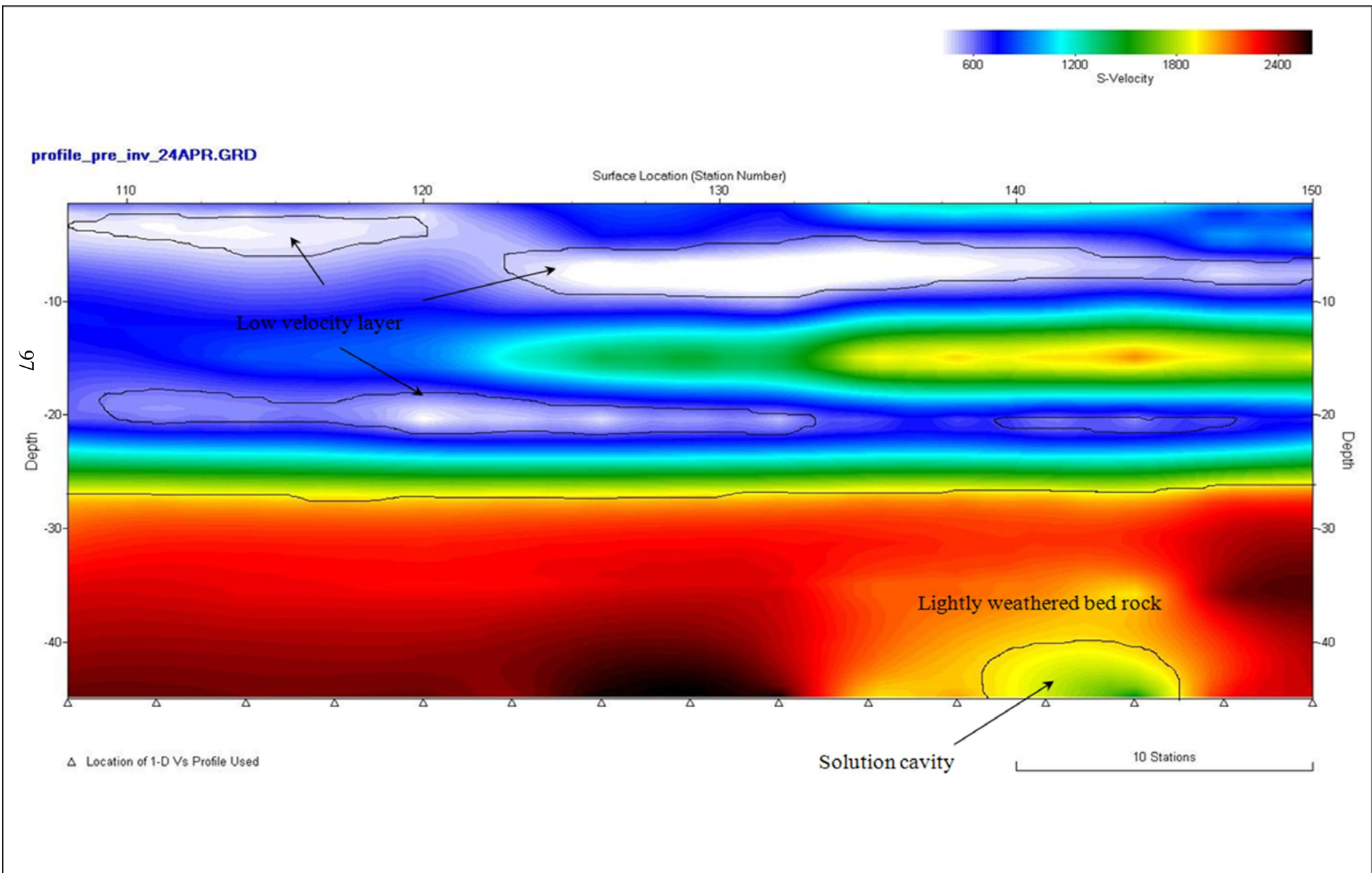


Figure 7.3 (a) Shear wave profile of Test Line 2 (MASW Test)  
 PENNDOT SITE – I Pennsylvania State University Golf Course Site

Drawing By: Ashutosh Srivastava  
 Date: 04/24/2008

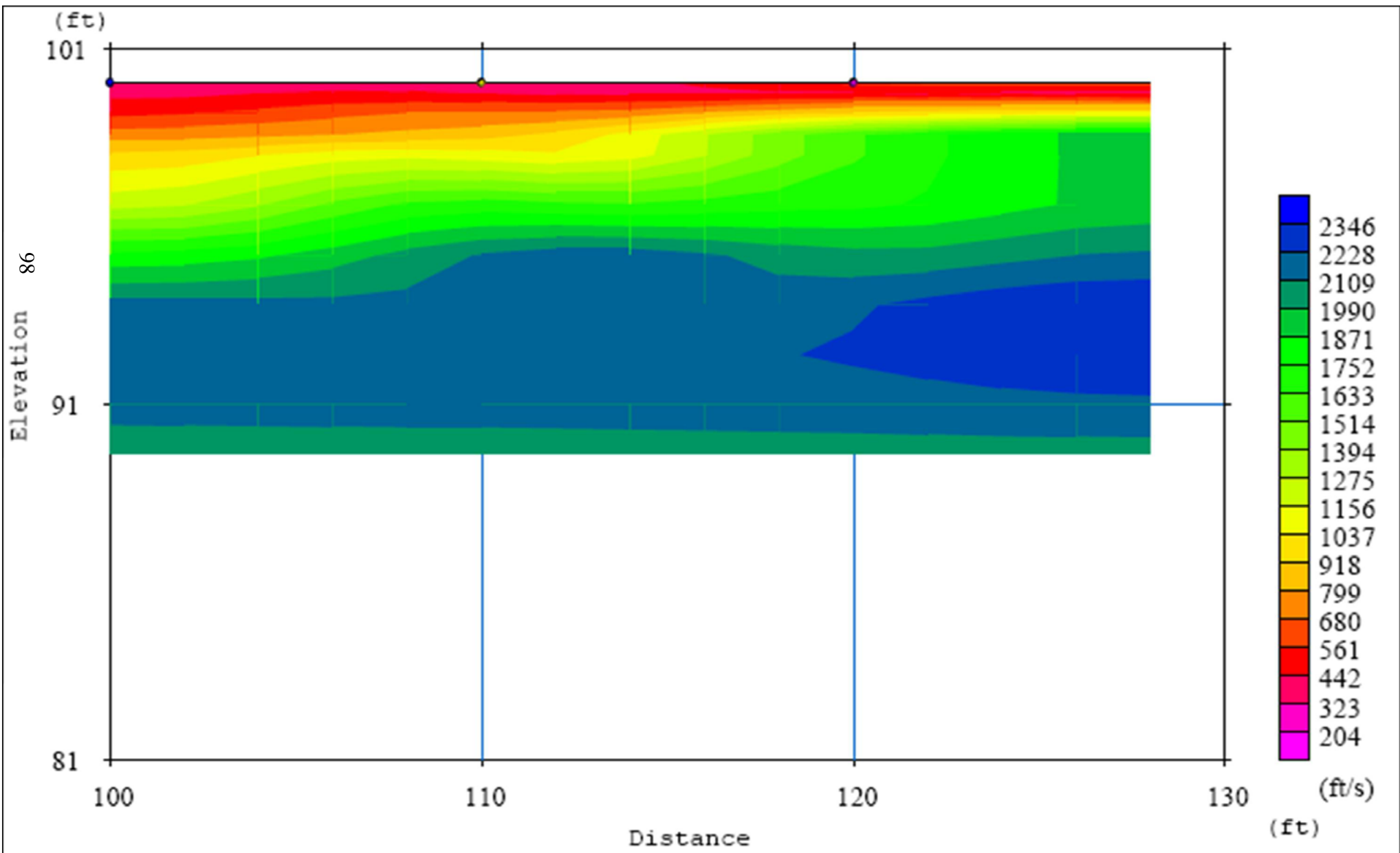


Figure 7.3 (b) Shear wave profile of Test Line 1 for span 100-128 feet (Refraction Test)  
 PENNDOT SITE – I Pennsylvania State University Golf Course Site

Drawing By: Ashutosh Srivastava  
 Date: 04/24/2008

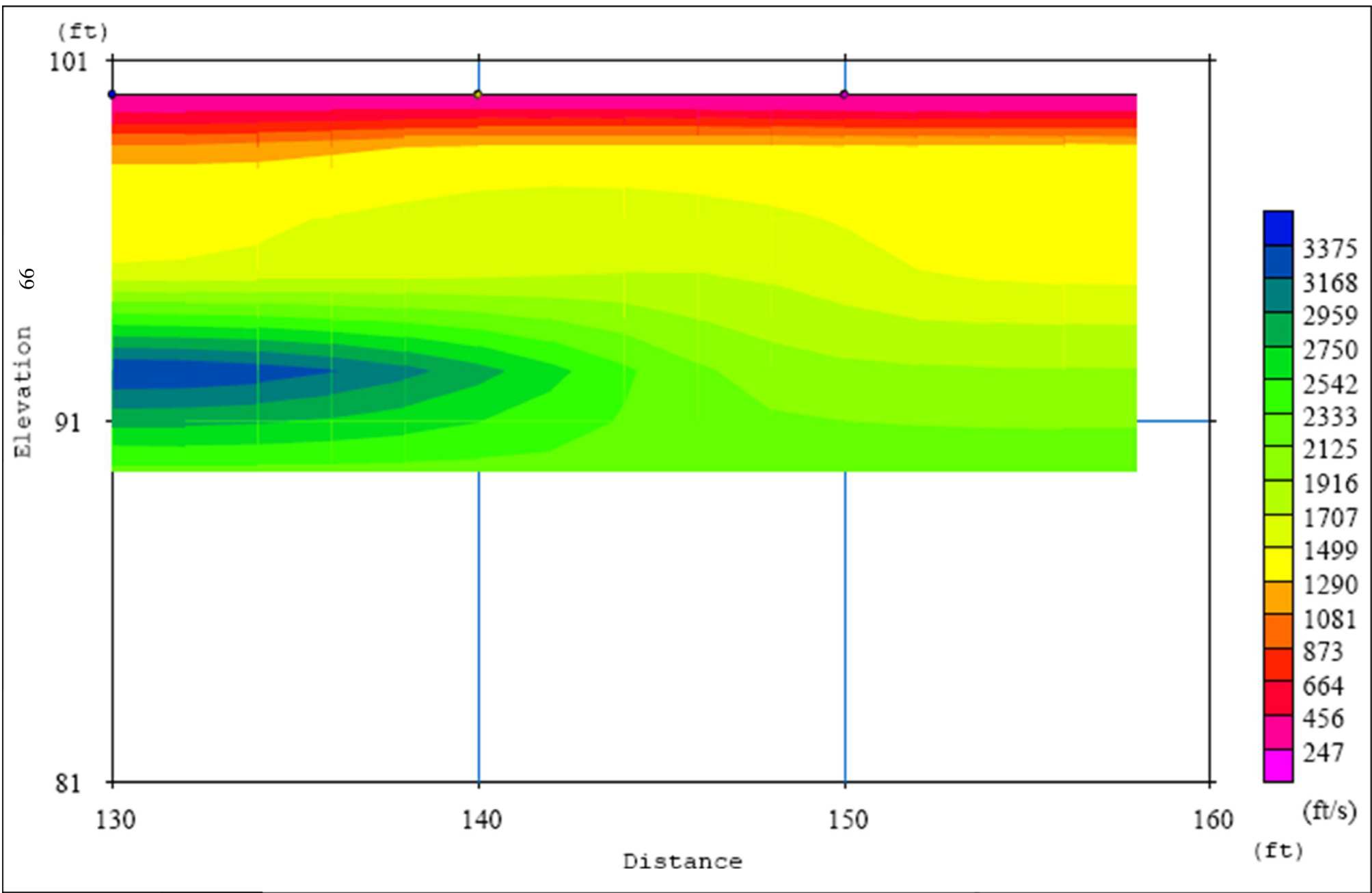


Figure 7.3 (c) Shear wave profile of Test Line 1 for span 130-158 feet (Refraction Test)  
 PENNDOT SITE – I Pennsylvania State University Golf Course Site

Drawing By: Ashutosh Srivastava  
 Date: 04/24/2008

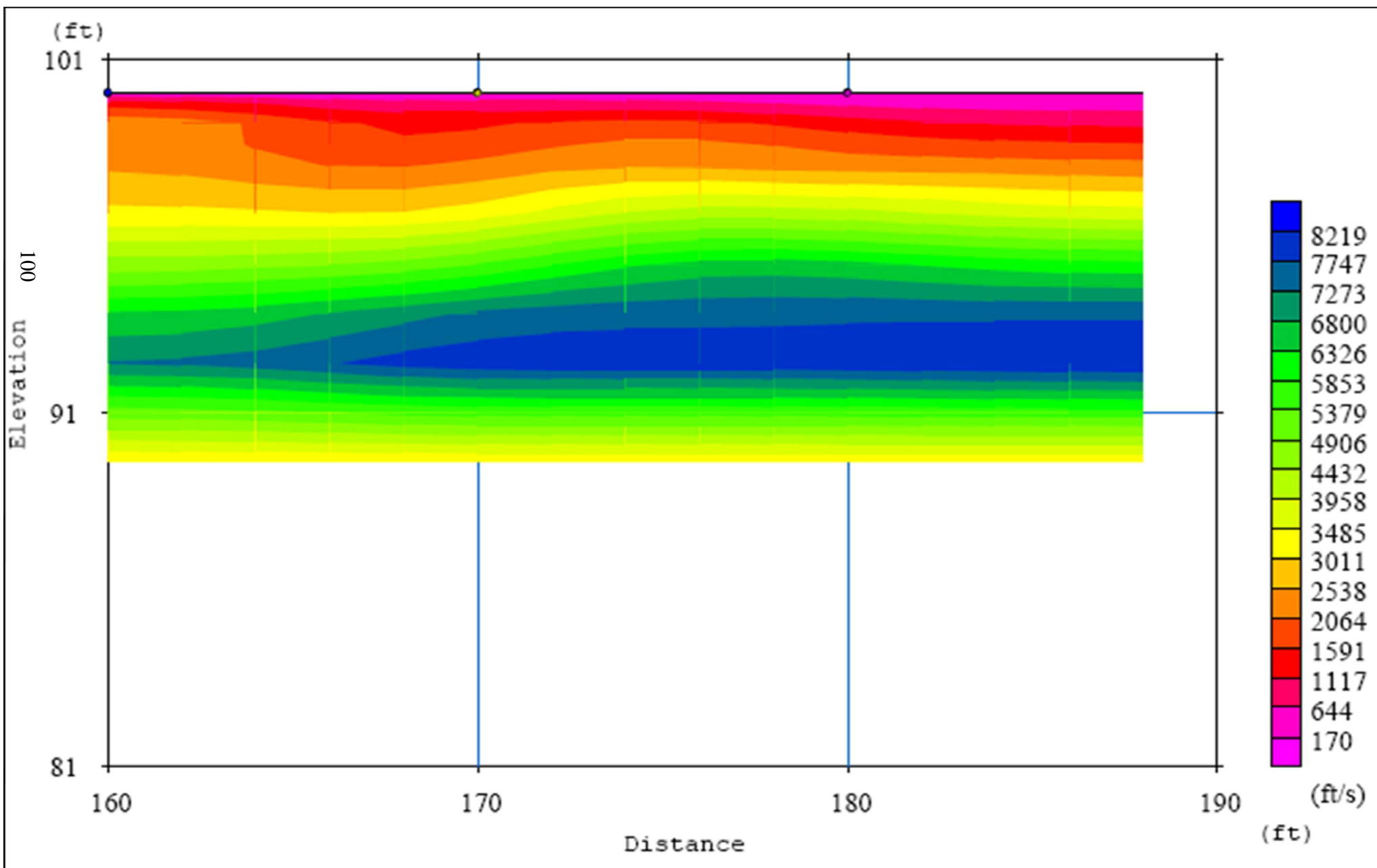


Figure 7.3 (d) Shear wave profile of Test Line 1 for span 160-188 feet (Refraction Test)  
 PENNDOT SITE – I Pennsylvania State University Golf Course Site

Drawing By: Ashutosh Srivastava  
 Date: 04/24/2008

### **7.3 Metzger Field (Lafayette College) Test Site and Setup**

MASW testing was conducted on May 19 and 20, 2008, on the Metzger Field (Lafayette College) site located in an open field near Braden Airpark to investigate the underground shallow cave. The survey consists of two lines running parallel to each other separated by 19 ft 7 in and approximately 50 ft from the fence separating the field and the Airpark (Figure 6.6 a).

MASW was conducted along the 100-ft test line, and the same geophone spacing of 3 ft was used for all test lines. The geophone array dimension,  $D$ , was 45 ft, and the two energy source offsets were 6 ft and 12 ft. A total of 43 tests were conducted on the test lines with a source receiver configuration (SRC) movement of 6 ft. The dynamic field data were collected using the parameters described in Chapter 6, and the data were processed using the protocol described in Chapter 5.

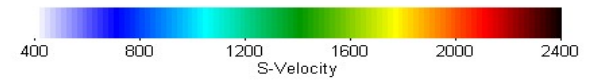
#### **7.3.1 Findings and Discussion of Tomography of Metzger Field Site**

The subsurface wave velocity profiles obtained from the MASW test conducted on the three test lines are shown in Figure 7.4. The presence of the void in the medium causes reflection of the portion of incident waves whose frequency content is dependent on the shape and size of the void. The results of electrical resistivity testing conducted in 2003 (Appendix A) on the same site shows the presence of extreme tomographical features such as caves, small localized voids, and loose soil layers near the surface. The presence of numerous wave velocity variations in a relatively small region can cause significant surface wave reflection resulting in a complex wave path. The presence of the caves may be resulting in the reflection of almost all of the wave energy. Thus, only a small amount of data is obtained from the geophones that are located at the end of the

array after the cave. The geophones that are placed between the cave and the source receive a direct wave, reflection of the direct wave from the small voids, and reflection of the direct wave from the cave and the waves from the complex reflections that are exchanged between the voids. In other words, due to the presence of numerous voids, the seismic energy may be trapped in the region and is disturbing the expected dispersion behavior of the surface waves.

### **7.3.2 Metzger Field Test Summary**

The MASW tests were conducted on the Metzger field at Lafayette College, Easton, Pennsylvania, to investigate the shallow underground cave. The presence of numerous low velocity regions along the cave resulted in complex reflections of surface wave energy along the wave path. This complex wave pattern cannot be analyzed with the current seismic wave analyzing software, so results were inconclusive for the Metzger Field site. A different test plan may need to be used to evaluate this site.



test1(Vs).GRD

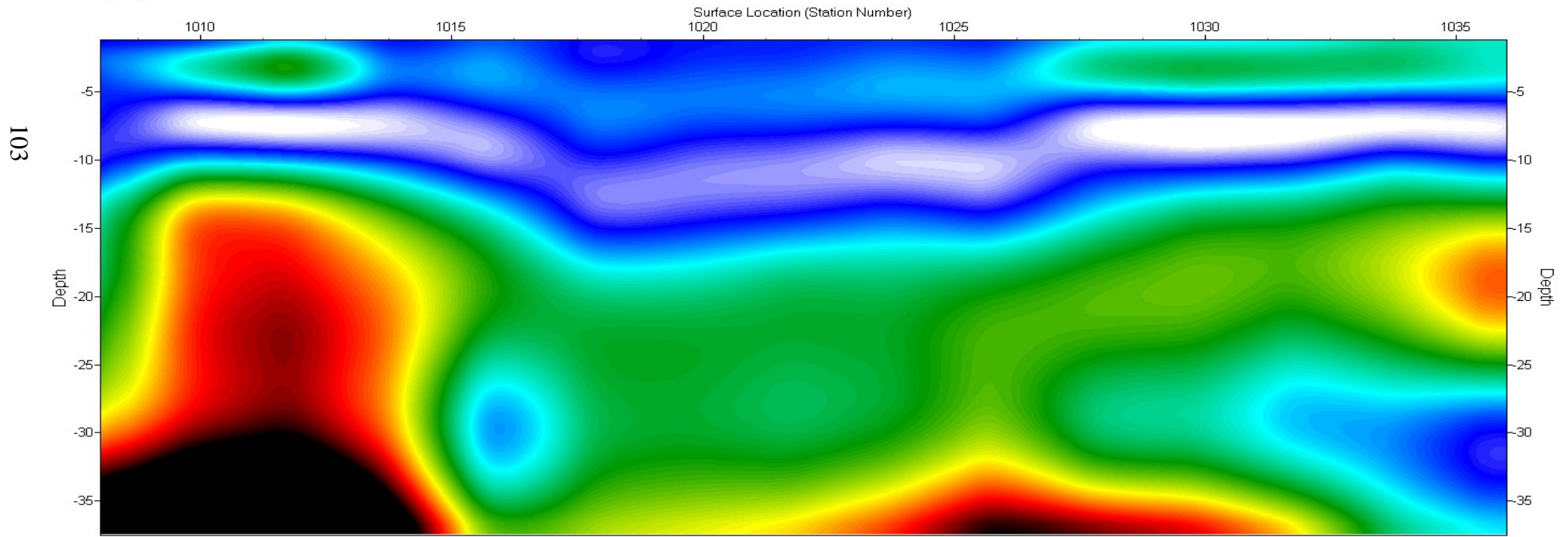
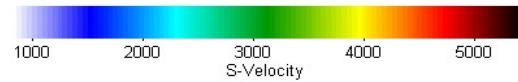


Figure 7.4(a). Shear Wave Profile of Control Line (MASW TEST).  
PENNDOT SITE – II Metzger Field (Lafayette College) Test Site  
Layout

Drawing By: Ashutosh Srivastava  
Date: 06/13/2008



12-2 14-2.GRD

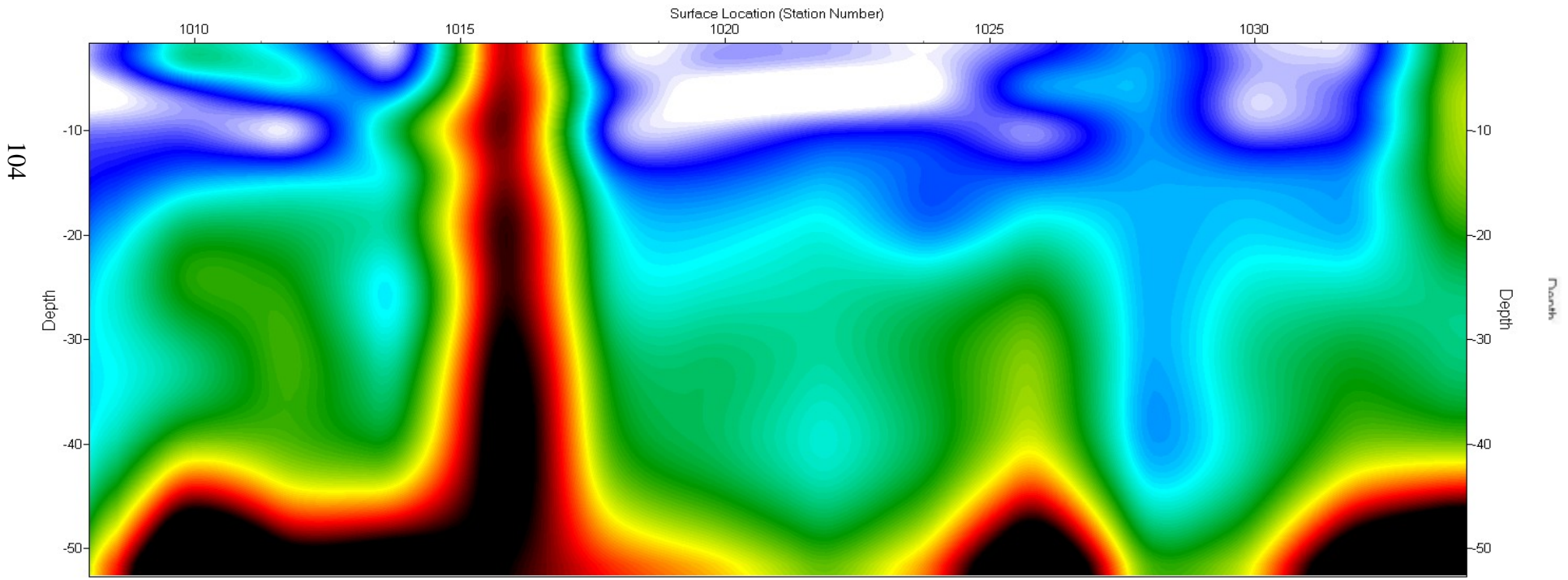
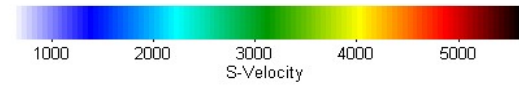


Figure 7.4(b). Shear Wave Profile of Test Line 1 (MASW TEST). PENNDOT SITE – II Metzger Field (Lafayette College) Test Site Layout

Drawing By: Ashutosh Srivastava  
Date: 06/13/2008



Line2\_2.GRD

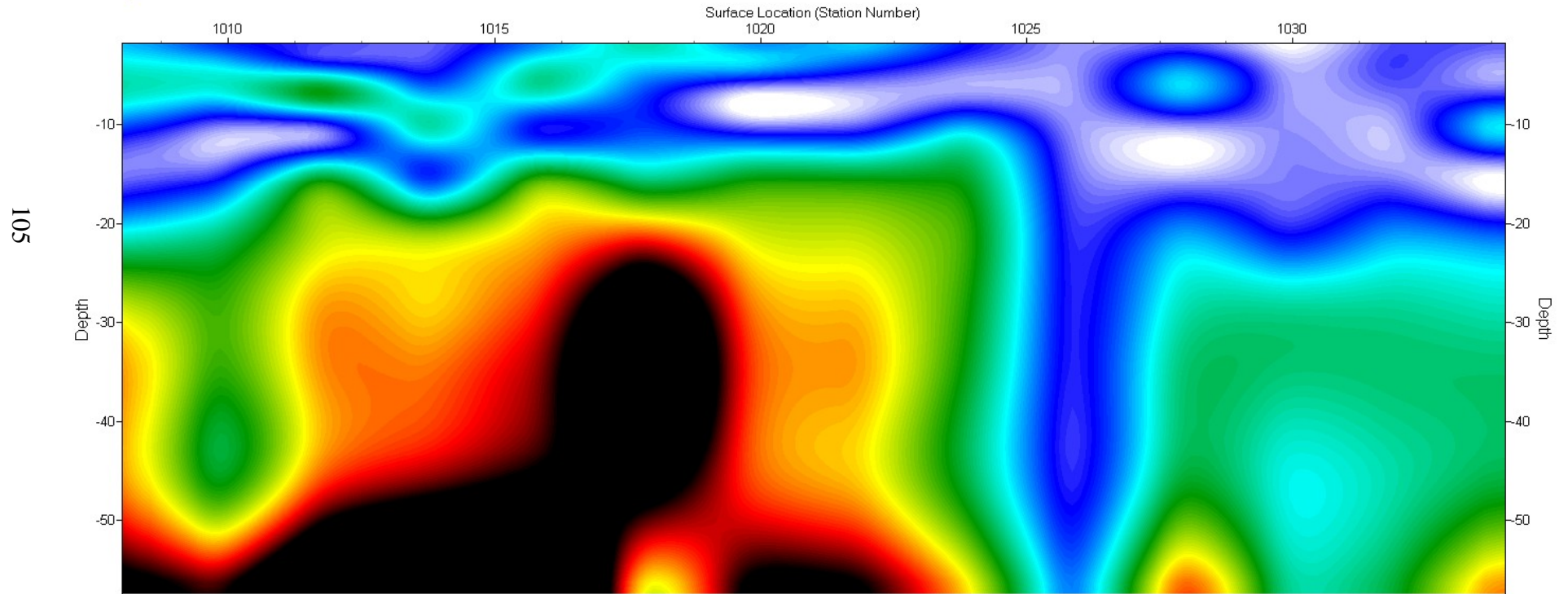


Figure 7.4(c). Shear Wave Profile of Test Line 2 (MASW TEST).  
PENNDOT SITE – II Metzger Field (Lafayette College) Test Site  
Layout

Drawing By: Ashutosh Srivastava  
Date: 06/13/2008

## **7.4 U.S. 220 N Test Site and Setup**

MASW testing and seismic refraction surveys were conducted on June 9, 2008, along US 220 N under the Harrison Road Bridge to identify the cause of several depressions located adjacent to the abutment of the bridge. The survey consisted of a single line running parallel to US 220 N under the Harrison Road Bridge at a distance of 8 ft from the outer edge of the shoulder (Figure 6.9 a).

The MASW test was conducted with 2-ft geophone spacing, geophone array dimension  $D$  of 30 ft, and two energy source offsets of 10 ft and 20 ft. A total of 16 MASW tests were conducted on the test line with source receiver configuration (SRC) movement of 6 ft. The refraction test was conducted with the same instrument setup used for MASW along the 100-ft test line. The geophone spacing was maintained at 2 ft. Initial and final offsets for the refraction tests were maintained at 20 ft for each geophone array spread. The dynamic field data were collected using parameters described in Chapter 6, and the data were processed using the protocol described in Chapter 5.

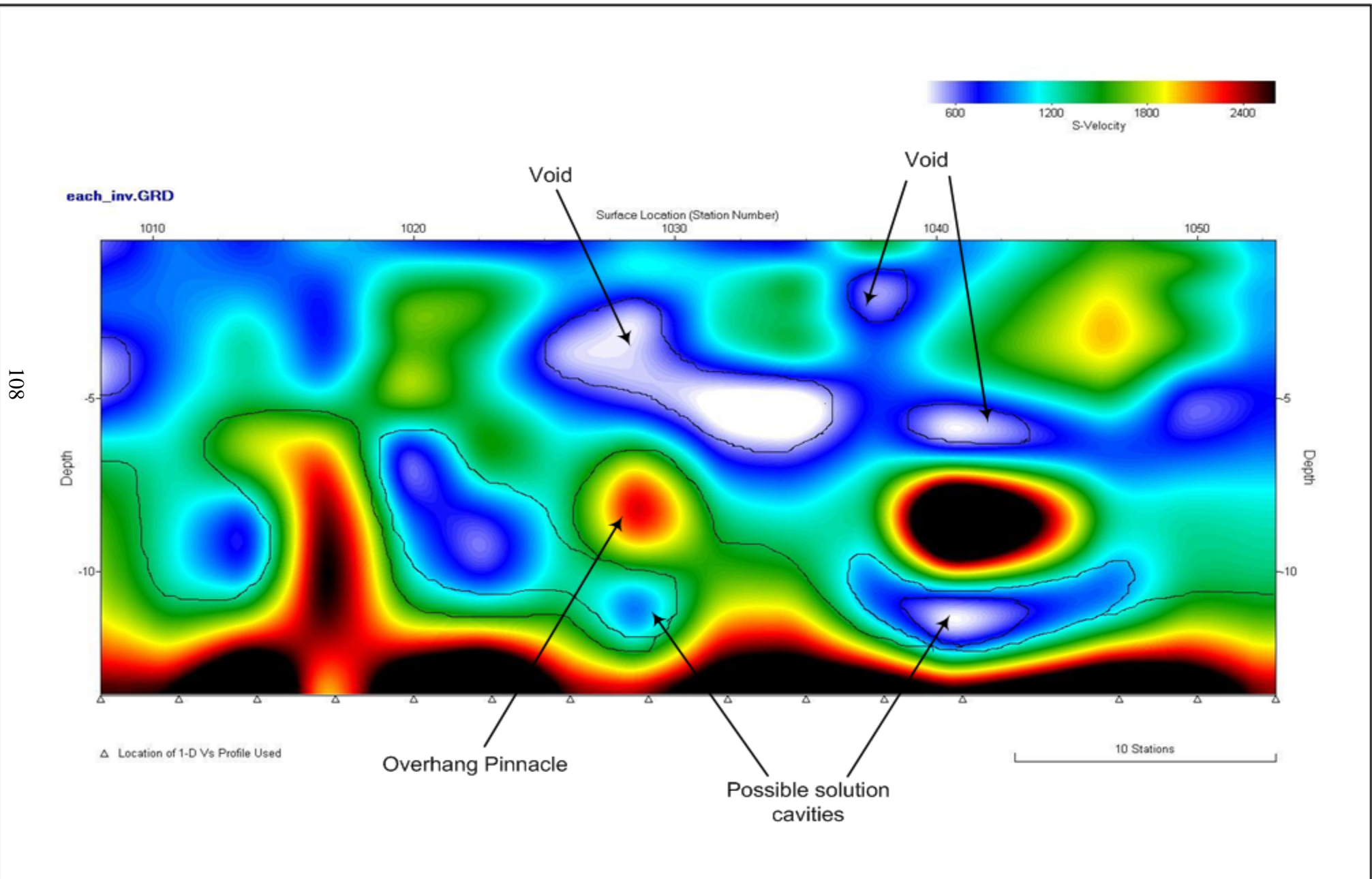
### **7.4.1 Finding and Discussion of Tomography of U.S. 220 N Test Site**

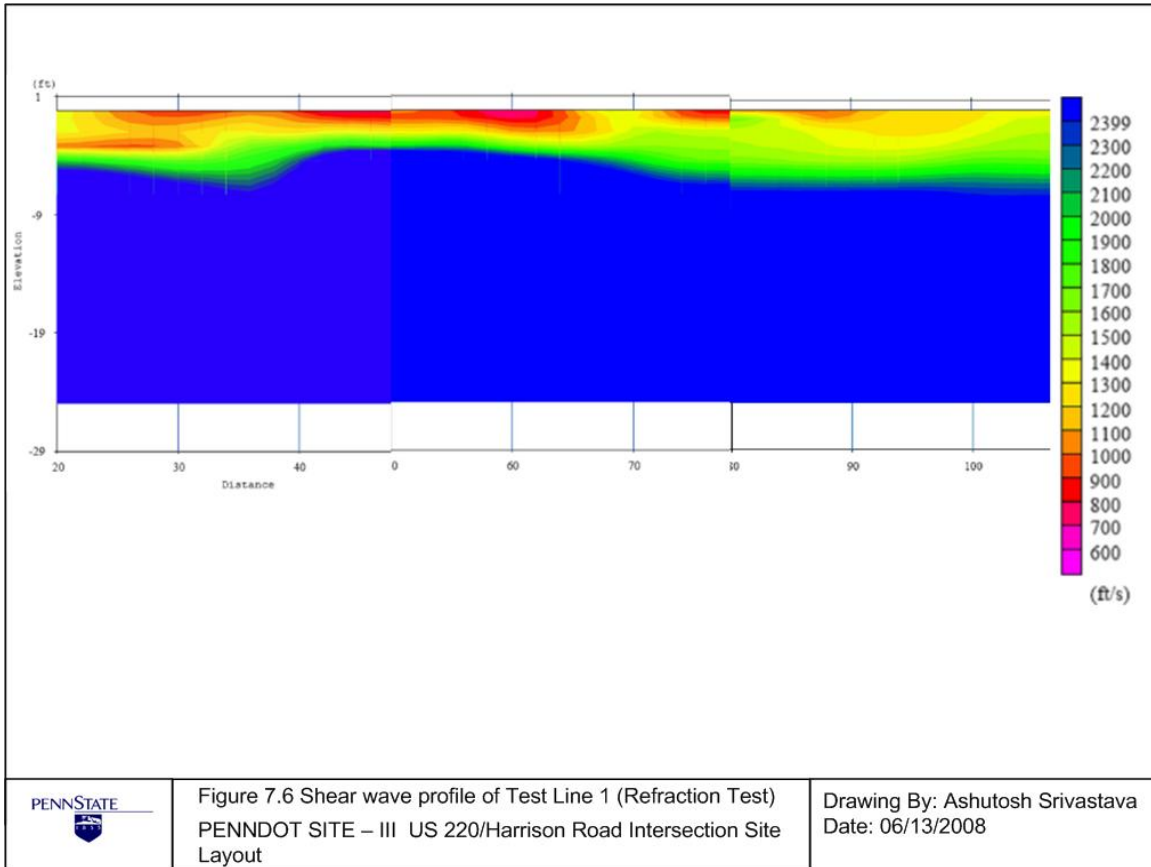
The subsurface wave velocity profiles for both types of seismic tests for the test line are shown in Figure 7.5 and Figure 7.6. The site consists of many surface depressions and few eroded regions, indicating an active subsurface tomography. As expected, the refraction survey was not able to capture the characteristics of all the rapidly varying tomographical features. The shear wave velocity plots from the refraction survey shows a very smooth variation in the tomographical features and thus fails to explain the surface depressions and erosion. MASW test results show the rapidly varying shear subsurface tomographical features. The bedrock depth

under the test line is almost constant at 13 ft. The shear wave velocity profile under the test line shows a void near the surface at the midsection coinciding with the majority of surface depressions. . The shear wave velocity profile shows two possible solution cavities that could be sinkholes in their developing stages.

#### **7.4.2 US 220 N Site Test Summary**

The subsurface shear velocity profile is highly variable. Two possible solution cavities are visible under the test line. A large bell-shaped shallow void is visible under the midsection, which explains the surface depressions around that region.





## Chapter 8 – Summary and Conclusions

### 8.1 Summary

This research provided an initial investigation into the applicability of MASW for use by PennDOT in evaluating and identifying sinkholes, including a step-by-step procedure for use of the equipment. Three sites were investigated: (1) the Penn State Golf Course, a site of known sinkhole activity; (2) the Lafayette College Athletic Field, a site of measured and investigated sinkhole and void activity for proof testing; and (3) the site at SR 220 (future I-99) under the Harrison Road overpass.

The golf course site provided an area for extensive equipment evaluation and troubleshooting due to its level terrain and proximity to the Penn State laboratories. Sinkhole activity was suspected at this site due to the presence of surface indicators (lack of vegetation, depressions, etc.). This site was successfully evaluated with the MASW technique with detection of some sinkhole activity coinciding with what would be expected for the region. The Lafayette cave site was intended to provide a comparison between MASW results and other test results from this site. The site had been thoroughly explored with resistivity testing as well as cores and some physical measurements of the cave. The MASW method with the test lines chosen was not well suited for this site due to likely interference from the proximity of multiple voids and the large cave. This site may need further investigation with a different test plan. The Harrison Road site provided data on a more typical PennDOT test case. The data coincided well with the expected results due to known sinkhole problems in the area. The data were acquired in a period of 4 hours and processed the same day.

## 8.2 Conclusions

The following conclusions can be drawn from this research:

- Seismic methods such as MASW can be effectively used to map the various subsurface tomographical features such as voids and the bedrock top surface, and can also identify the zones of weathered bedrock.
- The MASW method can be used for regions of rapidly varying tomography. It performed better in identifying the rapidly varying tomography.
- The MASW method is a quick and effective way to locate and evaluate potential sinkhole problems near PennDOT structures.

## 8.3 Implementation Plan

This report provides the first step in implementation of the MASW method for rapid subsurface evaluation for detection of sinkholes for PennDOT. Full implementation of the method would include the following:

- State-of-the-practice in MASW
- Documentation of the MASW method for different site types
- Training of PennDOT personnel in MASW use (with yearly updates)
- Manual and troubleshooting guide for using MASW for PennDOT applications

The first two items in the above list were covered by this report as a basis for full implementation. Step-by-step procedures for equipment setup, data acquisition, data analysis, and data interpretation are presented for use by PennDOT personnel.